LABORATORY INVESTIGATION AND FIELD PERFORMANCE EVALUATION FOR CHEMICALLY STABILIZED CEMENT TREATED SUB-BASES

A dissertation Submitted in partial fulfilment of the requirement for the award of the degree of

MASTER OF ENGINEERING
In
INFRASTRUCTURAL ENGINEERING

Submitted by:
SHEIKH HAZIM JAVAID
802023027

Under the Supervision of:

Dr. Tanuj Chopra

Assistant Professor,
Civil Engineering Dept.
TIET, Patiala

Mr. Rajesh Pathak

Associate Professor,
Civil Engineering Dept.
TIET, Patiala

Civil Engineering Department
Thapar Institute of Engineering and Technology,
Patiala, Punjab-147004 (India)

July - 2022

DECLARATION

I, hereby declare that this work which is being presented in the dissertation entitled **"Laboratory Investigation And Field Performance Evaluation For Chemically Stabilized Cement Treated Sub-Bases,"** in partial fulfilment of the requirement for the degree of master's of engineering in the field of Civil Engineering at Thapar Institute of Engineering and Technology (Patiala), is an authentic record of work carried out by me under the supervision of Dr. Tanuj Chopra (Assistant professor) and Mr. Rajesh Pathak (Associate professor), Civil Engineering Department, Thapar Institute of Engineering and Technology, Patiala, Punjab. This work has not been submitted elsewhere to reward any other degree. I am fully responsible for the contents of my project report.

Date: 29 July 2022

Sheikh Hazim
(802023027)

This is to certify that the above declaration made by the concern student is correct according to the best of my knowledge and belief.

Dr. Tanuj Chopra
Assistant Professor
Department of civil engineering
TIET, Patiala, Punjab

Sh. Rajesh Pathak
Associate Professor
Department of civil engineering
TIET, Patiala, Punjab

ACKNOWLEDGEMENT

The research work which is presented in this dissertation, is more of a teamwork, and I would like to thank many who have contributed their time and energy to the study.

First and foremost, I am grateful to my supervisor **Dr. Tanuj Chopra** and **Mr. Rajesh Pathak**, Department of Civil Engineering, Thapar Institute of Engineering and Technology, Patiala, who consistently kept me motivated and instilled good thoughts not only for research but for life as well. Their constant and enthusiastic support throughout is the root cause for the research work to see its end.

I would like to express my gratitude to **Dr. Prem Pal Bansal**, Head of the Department of Civil Engineering, Thapar Institute of Engineering and Technology, Patiala, for his kind cooperation and encouragement, which helped me in the completion of my work.

I am incredibly thankful to **Mr. Amarjit Singh** and **Mr. Jaspreet Singh** for helping me carry out the experimental work.

I would like to acknowledge **Zydex industries Pvt. Ltd.** Vadodara, Gujrat, India for sponsoring Nano-chemicals used in the study. I conscientiously acknowledge the cooperation, assistance and knowledge sharing imparted by the company during this research work.

I'd want to express my gratitude to **Mr. Junaid Altaf** and **Mr. Rohan Kumar**, who assisted with different aspects of this research and helped make the time informative, illuminating, enjoyable, and unforgettable.

Above all, I am grateful to The Almighty.

ABSTRACT

India is making significant investments in the transportation sector, but in many locations, the procurement and the processing cost of naturally available materials is exorbitantly increasing because of rapid depletion of these materials. In this work, soil that is readily available in the area, cement and nano-chemicals like Terracil and Zycobond are utilised to assess the impact of nano materials on California bearing ratio and compressive strength of chemically treated sub-base layer. XRD, SEM tests were carried out to identify the micro structure of different mixes. The addition of optimum dosage of nanoparticles had a very advantageous effect on UCS and CBR. The compressive strength of the soil aggregate mix treated with cement was improved by up to 103.4% by the addition of nano compounds. The California bearing ratio of the mix treated with optimum dosage of cement and chemical was increased by 219%. The different laboratory prepared mix were laid on the field (Intermediate lane, PMGSY road) to study a behaviour of mix. To examine the deflection and modulus for various mixes laid on the field, a deflectometric investigation employing a lightweight deflectometer was conducted. LWD was also used to calculate the 28-day modulus.

SEM, XRD analysis depicted that the nanoparticles promoted the pozzolanic reaction by transforming portlandite into C-S-H gel. According to the X-ray diffraction patterns, stabilisation by terrasil and zycobond results in the creation of additional peaks like CSH and changes the structure of pure soil when gypsum is added. SEM pictures of soil samples reveal a denser texture as a result of chemical stabilisation and a decline in the Si/Al ratio, which suggests increased shear strength in stabilised samples according to interpretation of energy dispersive X-rays (EDS).

TABLE OF CONTENTS

LIST OF FIGURES

LIST OF TABLES

LIST OF ABBREVIATIONS

MoRTH	Ministry of Road Transport and Highway.
IRC	Indian Road Congress.
LWD	Light Weight Deflectometer
ACTM	Automatic Compression Testing Machine
OMC	Optimum Moisture Content
MDD	Maximum Dry Density
CBR	California Bearing Ratio.
GSB	Granular Sub-Base.
WMM	Wet Mix Macadam.
BC	Bituminous Concrete.
CTSB	Cement Treated Sub-Base.
CTB	Cement Treated Base.
MSS	Mix Seal Surfacing
SAMI	Stress Absorbing Membrane Interlayer.
PMC	Premix Carpet.
DBM	Dense Bituminous Macadam.
LCCA	Life Cycle Cost Analysis.
VDF	Vehicle Damage Factor.
MSA	Million Standard Axles
LCV	Light Commercial Vehicle.
MAV	Multi-Axle Vehicle.
XRD	X-Ray Diffraction
SEM	Scanning Electron Microscopy

CHAPTER I
INTRODUCTION

Stabilization techniques, especially chemical techniques, have gained a drastic surge in recent decades. To adopt a cost-effective solution, improving ground using different becomes incumbent. Admixtures used with locally available soil should be added to improve the ground soil properties effectively because replacing of soil (in case of poor soil) could be exorbitant (Patel, Mishra and Pancholi, 2015). In a country like India, many soils are extensively being used and are problematic e.g. black cotton soil (Samal, et.al), (Kumar, Raju and Verma, 2020) , the only solution to these soil types is proper soil stabilization with additives.

Country like India, which is developing at a tremendous pace, where there is a massive construction in the road sector, new/alternative materials and technology in highway construction are of prime importance. Cement Treated Base (CTB), CTSB (because of its higher efficacy (Singh et al., 2020), waste plastic, geo-synthetics, recycling, fly-ash, modified bitumen (CRMB, polymer-modified, natural rubber), soil stabilization, and other IRC recommendations are available for use in highway building. To maximize potential time and cost savings, these materials/technologies must be promoted in the construction and maintenance of roads.

CTSB (Cement Treated Sub-Base) added with chemical additives is widely used as a sub-base layer in many road projects. It utilizes locally available soil, which reduces the cost of construction to a vast extent (Buazar, 2019), (Singh and Yadav, 2018) (Patil and Patil, 2013). Furthermore, the benefits of cement-treated soil with chemicals are not limited to its increased strength but also provides waterproofing, making it significantly more stable and long-lasting than untreated soil.

In regions where problems of groundwater intrusion exist, waterproofing plays a very crucial role as the water ingress can cause damage to the lower unbound layers. Cement's impact on critical elements like water content, curing time, compaction energy, and involvement in cement-treated soils' microstructure and engineering features have been thoroughly studied.(Catton, 1941). Other materials like Terra-zyme and Fly-ash are also used to improve the sub-base conditions.

In recent years, nanoparticles have attracted considerable scientific interest for many civil engineering applications. Of all the introduced nanoparticles, nano-SiO_2 plays the most significant role. Nanoparticles of SiO_2 exhibit high pozzolanic activity due to a high amount of pure amorphous SiO_2 (Farzadnia, Ali and Demirboga, 2013) (Kawashima *et al.*, 2013) (Givi *et al.*, 2010). The Nano-chemicals Terracil and Zycobond have been collected from Gujarat, India, for the stabilization studies. An experimental programme has been carried out on the Sandy soil treated with different dosages of Terracil, Zycobond and Cement. (Patel *et al.*, 2015) (Gayathri and Pal, 2021).

This study addresses the development of cement-treated soil strengthened with chemicals like Terracil and Zycobond as supplementary material. The inclusion of nanoparticles may reduce the cement consumption in the soil and accelerate the stabilization process. This study investigates changes in compaction, and unconfined compressive strength of cement-treated soil with chemicals.

During and after construction the LWD (lightweight deflectometer) is used as a field evaluation tool for different road assessment scenarios. Around the world, the use of a (LWD) for construction quality control is growing rapidly. The LWD can be used to check compaction during construction and to examine deflections thereafter, from which the modulus can be determined using back-calculating software such as LWD Mod, KGP back, and so on.

1.1 Flexible pavement:

Flexible pavement can be defined as a pavement layer comprising of a mixture of aggregates and bitumen, heated and mixed correctly and then laid and compacted on a bed of granular layer. It can also be defined as a pavement which are flexible in their structural action under the loads

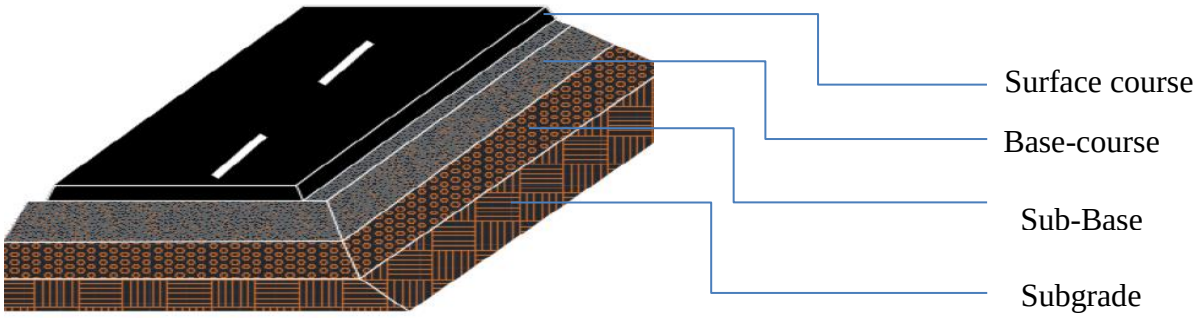

Figure 1.1: Conventional flexible pavement

1.2 Conventional Sub-Bases

In Highway Engineering Subbase is the layer that consist of aggregate that is laid on the subgrade. It can be skipped if the pavement will only be used by pedestrians, but it becomes incumbent for surfaces that are used to carry vehicular loads**.** The main load-bearing layer of the pavement is often the subbase. Its job is to uniformly distribute the load throughout the subgrade. Crushed stone, crushed slag or concrete, or slate are the most common unbound granular materials. There are in total of six gradation for GSB as per MoRTH.

Function of sub-base course layer:

- A sub-base course is a layer of material that is directly beneath a pavement's wearing course, while a sub base is a layer of material that lies between the base and the sub grade. The layer beneath a firm pavement is sometimes referred to as sub base.
- The flexible pavement's sub base layer is largely utilized to improve load bearing capacity by dispersing the load to the finite thickness and frost susceptible layer. When compared to the base layer, the materials employed are inferior.

Table. 1.1: Grading for Granular Sub-base Materials (MoRTH- 401.2.2)

IS sieve Designation	Grading I	Grading II	Grading III	Grading IV	Grading V	Grading VI
75.0 mm	100	-	-	-	100	-
53.0 mm	80-100	100	100	100	80-100	100
26.5 mm	55-90	70-100	55-75	50-80	55-90	75-100
9.50 mm	35-65	50-80	-	-	35-65	55-75
4.75 mm	25-55	40-65	10-30	15-35	25-50	30-55
2.36 mm	20-40	30-50	-	-	10-20	10-25
0.85 mm	-	-	-	-	2-10	-
0.425 mm	10-15	10-15	-	-	0-5	0-8
0.075 mm	<5	<5	<5	<5	-	0-3

Resilient modulus of Conventional Sub-base layer

The resilient modulus of the granular layer is determined by the resilient modulus of the foundation or supporting layer on which it rests, as well as the thickness of the granular layer. Because substantial deflections generated by loads result in de-compaction in the lower regions of the granular layer, weaker support does not allow for a greater modulus of the top granular layer. The following equation can be used to calculate the granular layer's modulus based on its thickness and the modulus value of the supporting layer.

$$M_{R\ Gran} = 0.2(h)^{0.45} * M_{R\ SUPPORT} \ldots\ldots\ldots \text{ (7.1) IRC 37, 2018}$$

Where,

h = Thickness of granular layer in mm

$M_{R\ Gran}$. *= Resilient modulus of granular layer (MPa)*

$M_{R\ SUPPORT}$ *= (Effective) Resilient modulus of supporting layer (MPa)*

1.3 Cementitious (cement-treated) Sub-base Layer (CTSB).

Cement-Treated Sub-Base (CTSB) is a type of Soil-Cement layer that describes an intimate mixture of native soils and/or manufactured aggregates with measured amounts of Portland cement and water to form a strong, durable, frost-resistant paving material after compaction and curing. (Pagar et al., 2018)

Indian Roads Congress (IRC) developed a Special Publication (SP) for the mix design of lime/cement treated base/subgrade. It saves money and helps to increase the life cycle of roads. The recommended minimum thickness and resilient modulus of the CTSB layer are 200mm and 600 MPa respectively.

CTSB with a grading IV strength of 0.75-1.50 MPa is not suggested for major highways, but it can be utilized for roads with less than 10 MSA traffic volume (Low volume roads). As per IRC-37,2018 the modulus value is taken as 400 MPa.

Several stabilizing agents can be used in treating CTSB. Reclaimed Asphalt Pavement material (RAPM) is used in treating base and subbase layers (Montepara et al., 2012). The sustainable valorisation of RAPM in the cement-treated base (CTB) layer by incorporating chemical stabilizers by the full-depth reclamation (FDR) method is done, which provides the best result in terms of strength parameters and durability properties of studied samples.

The gradation table for materials required in CTSB is given in MoRTH 400-4 and is shown below:

Table 1.2: Grading Limits of materials for stabilization with cement. (MoRTH 400-4)

IS Sieve Size	% by mass Passing Sub-base within Range
53.00 mm	100
37.5 mm	95-100
19.0 mm	45-100
9.5 mm	35-100
4.75 mm	25-100
600 microns	8-65
300 microns	5-40
75 microns	0-10

Resilient modulus of CTSB layer

For the Analysis and Design of pavements with CTSB layers, a design value of 600 MPa is recommended. CTSB with IRC: SP:89 grading IV and a strength range of 0.75-1.5 MPa is not recommended for national highways, but it can be used in roads with design traffic less than 10 msa and a modulus of 400 MPa. The CTSB layer's poisons ratio can be calculated as 0.25. The CTSB layer should be 200mm thick at the very least.

Advantages of Cement Treated sub-base

- For design traffic volume greater than 30 msa (all effective CBR values) the thickness of CTSB layer is less than that of conventional GSB layer. In case of 2msa traffic the thickness of CTSB is less than conventional up to a value of 10% effective CBR.
- Because of the improved load capacity of CTSB, the number of asphalt layers can be lowered, reducing construction time and costs.
- The inclusion of Portland cement and bituminous emulsion boosted the mixture's compressive strength, flexibility, pH, and CBR, according to the earlier research (Baghini, Ismail and Karim, 2015)
- The total cost of constructing flexible asphalt using the CTSB / CTB method is lower than with the traditional method since it eliminates the costs of hauling necessary equipment, machinery, and fuel consumption, among other things.

- Because it reduces material requirements, reduces initial construction costs, outperforms traditional materials, and reduces project maintenance costs, which have an impact on overall life cycle costs. This is also environmentally friendly.

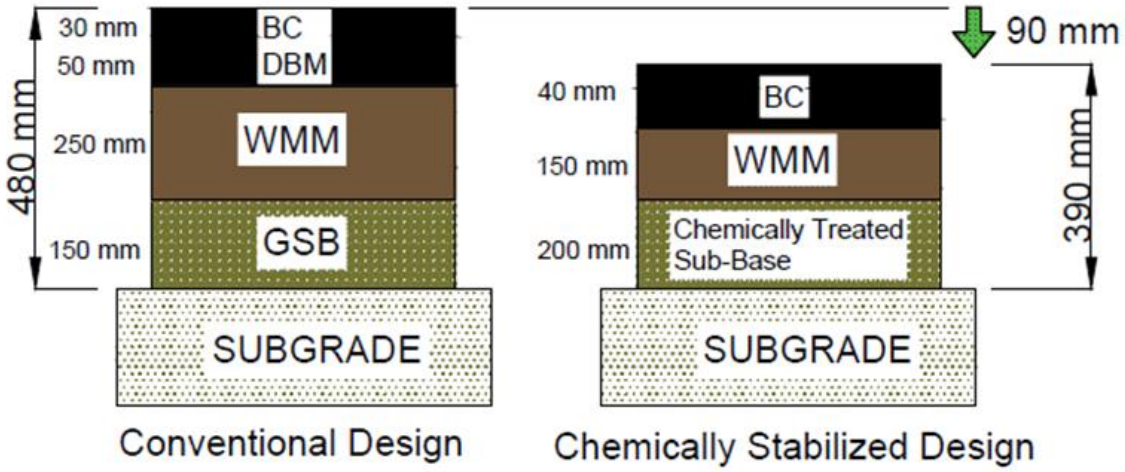

Figure 1.2: Conventional design vs Chemically stabilized design

The comparison between conventional and stabilized pavement design is displayed in the figure above. The crust thickness is reduced with the employment of Nano-technology and new techniques of stability.

Deflectometric Studies:

LWD, a dynamic stiffness device, has recently picked up steam as a portable and affordable tool for determining in-situ reactions such as deflections and surface modulus on thin bound and unbound layers(Guzzarlapudi, Adigopula and Kumar, 2016). The in-situ interactions were investigated using a popular method known as back calculation to estimate layer moduli. These in-situ responses were also utilized to predict the residual life of in-service pavement and define alternative maintenance techniques such as overlays, among other things. By analysing in-situ compacted stiffness, LWD devices can also be utilized as a quality control/quality assurance and structural evaluation tool. However, in India, the use of LWD for structural evaluation is restricted to low volume roads(Guzzarlapudi, Adigopula and Kumar, 2016) like PMGSY Roads.

CHAPTER 2
LITERATURE REVIEW

2.1 Literature review on Cement Treated Sub-base

Prabakar et al., (2004), in his paper discussed the type of foundations varies based on the availability of soil strata and the expense involved. Using varying amounts of fly ash ranging from 9 to 46 percent by weight of soil, three different soil types were evaluated. The primary objective is the usage of fly ash as a soil additive with an emphasis on improving soil engineering properties so that it can take more load from foundation structures. This research also supports the efficient use of fly ash as a cost-effective way to improve soil qualities. The current research focuses on soil characterization, fly ash behaviour, compaction, settlement, the California bearing ratio, shear strength parameters (C and φ), swelling characteristics, etc.

Al-Rawas et al., (2005) in his study discussed stabilization of expansive soil using lime, cement, combinations of lime and cement, Saroj (artificial pozzolan) and heat treatment. The untreated soil's chemical and physical qualities were first determined. The soil was then mixed with 3%, 6 %, and 9 % dry weight of lime, cement, and Sarooj.The soil was also combined with varying concentrations of lime (3 percent and 5%) and varied quantities of cement. The treated samples' physical results were determined. For comparison, untreated soil values were employed as a control point. With the addition of 6% lime, both the swell percent and the swell pressure were lowered to zero. Swelling potential was decreased to zero after a heat treatment. When compared to the other stabilizers, lime produced better outcomes.

Zabielska et al., (2008) in his paper discussed the use of power-industry wastes as a material for earthen structures depends on its compactibility. It has been proven that a fly ash/bottom ash mix crushed multiple times in Proctor's moulds is not representative. The connection between dry density of solid particles and water content was found for re-used waste samples. The impact of re-compaction on grain size distribution, solid particle density, specific surface, and sand equivalent of wastes was studied. Fly ash samples compacted using the Standard and Modified Proctor techniques were tested. Another objective of the research was to see if how cement additives affected the compactibility of a fly ash/bottom ash combination. To acquire compactibility curves, waste samples in their normal form and

with varied percentages of cement additives (2, 5, and 10%) were compacted using both impact compaction methods. It was discovered that adding cement enhanced the ρd max value while decreasing the optimum water content. After cement stabilization, linear regression connections for changes in compaction parameters are also provided.

Brooks, (2009), aims to improve expansive soil as a construction material by using flyash and materials such as rice husk ash (RHA). Strength experiments were conducted using remoulded expansive clay mixed with RHA and flyash. The use of a RHA-flyash blend as a swell reduction layer between a foundation's footing and the subgrade was investigated. To assess the study's significance, a cost comparison was done to prepare a roadway project's sub-base with and without admixture stabilizations. When the flyash content was increased from 0 to 25%, the failure stress and strains increased by 106 percent and 50%, respectively, according to the stress-strain behaviour of unconfined compressive strength. Unconfined Compressive Stress increased by 97%, but CBR improved by 47%, when RHA concentration increased from 0 to 12%. As a result, a 12 percent RHA content and a 25% flyash percentage are advised for fortifying the expansive subgrade soil. Because of its good performance in laboratory tests, a flyash content of 15% is recommended for blending into RHA to produce a swell reduction layer.

(Prasad, et al., (2011) worked on the increasing costs of conventional cconstruction materials and their depletion, resulting in the need to adhere to sustainability, alternative construction techniques, etc. Soil has been used worldwide to construct flexible pavements, etc. Many methods have been tried to improve the soil characteristics.

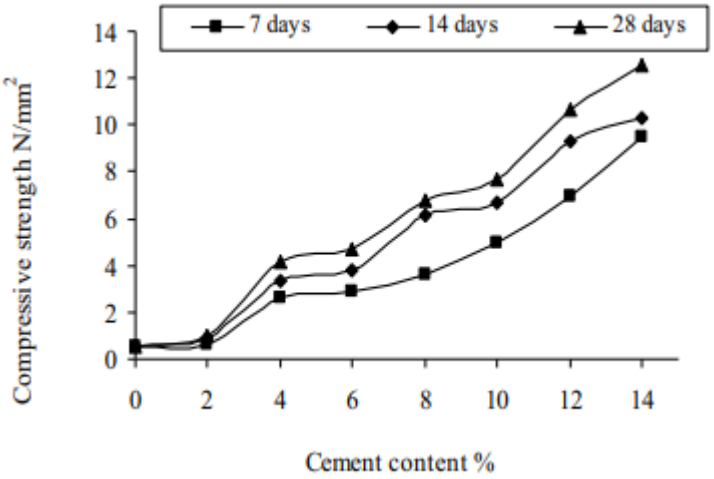

Figure 2.1: Compressive strength vs cement content

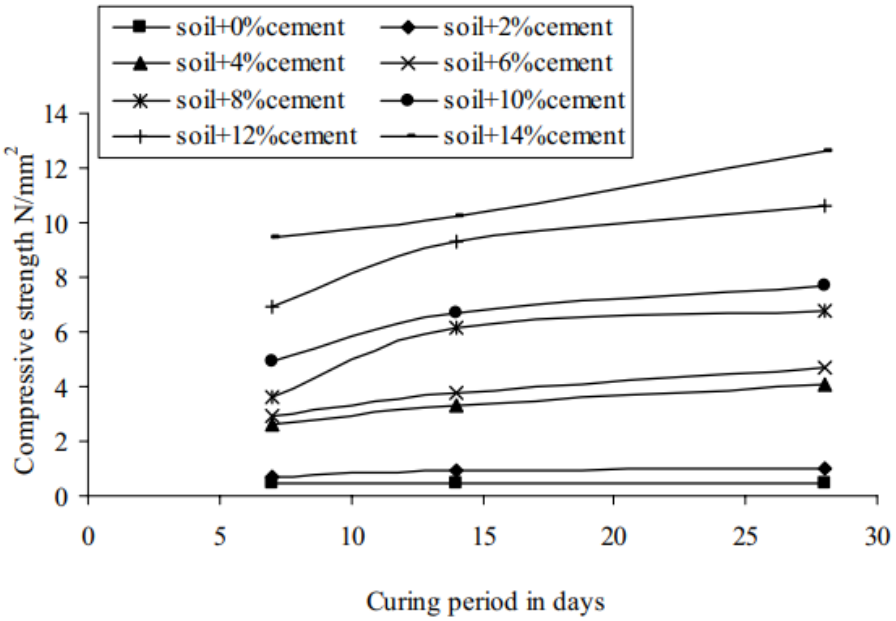

Figure 2.2: Curing days vs strength

In the present, comprehensive laboratory work is carried out to study the compressive strength characteristics of Cement stabilized gravelly soil from tests on cubes with cement content varying from 0-14% by weight after 7,14 and 28 days of curing. The strength is also assessed in terms of CBR values after 7and 14 days of curing. The compressive strength of cubes at 28 days for 10 and 12% cement stabilized soil are obtained in the range of M7.5 and M10 grade cement concretes. The results of study indicated the good potential of Cement stabilized gravelly soil in preparation of low-grade concrete for foundation beds of buildings, gravity retaining structures and pavements.

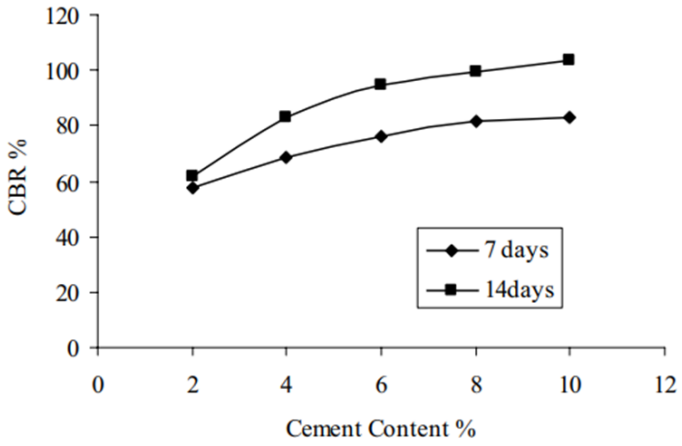

Figure 2.3: Variation of CBR for different cement proportions

Consoli, et al., (2011) in his study aims to assess the strength controlling parameters of a fine-grained soil moulded at three distinct water contents. In this research the primary work was to show that the effect of diverse soil structures formed during compaction of fine-grained soils at distinct water contents, The porosity of the specimens and the amount of

cement injected into them are critical factors in determining the goal strength of such materials. Water content (ω), cement content (C), porosity (η), and the porosity/volumetric cement content ratio (η/C_{iv}) were the regulating parameters studied. The current study included a number of unconfined compression tests. For the studied silt–cement mixtures, the results show that a linear function fits the unconfined compressive strength (q_u)–cement content (C) relationship for each specific water content studied, the strength (q_u) increases exponentially with the reduction in porosity (η), and a power function fits the strength (q_u)–porosity/volumetric cement content ratio (η/C_{iv}) relationship. Finally, a unique relationship may be established between the examined fine-grained soil's unconfined compressive strength (qu) and moulding water content (ω), porosity (η) and volumetric cement content (C_{iv}).

Samal, et al. (2012) worked on stabilizing Black Cotton (BC) soils, which are highly clayey in nature, by using Lime and Fly ash, which are used to improve the moisture changes and compressibility plasticity nature of those soils. This paper includes the evaluation of soil properties like Optimum moisture content, dry density and strength parameter (California Bearing ratio value). Various quantities of Lime and Fly ash (% by weight) are added to the BC soil and experiments are conducted on these soil mixes. The results show that the use of Lime and Fly ash increases the CBR values, i.e., soil strength to a great extent.

Patil, et al. (2013) deals with the effect of industrial waste like fly ash, pond ash, etc. and chemical additives like RBI. Grade 81 on the CBR value of soil. The CBR value of mix with different proportions of RBI. Grade 81 was determined. The RBI. Grade 81 was added in 2%, 4%, and 6% by weight of soil. The results show that the CBR value of treated soil with 2% RBI. Grade increases by 91.01%. The CBR result for untreated soil is 2.56% and for that of treated soil is 12.74% (with addition of 40% of pond ash and 4% OF RBI 81). The increase in CBR is 397% more than untreated soil. There is a slight increase in the soaked CBR value of soil with the addition of industrial wastes and when these are incorporated with RBI grade 81 there is a considerable increase in the CBR Another aim of the paper is to reduce the construction cost by using RBI 81 which uses regionally available soil.

Madurwar et al., (2013) investigated the result of using RBI 81 to stabilize red soil, kaolinite & laterite soil. This study showed that with the addition of RBI 81 grade, both soaked and un-soaked CBR increased significantly for kaolinite, red & laterite soil. In this experiment, different percentages of RBI 81 i.e. (0%, 2%, 4%, 6% & 8%) were used and 1% water content at OMC was added for the specimen preparation. C.B.R. tests were performed on

those samples which were cured for 0, 7 & 11 days. CBR test on sample cured for 11 days was performed after soaking for 4 days. After all experiments, the study concluded that soaked CBR increased by 16, 14, 4 folds with an optimum percentage of RBI 81 for red soil, lateritic and kaolinite respectively.

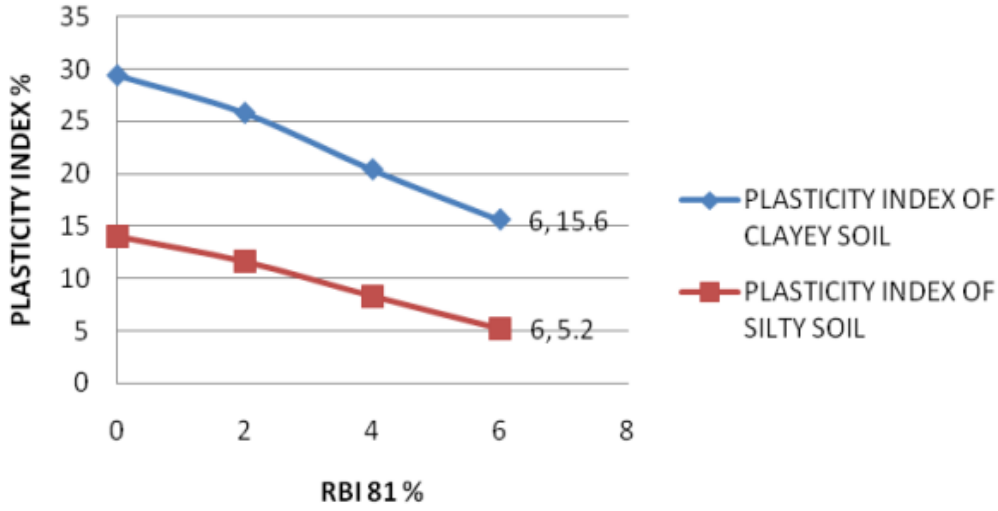

Figure 2.4: Variation RBI % and plasticity index

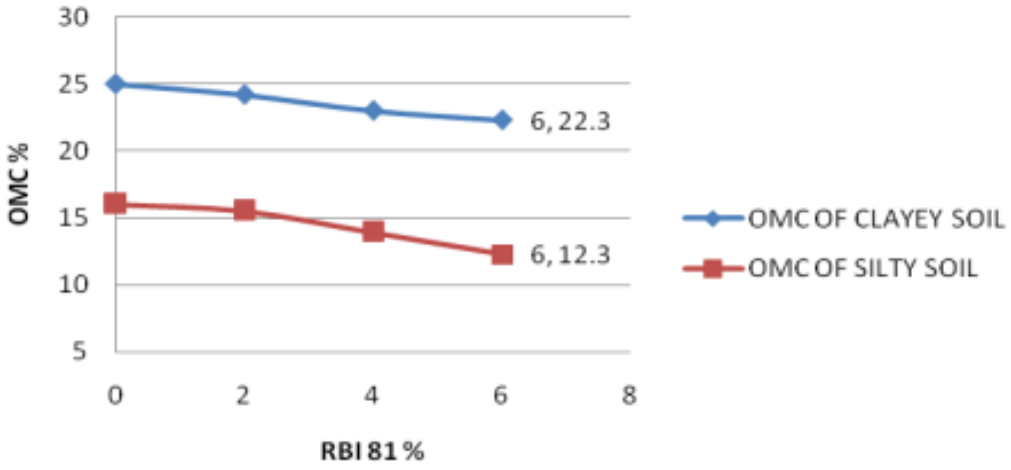

Figure 2.5: Variation RBI % and Optimum moisture content.

Pancholi, et al. (2015) , highlighted in his paper, that it is always advisable to use the regionally available soil and materials. In the case of their unsuitability, soil should be treated with chemical stabilizers so that the properties are corrected as per the design requirements. Terrasil was utilized as a stabilizer for altered measurement, i.e. 0.041% by dry aggregate weight of soil test. With the addition of 0.041% Terrasil, the soil's liquid limit and plastic limit decreases. For treated soil, the film of adsorbed water is reduced thereby reducing

swelling capacity. The results concluded that the permeability values decreased and the thickness reduced by about 25% when the soil was treated with 0.041% of Terrasil.

(Shooshpasha, et al. (2015) in his paper studied the effects of cement stabilization on the geotechnical characteristics of sandy soils. Lime Portland cement was used as a stabilizing ingredient in percentages of 2.5, 5, and 7.5 percent by dry weight of the soils. The interpretation of findings from unconfined compression testing and direct shear tests is used to provide a mechanical examination of the soil. For unconfined compression and direct shear tests, cylindrical and cube samples were manufactured at optimum moisture content and maximum dry unit weight. After being cured for 7, 14, and 28 days, the samples were analyzed. According to experimental examinations, the use of cemented specimens improved strength parameters, reduced displacement at failure, and transformed soil behaviour to a detectable brittle behaviour.

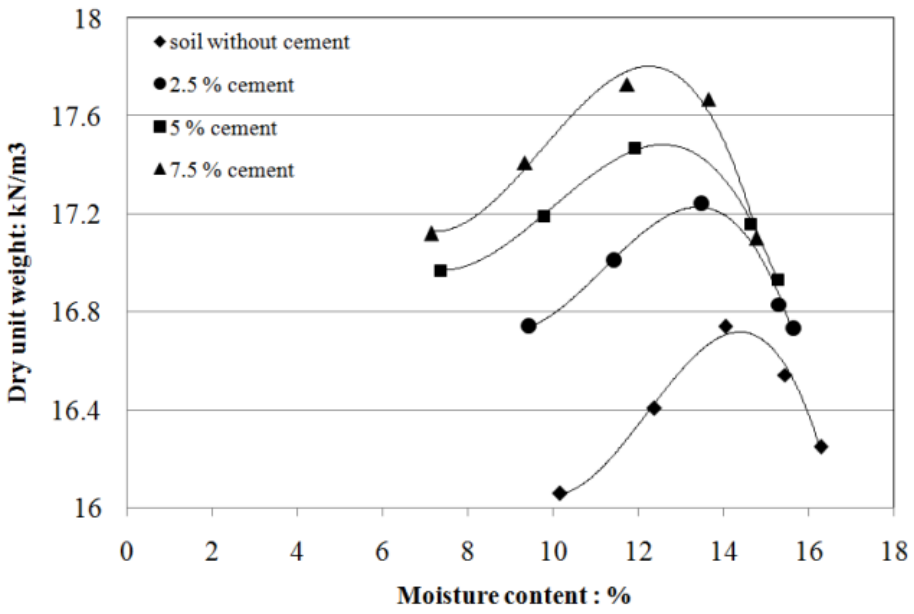

Figure 2.6: Compaction curve for mixes with different cement proportions

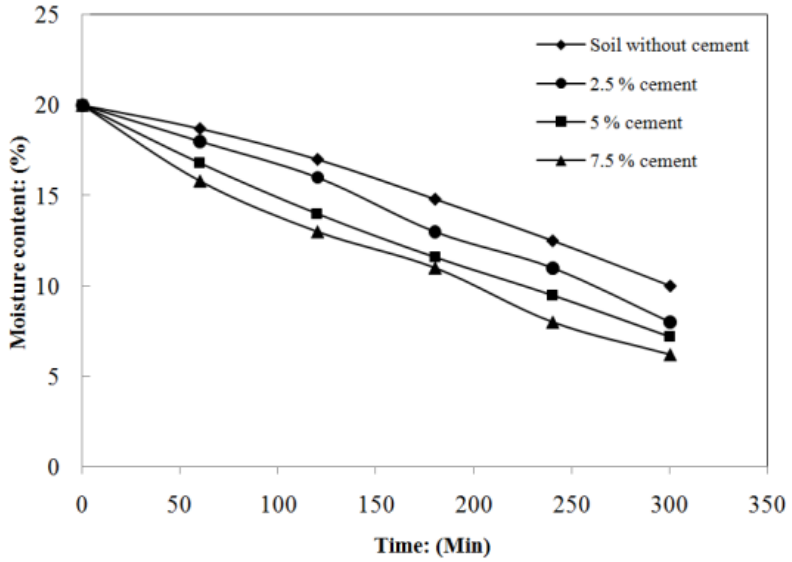

Figure 2.7: Solidification of sandy soil with different proportions of cement.

Patel, et al., (2015) worked to focus on soil engineering properties (with and without stabilizer: standard compaction; four days-soaked California Bearing Ratio (CBR), permeability test and cyclic loading test according to codal procurement. A concoction: Terrasil was utilized as stabilizer for altered measurement i.e. 0.041% by dry aggregate weight of soil test according to the convention of Zydex Industries, Vadodara. Test outcome showed that designing properties got modified and CBR on stabilized clayey samples increased considerably. Also the expense is reduced, which profits the engineers, pavement designers, etc.

Patel, et al., (2015) et al. investigated natural soil to determine physical and engineering properties based on Indian standards (1948-1970) and property changes caused by Terrasil and Zycobond expansion as a stabilizer. Another fundamental goal was to investigate the transformation of the soil index properties of untreated weak local soil and limit the volume change potential of a highly plastic soil by using dosages as stabilizers (Terrasil + Zycobond). The study showed various tests like liquid limit, Plastic limit, Free swell index and CBR that were carried out as per Indian standards.

GVLN Murthy et al. (2016) worked out that the solution to pavement deterioration is the treatment of soil with chemical stabilizers. The paper showed that in silty clay soils, the engineering properties are improved by adding chloride salts like NaCl, MgCl2, and CaCl2.

Chloride salts increase the maximum dry density (MDD) by decreasing the optimum moisture content (OMC). The effect of stabilization agent on compaction characteristics, consistency limits, and compressive strength is studied with different amounts of salts (15%, 20%, and 25%). The study concluded an increase in MDD and a decrease in OMC when the chemical compound percentage increases. Also, with an increase in additive content, the LL, PL, and plasticity index decrease. Furthermore, the UCS and bearing capacity of the soil increases as the quantity of chemicals is increased.

Ateş, (2016) researched the use of glass fiber-Portland cement as reinforcement to improve the structural and mechanical qualities of sandy soils. UCS tests were used to determine the soil's mechanical behavior. Glass fiber and cement added to sandy soils increased engineering attributes and mechanical strength, decreased displacement at failure, and made the soil more brittle. At a glass fibre concentration of 3%, maximum strength was achieved, whereas subsequent increases in glass fibre resulted in a drop in the mechanical characteristics of the cement and sandy soils.

Rathod, (2017) discussed in his paper about soil stabilization techniques for improving the strength of the in-situ soil especially in road construction, and one of the techniques is using chemical additive. Chemical improvement is a time-saving approach for improving the density and strength of subgrade, sub-base layer, and otherwise unsuitable materials in-situ, eliminating the need for costly excavation and replacement with borrow material. The results of the earliest stages of a study programme to explain the process and behavior of the liquid chemical and engineering characteristics of three natural residual soils at laboratory scale are presented in this paper.

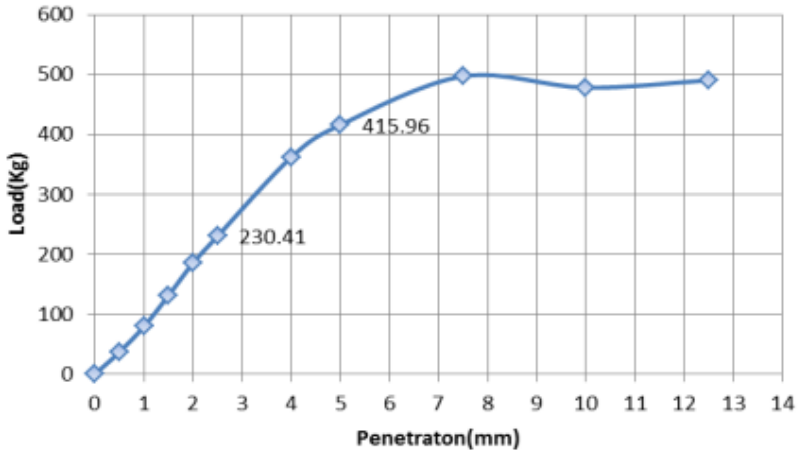

Figure 2.8: Compaction curve of Black cotton soil treated with Terracil

This study aims to improve the engineering properties of two natural residual soils that have been blended with various liquid chemical amounts. To assess the usefulness and

performance of this chemical as a soil stabilizing agent, a series of laboratory tests on engineering parameters, such as the Modified Proctor Test, consistency limits, moisture-density relationship (compaction), and California Bearing Ratio, were conducted.

Singh & Yadav, (2018) worked on improving various sub-grade soil properties by using soil stabilizer and locally available materials. They carried out the standard proctor test on treated and untreated soil samples. The soil was treated with different proportions of RBI 81 and moorum and tested for soaked CBR value, MDD, OMC, which resulted in the soil mix: RBI. Grade 81 in the proportion of 100:0, 98:2, 96:4 and soaked CBR values came out to be 2.56%, 4.89%, and 8.79%. For mix of soil-moorum the proportions of RBI grade 81 was 100:0:0, 90:10:0, 80:20:0, the soaked CBR values came out to be 2.56%, 2.41%, 2.84%. For another mix of soil: moorum, RBI 81 proportion of 78:20:2, 76:20:4, the soaked CBR values came out to be 4.56%, 14.76% respectively. This implies that the using moorum soil along with RBI 81 has a very good impact on the stabilization of subgrade soil and also the construction cost can be reduced to a great extent.

Buazar, (2019) studied the Impact of Biocompatible Nano silica on Green Stabilization of Subgrade Soils. The paper discusses the effect of green Nano silica additives (0.5, 1, 1.5, and 2% of the total dry weight) on soil subgrade. The preparation of Nano silica is studied and approved by ICP, TEM, FTIR, and XRD analysis and when produced, showed an amorphous structure with an average size of 20mm. Soil properties such as Atterberg limits, MDD, OMC, and shear strength of the treated soil were higher than untreated soil. The stabilized soil showed a rise in the angle of internal friction, cohesion, shear strength, Max Dry Unit Weight by factors of 2.17, 3.07, 2.21, and 1.5, respectively. The CBR strength of Nano silica-cured soil is 5.83 times higher than that of the original subgrade soil and the optimum Nano silica content came out to be 1.5%

Kumar et al., (2020) worked on Black Cotton (BC) Soil because of its unsuitability when it comes in contact with water, which is mainly due to its high expansive nature. The study worked on making the BC soil impervious and increase its bond strength. It concluded that the use of the chemicals Terrasil and Zycbond increases the bond strength between soil particles and by permanently changing the soil properties, it creates a protective layer. It also makes the soil feasible for most infrastructural projects by exponentially increasing its CBR value.

V. Padmavathi, (2020) worked on soil stabilization techniques to improve the base soil's strength and increase the resistance to softening when saturated by bonding the particles.

This study shows nano-materials like Terrasil, Zycobond and Cement as admixtures to improve the strength properties both at OMC and SMC conditions of a c-ϕ soil (SC) with 31% fines a plasticity index value of about 15%. The addition of Terrasil to the base soil developed water tightness. The strength properties were improved when Zycobond and Terrasil are used independently as additives and in combination with Cement. Paving blocks of size 19 cm × 23 cm × 10 cm prepared with 3% of Cement, Zycobond and Terrasil yielded uniaxial compressive strength of 1.28 MPa after 14 days of curing.

Singh et al., (2020). discussed the Efficacy of Cement Treated Base/subbase in his paper. Cement treated base/subbase (CTB/CTSB) refers to an intimate mixing of native soils with measured proportions of ordinary Portland cement (OPC) and water that hardens after compaction and curing to make a robust, durable, and frost resistant paving material. CTB/CTSB has the advantage of providing a stiffer and stronger basis than an unbound granular base. Furthermore, a wide range of in situ soils can be utilized, eliminating the requirement to transport low-cost chosen granular aggregates. According to this paper, the efficacy of CCS in powder and liquid form has been employed to improve pavement performance at 7 locations in and around Nashik, Maharashtra, India. These CCS fill up the gaps between soil particles, forming a flexible and impermeable connection. A thorough programme has been developed, including a preliminary site survey, pavement design using IITPAVE, experimental research on in situ soil with and without CCS, and field performance tests. 4 percent cement as a source of CaO and 750 ml/cum of CCS in liquid form, and 9.8 percent cement and 0.2 percent CCS in powder form are used in the proposed design mix. The compressive strength and durability of the CCS are assessed to determine its efficacy. Actual construction work is carried out on site based on the results of the laboratory inquiry, and field performance tests such as fast moisture meter, dynamic cone penetrometer, sand replacement, and so on are carried out to guarantee quality is maintained on the job site. According to the investigation findings, the current bad conditions and difficulties in the pavement stretch have been resolved, and the cement loss is well within acceptable limits. The use of commercial chemical stabilizers can thereby improve pavement performance (CCSs). However, comprehensive laboratory testing is recommended to determine the best amount for pavement stability.

Zahoor & Jassal, (2020) replaced regionally available materials and increased properties such as soil strength and load carrying capacity. Using Terrasil and Zycobond, made by Zydex industries, as a replacement for soil stabilization. also leads to an increase in soil particle bondage, CBR and decreased swellingg. This chemical (Terrasil and Zycobond) mixes with

water and is sprayed on the subgrade which helps the soil particles to get compacted upto 200mm . Also, it is sprayed at the top of the subgrade to make the soil water repellent and reduce permeability to 10-7 to 10-8 cm/sec.

Table 2.1: Chemical composition of Terracil

Chemical Compound	Value in range, %
Hydroxyalkyl- alkoxy-alkylsilyl	65-70%
Benzyl Alcohol	25-27%
Ethylene glycol	3-5%

Raghwa & Sonthwal, (2021) discussed to reduce the cost of soil stabilization by using cheap and easily available materials like Terra-zyme and Fly-ash, which are the waste products of industries. These materials are used to facilitate several soil properties, like having a very drastic impact on the strength characteristics of the soil. A concoction of Terra-zyme and Fly-ash greatly reduces the construction cost.

2.2 Literature Review on Deflectometric Studies

Montepara et al., (2012) discussed that there are two methods for recycling reclaimed asphalt pavement (RAP) in pavement engineering: hot recycling and cold recycling. Another option for the sub-base layer is to combine it with natural aggregates. The preliminary findings of a research effort conducted on a test track created specifically to investigate the impact of a sub-base layer mixture including 50% natural aggregates and 50% RAP on pavement performance are presented in this paper. The research is based on LWD and FWD analyses, with results compared to those obtained on the next segment of the test track, which is constructed entirely of natural aggregates.

Guzzarlapudi et al., (2016).On a low-volume road, static and dynamic deflection methods using lightweight deflectometer and traditional Benkelman beam deflectometer are used to compare subgrade moduli. Field and laboratory tests are conducted at 40 test locations over a 2-kilometer stretch of in-service road that contains three types of cohesive soils (CH, CI, and CL). The static and dynamic reactions of the pavement are calculated to determine the static, back calculated, and composite moduli of the subgrade. The back calculated and composite moduli of the subgrade are confirmed using repeated triaxial tests at a specified moisture content. The composite and laboratory moduli of subgrade are approximately consistent with 2 percent to 7 percent variation, respectively. Static modulus values are on

the lower side when compared to dynamic moduli values, whereas the composite and laboratory modulus of subgrade are on the lower side when compared to dynamic moduli values. Correlation investigations of static and dynamic moduli of various types of subgrade soils reveal an excellent correlation of determination (R2) that ranges from 0.75 to 0.91. Validation of static moduli with California bearing ratio (CBR) related subgrade moduli indicates a moderate correlation of 0.67 to 0.74 for different types of soils, however dynamic moduli shows an excellent correlation of 0.74 to 0.93. As a result of the comparison, the lightweight deflectometer delivers reliable subgrade moduli values and can be used as a rapid instrument for measuring subgrade strength on low-volume highways.

Singh et al., (2020) discussed in comparison to conventional layers, cement stabilization in granular material is an excellent technology for increasing the rigidity of base and sub base layers while also reducing their thickness. Furthermore, in the short and long term, cement base layers can improve the fatigue behaviour of asphalt surface layers and subgrade rutting. No performance data for CTB and CTSB layers in in-situ settings is available in our country. The resilient modulus (M_R) of stabilized pavement layers is investigated in this work using field data collected on in-service flexible pavement sections, which may be relevant for design purposes. In this study the major part was to compare M_R values for cement stabilized layers utilizing non-destructive methods such as the Falling Weight Deflectometer (FWD) and destructive methods such as cores. The field data was gathered along the State Highway (SH) and the Major District Road (MDR) in the Lucknow, Uttar Pradesh area. During field assessments, no visual discomfort was noticed on either of the road sections. Two 500-meter-long study sections on SH and one on MDR have been identified for the study. The in-situ cores were collected from CTB and CTSB layers and examined for MR values using Unconfined Compressive Strength (UCS) according to IRC:37-2018. For the CTB and CTSB layers, FWD deflection data was used to determine M_R values using back calculation software. Furthermore, test pits on the existing pavement were used to establish the thickness and qualities of each layer.

2.3 Micro structural analysis

Guefrech et al., (2011) The characteristics of cement mortars containing nano-SiO2 were investigated experimentally. The primary component of a pozzolan, amorphous or glassy silica, combines with calcium hydroxide produced by calcium silicate hydration to yield calcium hydroxide. The amount of surface area accessible for reaction determines the rate of the pozzolanic reaction. As a result, adding nano-SiO2 particles to high-performance concrete

is a possibility. Nanoparticles of silica amorphous were included at a rate of 3 and 10% by weight of cement to evaluate the impact of adding nanoparticles on the behaviour of pastes and cement mortars. The compressive strength of various mortars increases as the amount of nano-SiO2 increases. The impact of nano-SiO2 on consistency and reliability

Nima et al., (2012) looked at a variety of changes that have occurred as a result of technological improvement. High-performance concrete is the most recent type of concrete available, and it uses a variety of chemical and mineral admixtures to improve mechanical and durability properties. As the importance of sustainability became more apparent in the concrete industry, many researchers focused on micro-sized mineral admixtures such as silica fume, fly ash, rice husk ash, slag, and other admixtures to replace Portland cement, which is responsible for nearly 7% of carbon dioxide emissions into the atmosphere. Scientists have recently been able to analyze nanoscale admixtures and their effects on concrete structure thanks to advances in technology. This research examines nanomaterials in cement composites and how they can help concrete achieve better characteristics.

Stefanidou, et al. (2012) discussed the evolution of nanotechnology offers materials with new qualities, and a lot of work has been put into introducing nanoparticles into cement pastes in order to improve their properties and produce better performing materials in recent years. Nano-SiO2 generated by pyrolysis with a specific area of 200 m2/g was added to high-strength cement pastes at various percentages (0 percent, 0.5 percent, 1 percent, 2 percent, and 5 percent) in the current study. At various ages, the mechanical and structural properties of these pastes were evaluated. Large, idiomorphic crystals of Ca–Si composition were generated as a result of nanoparticles acting as nuclei for crystallization, assisting in the production of materials with dense structure, reduced porosity, and improved strength up to a specific percentage.

Farzadnia et al., (2013) studied the use of clay in cement composites and found that it improved the characteristics of concrete. However, little is known about nanoclays and their impact on cement composite mechanical characteristics and durability. Halloysite nanoclay is one of the nanoclay subcategories that has been unfairly overlooked in the manufacture of cement composites. The outer surface of the halloysite nanotubes possesses SiO2-like properties, while the inner cylinder core has Al2O3-like capabilities, which together may improve the cement matrix. The mechanical characteristics, flowability, thermal behaviour, and durability of mortars containing 1, 2, and 3% halloysite nanoclay were studied

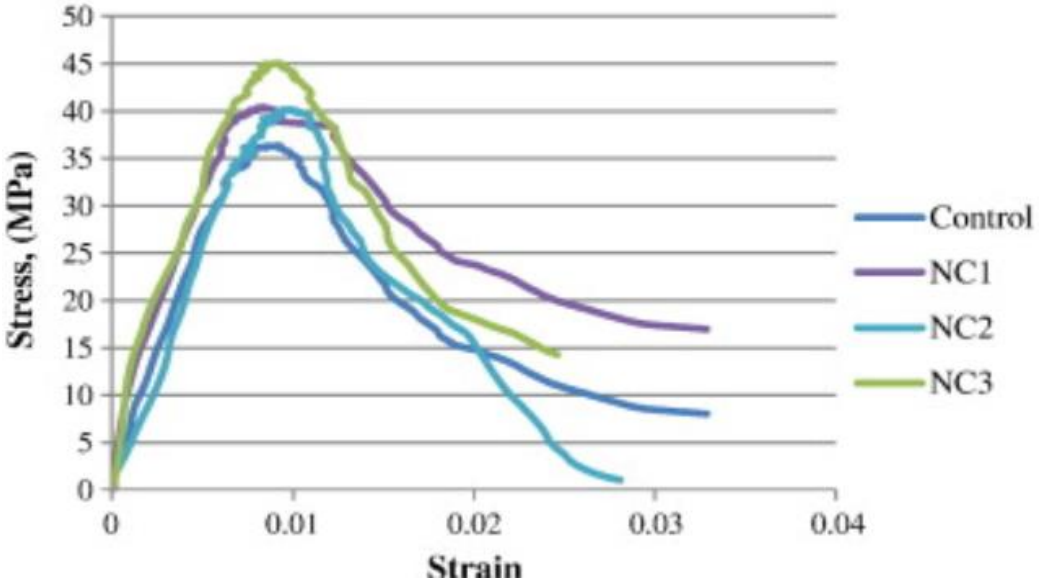

Figure 2.9: Stress strain for different mixes.

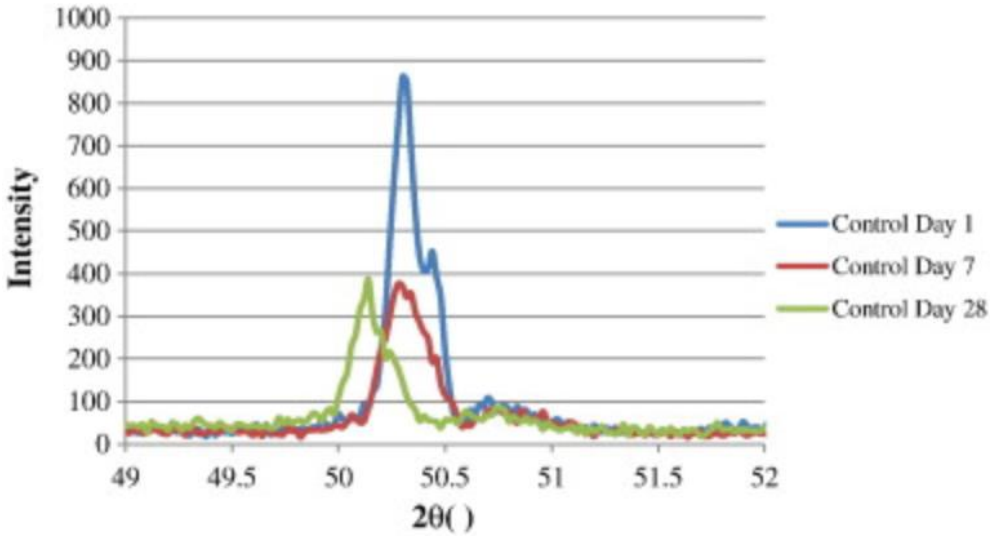

Figure 2.10: Intensity and 2theta variation for different mixes

Samples with 3 percent and 2 percent nanoclay enhanced their compressive strength and gas permeability by 24 percent and 56 percent, respectively. The microstructure and chemical content of samples containing halloysite nanoclay were investigated using SEM, XRD, and DSC testing.

2.4 Objectives:

The key objectives of the study are:

- To determine the optimum percentage of cement and chemical for the stabilization of the sub-base layer.
- To study the engineering properties and effectiveness of the stabilized mix.
- To perform field performance evaluation for chemically based cement treated sub-bases using light weight deflectometer.
- To Analyse and design the most effective/economical section for low volume roads.
- To analyse the microstructue of the mix by SEM and XRD.

2.5 Outline of the thesis:

The thesis is divided broadly into six chapters. Chapter I gives the basic introduction of stabilization and cement-treated sub-bases. The second chapter is the literature review, in which the previous research work regarding sub-base stabilization is mentioned. The methodology and experimental programme are discussed in full detail in Chapter III. The chapter IV has the results and discussions of all the experiments we performed in chapter III. 5th chapter comprises the analysis and design of the pavement section using the mix design prepared in the lab.

CHAPTER-3

METHODOLOGY AND EXPERIMENTAL PROGRAM

3.1 Methodology

This chapter will discuss the procedure that was followed throughout the entire study. The process was carried out in steps, beginning with material selection, testing, and then mix design. The casting process was conducted when the mix design was completed, and the casted samples were then tested in the laboratory. A similar mix design was created on the field, and testing was conducted to compare lab and field results. The flowchart representing the process is shown in the figure below,

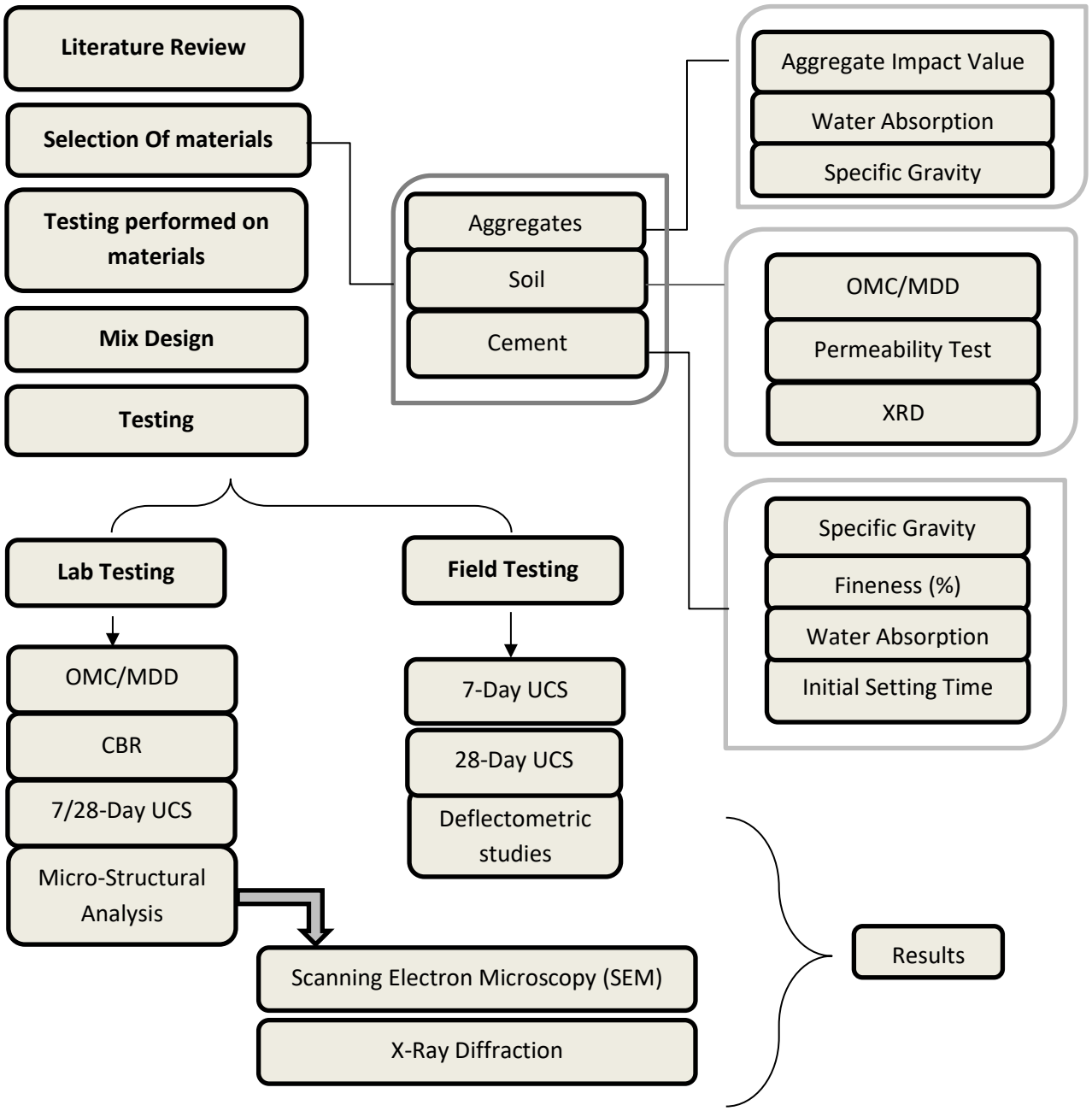

3.2 Materials Used

3.2.1 Coarse Aggregates:

Aggregates are a necessary component of every pavement. Aggregates are utilized as a stabilizing ingredient for each pavement layer to carry severe traffic loads. The aggregates are examined in accordance with MoRTH norms and IRC codal criteria. The aggregates employed in this research are 40mm, 20mm, and 10mm in size. The following tests are used to assess the quality of the aggregates used in the study.

Figure 3.2: Different sizes of Aggregates

Table 3.1 Physical properties of Coarse Aggregates.

S. No.	Properties	Tests	Description (Max %)	Relevant IS-codes
1	Strength	Los Angeles Abrasion Value	35%	IS:2386 Part IV
		Aggregate Impact Value	27%	
2	Durability and other Parameter	Soundness	12%	IS:2386 Part V
		Water Absorption	2%	IS:2386 Part III
3	Grain size Analysis and particle shape	Combined Flakiness and elongation Index	35%	IS:2386 Part I

a. Aggregate Impact Value (AIV)

This test method has been followed as per IS-2386 Part IV. The AIV test provides the aggregate strength results value under impact loading conditions. With this property, the toughness of the aggregates is defined to resist the impact load. The maximum allowable value is 18%.

Table 3.2 AIV values for different aggregates.

S.No.	Aggregate Type	(AIV)
1	40mm aggregate	13.5
2	20mm aggregate	15.3
3	10 mm aggregate	22.8

Table 3.3 Aggregate Impact value Classification.

Aggregate Impact Value (%)	Classification
<20	Exceptionally Strong
10-20	Strong
20-30	Satisfactory for road surfacing
>35	Weak for road surfacing

Specified limits of percent aggregate impact value for different types of road construction by Indian Roads Congress is given below

Table 3.4 Type of pavement vs Max AIV

Type of pavement	**Aggregate impact value not more than (%)**
Wearing Course	30
Bituminous surface dressing	
Penetration macadam	
Bituminous carpet concrete	
Cement concrete	
Bitumen bound macadam base course	35
WBM base course with bitumen surfacing	40
Cement concrete base course	45

b. Water absorption

The aggregate's absorption capacity is the maximum amount of water it can absorb. Water absorption provides information about the aggregate's interior structure and strength. Aggregates with higher absorption are porous in nature and are normally deemed undesirable until strength, impact, and hardness testing show that they are acceptable. The method has been followed as per IS-2386 Part 3. The maximum value for water absorption test is allowed is 2%. All the tests were in accordance with IS-2386 part 3.

Table 3.5 Type of aggregates and corresponding Absorption values

Aggregate type	**Average Absorption Values**
40mm Aggregates	0.39
20mm Aggregates	0.48
10mm Aggregates	0.61

.

c. Toughness and abrasion resistance

Aggregates have shown to have good toughness and abrasion resistance, allowing them to withstand breakdown during construction and after paving in traffic. The aggregates will burst out of the pavement if they break down, resulting in a fractured road surface. As a result, the maximum impact value is 27%, and the maximum loss abrasion value is 35%.

d. Specific Gravity of Aggregates

The specific gravity of coarse aggregates is described because the weight of aggregates dried to a regular weight in an oven at 100°C divided with the aid of using absolutely the quantity of the mixture particles, along with natural voids, within the aggregate particles, according to the IS: 2386 (Part III).

Table 3.6: Aggregate size and bulk specific gravity.

S.No.	Aggregate Size	Bulk Specific Gravity
1	40mm	2.76
2	20mm	2.7
3	10mm	2.62

3.2.2 Fine Aggregate (Soil)

In this study, soil from Punjab's Chowkiman district was used. The physical parameters of this soil were determined using standard protocols indicated in BS 1377-2, including specific gravity, direct shear test, and particle size distribution. The particle size distribution curve of soil is depicted in the figure 3.4. The soil is described as Poorly graded sand with silt (SP-SM). The optimal moisture content (OMC) and maximum dry density (MDD) are 1.87g/cc and 9.30 percent, respectively. A characteristic X-ray diffraction (XRD) plot of the soil, shown in figure 3.5, indicates that the soil is classified as poorly graded sand with silt.

Figure 3.3: Soil (Fine Aggregates)

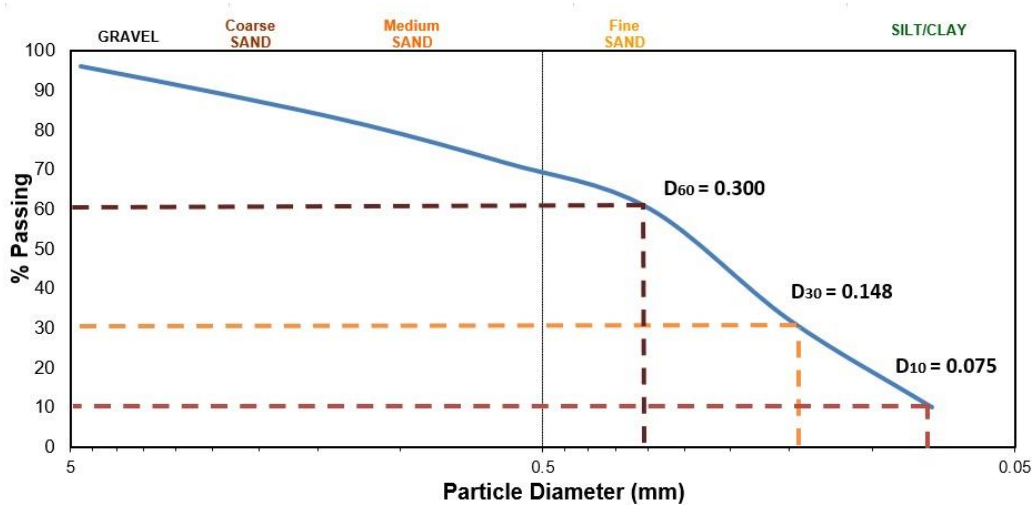

Figure 3.4: Grain size distribution curve

If the percentage of fineness is in between 5% and 12% dual notation is used, both the gradation and type of fine-grained soil is indicated.

Coefficient of uniformity, Cu= D_{60}/ D_{10} = 4.225

Coefficient of curvature, Cc= D_{30}^2/ ($D_{60} * D_{10}$) = 1.02

Classification of Soil = SP-SM (Poorly graded sand with Silt)

Table 3.7 Properties of the soil

Natural water content (%)	3
Compaction properties	
Maximum dry density (g/cc)	1.87
Optimum water content (%)	9.30
Specific gravity	2.48
Soil classification	SP-SM
Chemical properties	
Silica (SiO_2) (%)	70.23
Alumina (AL_2O_3) (%)	16.13
Iron oxide (Fe_2O_3) (%)	5
Potash (K_2O) (%)	1.4
Magnesia (MgO) (%)	0.15
Loss in ignition (%)	1

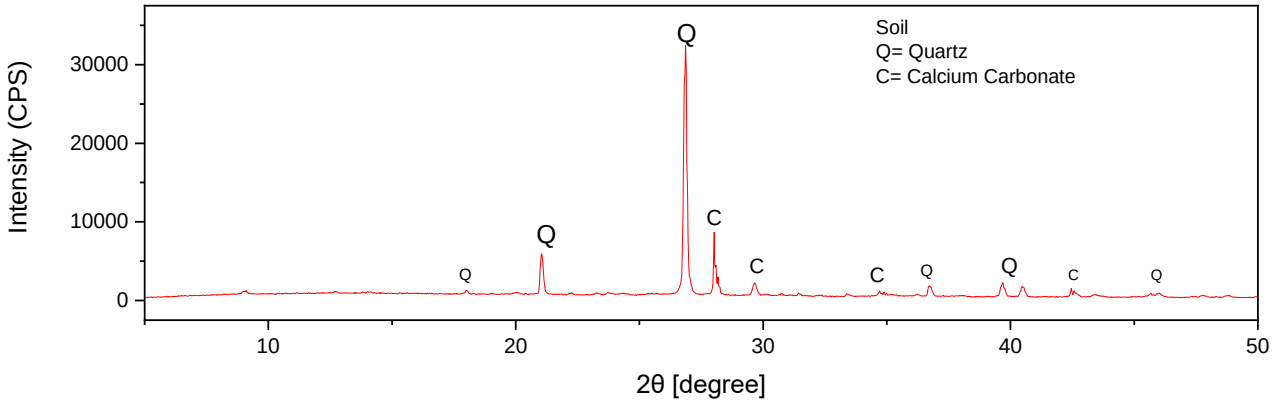

Figure 3.5: XRD of Soil

3.2.3 Cement

An ordinary Portland cement of Grade 43 in compliance with IS-8112 obtained from the Cement manufacturing company in Patiala was used in the study. The different properties of the Cement are given in the table below. The specific gravity of the Cement is 3.12 g/cm^3.

Table 3.8 Properties of the Cement

Physical properties	
Specific gravity (g/cm^3)	3.12
Fineness (%)	3
Water absorption (%)	0.41
Initial setting time (min)	30
Chemical composition	
Silica (SiO_2) (%)	22.3
Alumina (Al_2O_3) (%)	5.4
Iron oxide (Fe_2O_3) (%)	3.23
Calcium oxide (CaO) (%)	54.32
Potash (K_2O) (%)	1.02
Magnesia (MgO) (%)	2.9
Sulphur trioxide ($S0_3$) (%)	1.8
Sodium oxide (Na_2O) (%)	0.22
Loss on ignition (%)	1.9

3.2.4 Nano-Chemicals

a. Terracil:

It's an organ-silane molecule that combines with soil particles to change them from water-loving (Hydrophilic polar) to water-hating (Hydrophobic non-polar) particles. This makes the soil less water-sensitive and allows it to be compacted for greater soil particle interlocking. It provides or develops a permanent water-resistant Nano-coating on all types of soils, aggregates, and other surfaces. Because it chemically bonds to surfaces indefinitely, this siloxane is non-leachable. It generates a strong covalent link structure that allows the treated material to breathe, allowing air to flow through its structure while maintaining thermal insulation freely. Terrasil prevents damage due to the rise of water(capillarity), cracking of soil, and resistance to ultraviolet rays. It is highly soluble in water. (Padmavathi et al., 2018)and (Shirahatti et al., 2016) explains the chemical action of Terrasil and surface silicate structure after Terracil reaction. The chemical action of Terracil is shown in figure 3.6

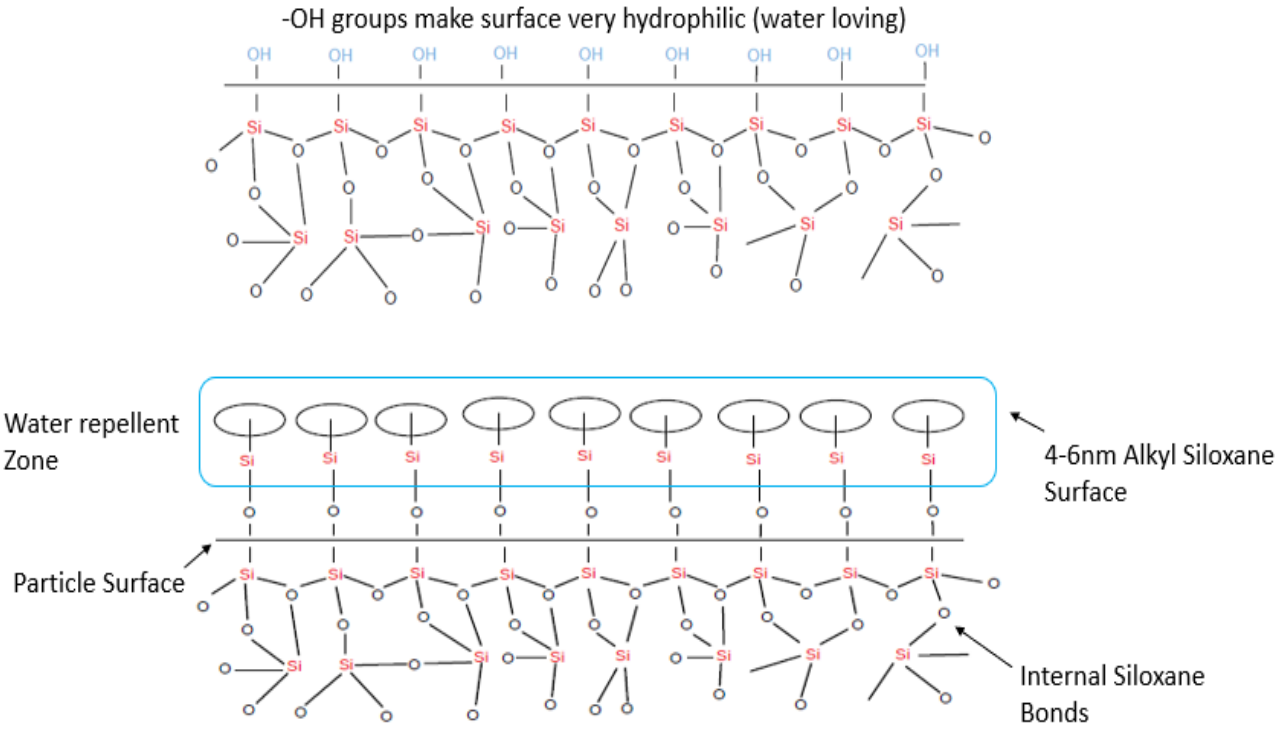

Figure 3.6: Chemical action of Terracil

Table 3.9: Physical and chemical properties of Terracil

Physical State	Liquid
Colour	Pale Yellow
Odour	Slightly Aromatic
Boiling Point	Approx. 200^{o}C
Flash Point	90^{o}C
Density	1.04g/ml
Solubility	Miscible with ethanol, methanol, alcoholic
Viscosity	100-500 cP @ 25^{o}c
Explosive property	Non-Explosive
Oxidizing Property	Non- Oxidizing

Figure 3.7: Terracil

a. Zycobond:

Zycobond is a next-generation co-polymer acrylic and nanotechnological additive. It's best used for soil stability, topical irrigation, and surface layer sealing as a rolling and dust treatment. It's a Nano polymer having particles that are less than 90 nanometres in size. It disperses in the soil, bonding the soil particles and providing erosion resistance, dust control, and fatigue resistance. Terrasil combined with Zycobond gives the soil strong bonding characteristics and provides long-term erosion control. Terrasil bonding are durable and long-lasting, and because they resist UV degradation. Properties of Zycobond is shown is the table below,

Figure 3.8: Zycobond

Table 3.10: Physical and chemical properties of Zycobond:

Physical State	Liquid
Colour	Translucent
Odour	Faint Odour
pH	Approx.5.0-5.6
Boiling Point	Approx. 100^{o}C
Flash Point	>70^{o}C
Density	1-1.02g/ml
Solubility	Partly Soluble
Viscosity	20-200 cP @ 30^{o}c
Incompatible Materials	Metal salts
Oxidizing Property	Not fire propagating

3.3 Mix Design

Cement-Treated Sub-Base (CTSB) is a type of Soil-Cement that describes an intimate mixture of native soils and/or manufactured aggregates with measured amounts of Portland cement and water that hardens after compaction and curing to form a strong, durable, frost-resistant paving material after compaction and curing. CTSB is versatile/adaptable because it can be blended in place and compacted thereafter, or it can be blended at a central facility and brought to the placement area, where it is spread on a prepared subgrade and compacted.

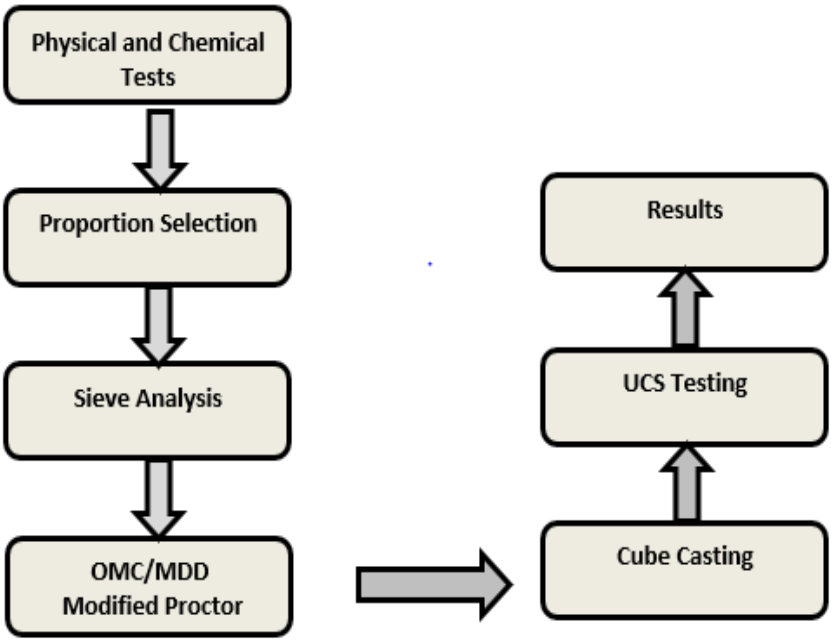

Figure 3.9: Flow Chart for mix design

3.3.1 Procedure for mix-design

1. The Physical and chemical testing of materials used in the CTSB like aggregate, cement, soil and water.
2. Selection of Proportion of Material like GSB, soil and cement (% weight) to form CTSB and the gradation is done using MoRTH table 400-4.
3. Sieve Analysis of final CTSB is done and compared with MORTH table 400-4 to check that the values are coming in range.
4. Then, Modified Proctor test is done to determine (MDD) and (OMC) of mix with cement content according to IS 2720 (Part 8).
5. Find Uniformity Coefficient as specified.
6. 10% Fines value is determined according to IS 2386 (Part 4)
7. Water absorption of material larger and less than 10mm in size is found out according to IS 2386 (part 3).
8. Then cubes are casted with the help of Vibratory Hammer (DLC- Hammer).

3.3.2 Sieve Analysis

The sieve analysis, often known as the gradation test, is a fundamental test that is performed to check the gradation of the material. In order to determine compliance with design, production control requirements, and verification criteria, the sieve analysis analyses the gradation (the distribution of aggregate particles by size within a particular sample). To mention a few applications, gradation data can be used to calculate relationships between

various aggregates or aggregate blends, assess compliance with such blends, and predict trends during production by graphically showing gradation curves. Sieve analysis is an excellent quality control and quality acceptance method when used in conjunction with other tests.

3.3.3 Gradation of aggregates

Aggregate Grading is a measurement of how evenly the sizes of the particles in an aggregate are spread. A well-graded aggregate will contain a wide variety of particle sizes and a good representation of each particle size. Blending numerous aggregates of various grades can change an aggregate's grading. The table below shows the gradation for 10 mm, 20 mm, and 40 mm aggregates.

Table 3.11 Average Percentage passing for 40 mm Aggregates.

IS Sieve size (mm)	Wt. of material retained (kg)	Cumulative wt. retained (kg)	Cumulative retained (%)	Passing (%)
53.00	0.00	0.00	0	100
37.50	0.150	0.15	3	97
19.00	4.094	4.244	84.88	15.12
9.50	0.726	4.97	99.4	0.6
4.75	0.00	4.97	99.4	0.6
0.600	0.00	4.97	99.4	0.6
0.300	0.002	4.99	99.8	0.2
0.075	0.001	5.00	100	0

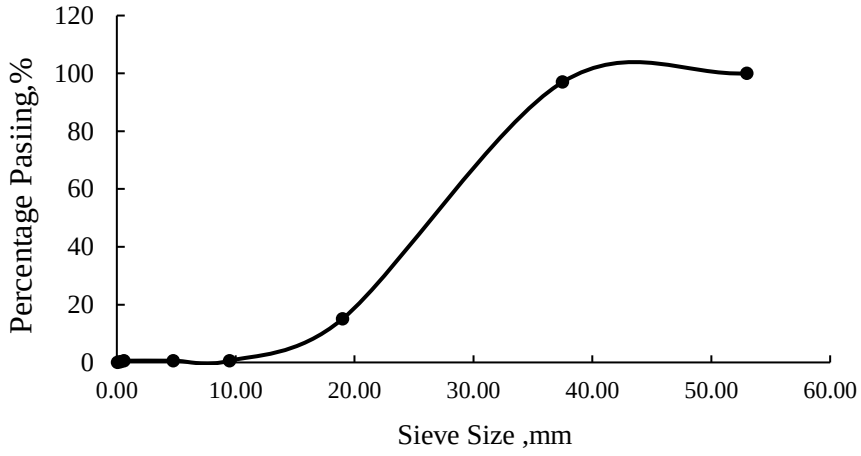

Figure 3.10: Gradation curve for 40mm aggregates.

Table 3.12: Average Percentage passing for 20 mm Aggregates

IS Sieve size (mm)	Wt. of material retained (kg)	Cumulative wt. retained (kg)	Cumulative retained (%)	Passing (%)
53.00	0.00	0.00	0	100
37.50	0.00	0	0	100
19.00	0.180	0.18	3.6	96.4
9.50	4.356	4.536	90.72	9.28
4.75	0.45	4.986	99.72	0.28
0.600	0.002	4.988	99.76	0.24
0.300	0	4.988	99.76	0.24
0.075	0	4.988	99.76	0.24

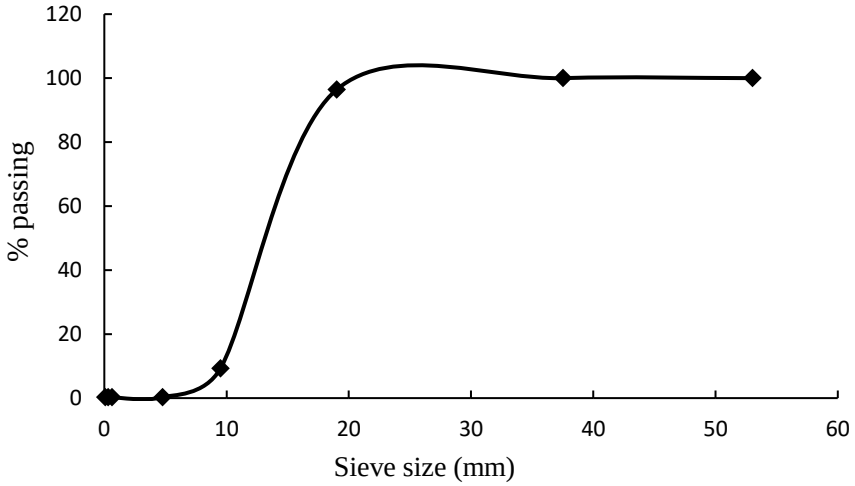

Figure 3.11: Gradation curve for 20mm aggregates.

Table 3.13 : Average Percentage passing for 10 mm Aggregates

IS Sieve size (mm)	Wt. of material retained (kg)	Cumulative wt. retained (kg)	Cumulative retained (%)	Passing (%)
53.00	0.00	0.00	0	100
37.50	0.00	0.00	0	100
19.00	0.00	0.00	0	100
9.50	0.928	0.928	18.56	81.44
4.75	3.152	4.08	81.6	18.4
0.600	0.784	4.86	97.28	2.72

0.300	0.084	4.95	98.96	1.04
0.075	0.032	4.98	99.6	0.4
Pan	0.016	5.00	99.92	0.08

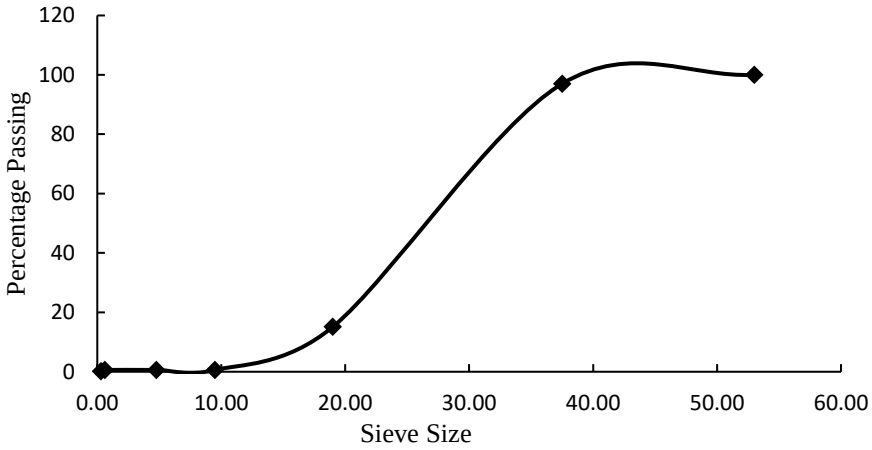

Figure 3.12: Gradation curve for 10mm aggregates

Table 3.14: Percentage Passing of aggregates of different sizes and obtained grading

IS Sieve size (mm)	**Percentage passing (%)**							
	40mm	**20mm**	**10mm**	**soil (FA)**	**Range**	**Mid-Point**	**Obtained Grading**	**Square of Difference**
53	100	100	100	100	100	100	100.00	0.00
37.5	96.04	100	100	100	95-100	97.5	99.41	3.63
19	3.11	97.57	97.7	100	45-100	72.5	84.89	153.39
9.5	0	2.39	79.19	100	35-100	67.5	75.96	71.53
4.75	0	0	17.07	93.3	25-100	62.5	59.39	9.65
0.6	0	0	1.69	85.725	8 to 65	36.5	51.77	233.26
0.3	0	0	0.36	69.45	5 to 40	22.5	41.74	370.25
0.075	0	0	0	14.3	0-10	5	8.58	12.82
								854.53

Table 3.15: Mixes with corresponding proportion of aggregates

Mixes		40 mm (%)	20 mm (%)	10 mm (%)	Soil (%)
20% Aggregates	80% Soil	10	5	5	80
30% Aggregates	70% Soil	15	5	10	70
40% Aggregates	60% Soil	15	5	20	60
50% Aggregates	50% Soil	25	5	20	50
60% Aggregates	40% Soil	30	5	25	40
70% Aggregates	30% Soil	30	15	25	30
80% Aggregates	20% Soil	25	25	30	20

Table 3.16: Passing percentages of different CA/FA proportions.

Mixes →	20% CA 80% FA	30% CA 70% FA	40% CA 60% FA	50% CA 50% FA	60% CA 40% FA	70% CA 30% FA	80% CA 20% FA
PERCENTAGE PASSING (%)	100	100	100	100	100	100	100
	96.2	87.92	98.52	93.8	93.48	82.6	96.2
	90	84.72	84.78	74.8	69.8	71.2	74.48
	81.28	74.22	66.86	54.68	47.28	37	33.68
	77.32	66.22	56.3	47.12	38.54	29.6	20
	58.58	52.74	14.62	36.58	31.54	24.36	15.32
	48.58	43.94	11.8	30.04	26.48	20.04	12.82
	7.28	4.66	2.06	3.04	2.84	2.74	2.5

The blending proportion for mix with 60% soil and 40% aggregate is shown in the table and is satisfying the range of MoRTH 400-4.

Table 3.17: Blending proportion of 60% soil and 40% aggregates.

IS Sieve size (mm)	Weight of material Retained	Cumulative Weight Retained (g)	Cumulative Retained (%)	Passing (%)
53	0	0	0	100
37.5	74	74	1.48	98.52
19	687	761	15.22	84.78
9.5	896	1657	33.14	66.86
4.75	528	2185	43.7	56.3
0.6	2084	4269	85.38	14.62
0.3	141	4410	88.2	11.8
0.075	487	4897	97.94	2.06

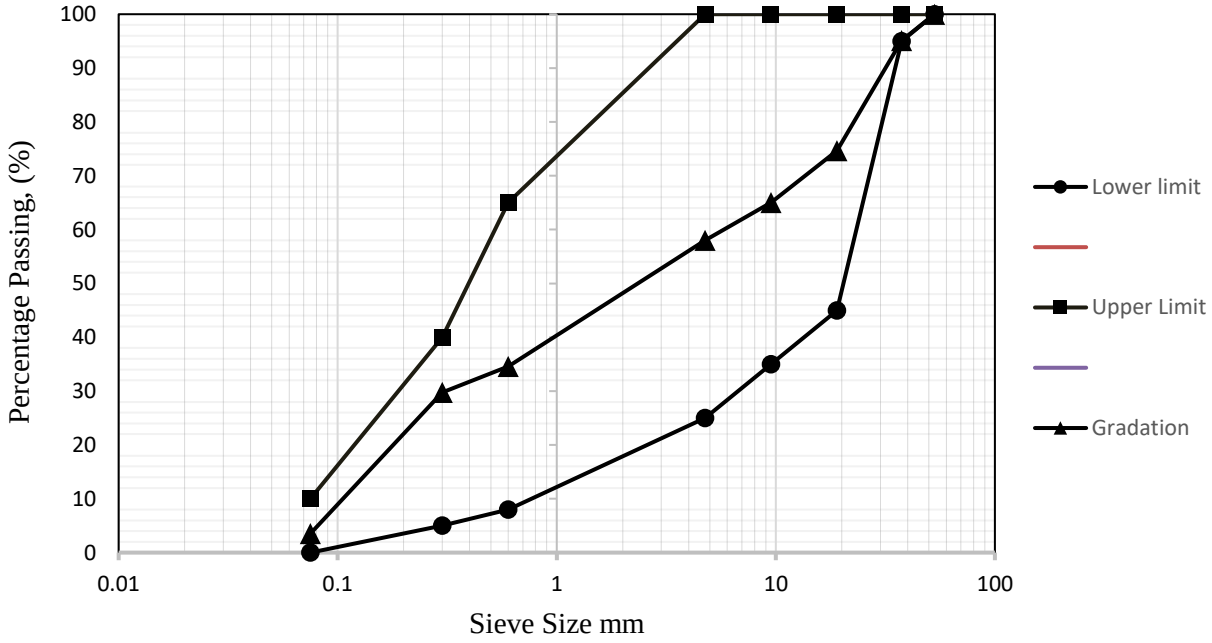

Figure 3.13: Gradation line of mix

The gradation line in the picture above is almost in the middle of both the upper and lower limits, indicating that the range is satisfied asper MoRTH 400-4.

Seven mixes were produced with varying proportions of coarse and fine aggregates, and several tests were done, including proctor compaction, California bearing ratio, and unconfined compression strength test.

Table 3.18: Mixes with different CA/FA proportion.

Mix Nomenclature	Mix Description
SA1	20% Soil (FA) 80% Coarse Aggregates
SA2	30% Soil (FA) 70% Coarse Aggregates
SA3	40% Soil (FA) 60% Coarse Aggregates
SA4	50% Soil (FA) 50% Coarse Aggregates
SA5	60% Soil (FA) 40% Coarse Aggregates
SA6	70% Soil (FA) 30% Coarse Aggregates
SA7	80% Soil (FA) 20% Coarse Aggregates

3.4 Compaction Test

This test is in accordance with IS 2720 Part 8. A modified proctor compaction test was carried out to calculate the optimum moisture content and maximum dry density of different control mixes. The apparatus consisted of a mould of volume (2250 cc), and a hammer of weight 4.9kgs with a dropping height of 450mm. The sample was laid in 5 layers with fifty-six blows per layer. The compaction of soil was performed using Automatic compactor in which the diameter of the mould is 10cm and the height is 15cm. The soil was compacted using an automatic compactor with a mould of 10cm diameter and a 15cm height. The mix samples which included the soil and aggregates were compacted using modified proctor test.

Figure 3.14: OMC/MDD of soil using automatic compactor.

The optimal moisture content and maximum dry density of 7 mixtures (Soil + Aggregate) were investigated in this study. The graphs clearly show that as the percentage of aggregates increases the maximum dry density while the optimal moisture content decreases.

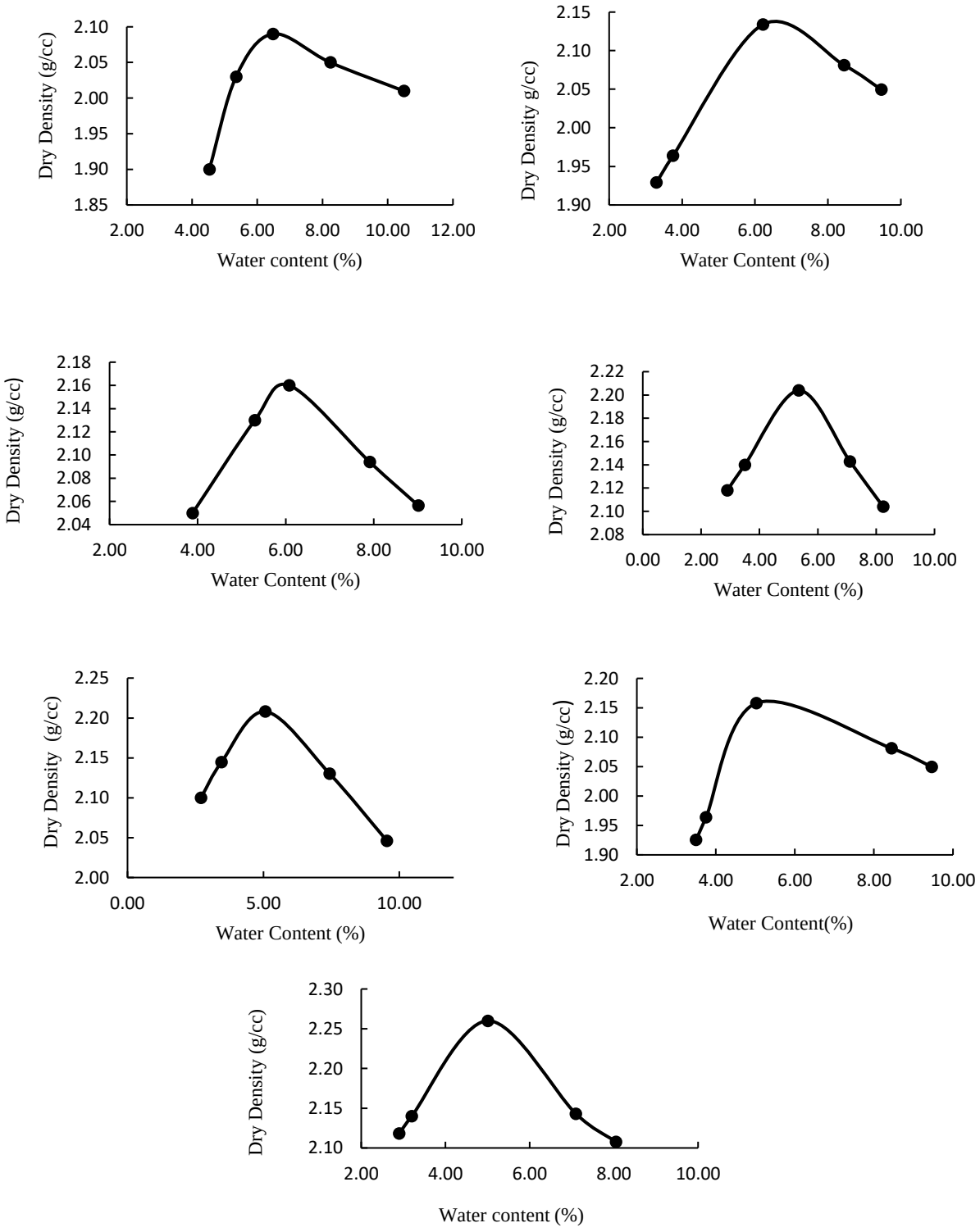

Figure 3.15: OMC/MDD of different mixes (i) SA7, (ii) SA6, (iii) SA5, (iv) SA4, (v) SA3, (vi) SA2, (vii) SA1.

The individual graphical representation of different mixes is shown in the figure 3.15 and the comparison of OMC/MDD for all mixes are shown in the figure 3.16.

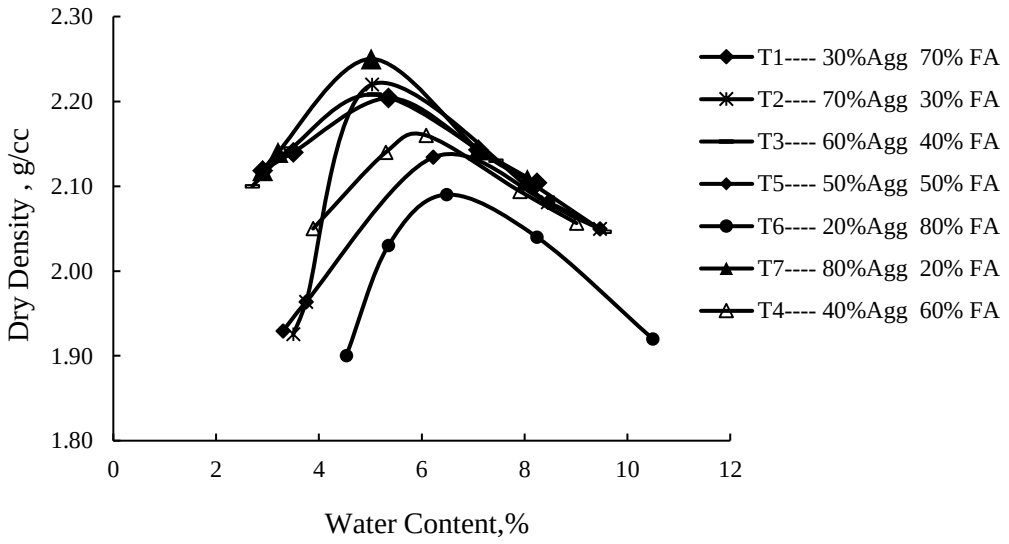

Figure 3.16: Comparison of MDD/OMC of different Mixes.

Table 3.19: OMC and MDD of mixes with different Aggregates to Soil proportions

S.No.	Mix type (Control Mix)	Optimum Moisture Content and Maximum Dry Density.	
		OMC	MDD
1	SA1-20% Soil 80% Aggregates	5.01	2.25
2	SA2-30% Soil 70% Aggregates	5.03	2.22
3	SA3-40% Soil 60% Aggregates	5.07	2.21
4	SA4-50% Soil 50% Aggregates	5.35	2.20
5	SA5-60% Soil 40% Aggregates	6.08	2.16
6	SA6-70% Soil 30% Aggregates	6.22	2.13
7	SA7-80% Soil 20% Aggregates	6.48	2.09

The optimum moisture content and maximum dry density of various combinations are displayed in the table. The table demonstrates that as the proportion of soil increases, OMC rises while MDD falls, and vice versa.

3.5 Unconfined compressive strength tests (UCS)

UCS tests was performed on the cubical specimens at 7 days, in accordance with IS 14858:2000 using ACTM (Automatic compression testing machine). The test was conducted using compression testing equipment with a 0.2 N sensitivity and a Pace load of 5 percent per minute. During the unconfined compression test, smooth metal sheets were inserted at the bottom and top of each specimen to reduce end effects. Three identical samples were prepared and test was performed on them to minimize any mistakes caused by variations in the material and testing conditions, with the average value used in the reports.

Figure 3.17: ACTM machine, Samples for UCS testing.

(a) Perpetration of specimen

Use the prepared mix to make a 150 mm x 150 mm x 150 mm cubical specimen mould. The first mould must be assembled on its baseplate, and a second mould must be placed on top of it without its baseplate. A quantity of stabilised mix sufficient to give a specimen of 150 - 165 mm depth after compaction (approximately 8 kg) shall be compacted into the mould in five equal layers, each layer being compacted with a tamper fitted to a vibrating hammer (if a vibrating hammer is not available, compact with a 4.90 kg hammer to give 56 evenly distributed blows and dropped from a height of 450 mm. Before adding the next layer, previous layer must be scarified with a palette knife. Remove the upper mould after proper

compaction and strike off the extra material with a straight edge tool. If there are any regularities on the surface sample, the same material is filled and the surface is smoothed.

Figure 3.18: Preparation of Mix

(b) Curing of Samples

Curing of mould for 7+4 days prior to testing is required for cement and chemicals to complete their initial reaction and begin to show strength and waterproofing effect. Another method of curing is to completely wrap the mould in a damp gunny bag and keep it wet for the duration of the curing period, or to keep the mould snugly packed in a plastic zip lock bag so that the moisture inside the mould does not escape. Remove the gunny bags or plastic bags from the mould after 7 days and let them dry in the sun or under a heat bulb.

Figure 3.19: Moulds wrapped with plastic sheets

Figure 3.20: Drying of Samples under the Sun (4-days)

The strength of the mixtures with varying proportions of soil and aggregates was tested using UCS on an ACTM (Automatic compression testing machine). The maximum unconfined compressive strength for SA5 (60 percent soil and 40 percent aggregates) was 1.7 MPa.

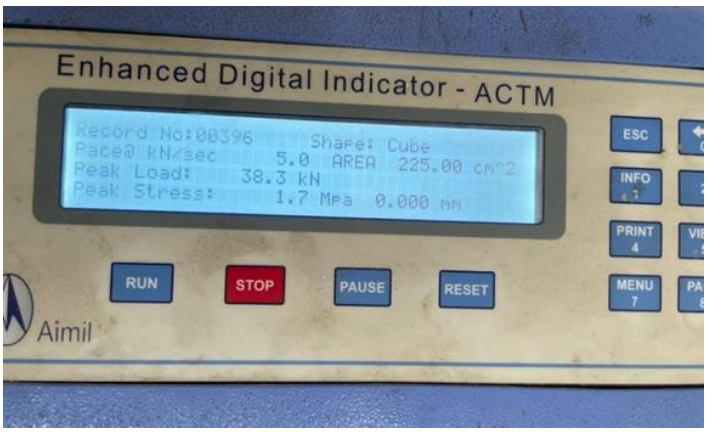

Figure 3.21 UCS values for SA5

Table 3.20: Average UCS values of different mixes

S.No.	Mix type (Control Mix)	Average 7- days UCS (MPa)	Average 28- days UCS (MPa)
1	20% Soil 80% Aggregates (SA1)	0.6	1.4
2	30% Soil 70% Aggregates (SA2)	0.8	1.9
3	40% Soil 60% Aggregates (SA3)	0.86	1.96
4	50% Soil 50% Aggregates (SA4)	1.33	2.42
5	60% Soil 40% Aggregates (SA5)	1.76	3.5
6	70% Soil 30% Aggregates (SA6)	1.26	2.53
7	80% Soil 20% Aggregates (SA7)	1.03	2.33

SA5 mix was chosen for further analysis (because of its high strength) and was subjected to several cement treatments (2%, 3%, and 4%). The table 3.21 shows the related average UCS values.

Figure 3.22: (i) Sample before loading (ii) Sample after loading

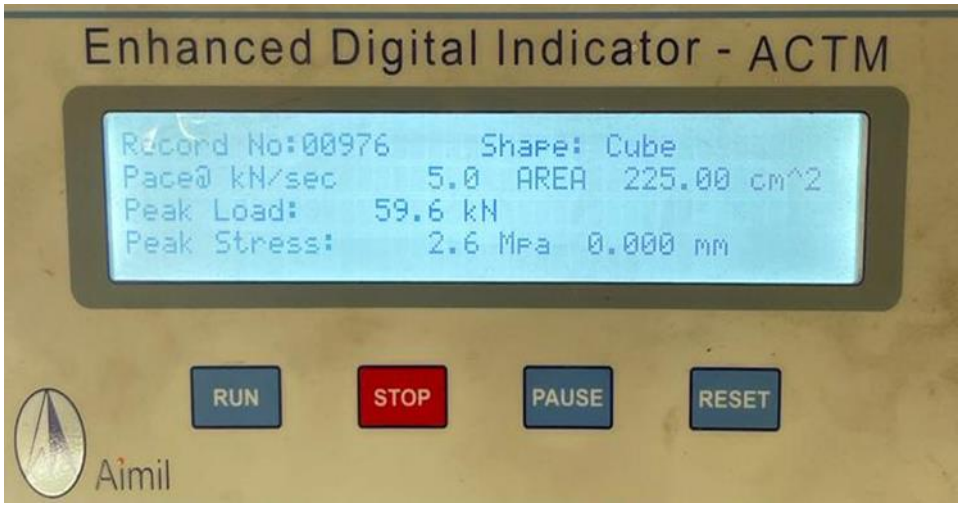

Figure 3.23: UCS values of (SA5C4)

Table 3.21: Average 7/28 days UCS values of (SA5) mix treated with different proportions of cement.

Mix No. 5 with different Cement proportions	**Average Unconfined Compression Strength (MPa)**	
	7-days	**28-days**
60% Soil 40% Aggregates + 2% Cement (SAC2)	2.03	4.13
60% Soil 40% Aggregates + 3% Cement (SAC3)	2.23	4.65
60% Soil 40% Aggregates + 4% Cement (SAC4)	2.60	4.92

The table above shows the average UCS values of SA5 mix treated with different proportions of cement (2%, 3%, 4%). The table 3.21 clearly shows that when the cement percentage increases, the average UCS values increase, but because only 1.5-3 MPa strength is required for CTSB as per IRC 37-2018, there is no need to exceed the cement percentage beyond 4 percent as it will be uneconomical. The earlier studies have also shown that with increase in the cement proportions there is an increase in the strength efficacy (Singh et al., 2020). Different proportions of cement were then treated with varying proportions of chemicals and tested for unconfined compressive strength, and the average values are shown in the table 3.22.

Table 3.22: Average UCS values of SA5 mix treated with different proportions of cement and chemicals.

Mix 5 with cement and chemical	**Nano-Chemical Dosage (Kg/m^3)**	**Average 7Days-UCS (MPa)**	**Average 28Days-UCS (MPa)**
60% Soil 40% Aggregates + 2% Cement (SAC2)	0.2 Nano-Chemical (SAC2CH1)	2.4	4.1
	0.4 Nano-Chemical (SAC2CH2)	2.9	5.3
	0.6 Nano-Chemical (SAC2CH3)	3.43	6.1
	0.8 Nano-Chemical (SAC2CH4)	3.1	5.8
60% Soil 40% Aggregates + 3% Cement (SAC3)	0.2 Nano-Chemical (SAC3CH1)	2.7	4.3
	0.4 Nano-Chemical (SAC3CH2)	3.2	5.9
	0.6 Nano-Chemical (SAC3CH3)	3.58	6.3
	0.8 Nano-Chemical (SAC3CH4)	3.44	6.1
60% Soil 40% Aggregates + 4% Cement (SAC4)	0.2 Nano-Chemical (SAC4CH1)	5.4	9.3
	0.4 Nano-Chemical (SAC4CH2)	5.9	10.2
	0.6 Nano-Chemical (SAC4CH3)	6.4	13.6
	0.8 Nano-Chemical (SAC4CH4)	6.1	11.8

As the percentage of the chemical increases the UCS increases till a dosage of 0.6kg/m^3 after which the UCS value drops. The UCS value for the mix (SAC4CH3) is shown in the figure 3.23.

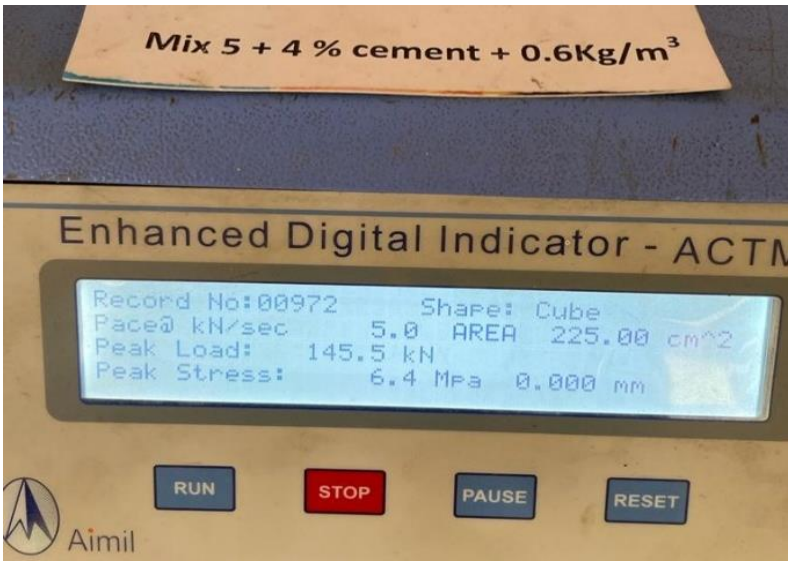

Figure 3.24: UCS value of (SAC4CH3)

3.6 California Bearing Ratio (CBR)

The California Bearing Ratio Test is a penetration test used to determine the strength of the subgrade of roads and pavements. These tests' results are combined with empirical curves to establish the thickness of the pavement and its constituent layers. This is the most extensively used method for flexible pavement design.

In this experiment, a cylindrical mould with an inner diameter of 150mm and a height of 175mm was employed, along with a removable collar of 50mm height and a 10mm thick base plate. With a large weight hammer (4.89kgs) and a dropping height of 450mm, the sample soil is filled and compacted in 5 layers.

Figure 3.25: CBR Test Machine

Procedure for Penetration Test

Place the surcharge-weighted mould on the CBR test equipment. With the smallest feasible load, seat the piston in the specimen's centre. Set the dial gauge for stress/strain to zero. Apply a load to the piston so that it penetrates at a rate of 1.25mm/min. Note the load readings for 0.5, 1.0, 1.5, 2.0, 2.5, 3.0, 4.0, 5.0, 7.5, 10, and 12.5 mm penetrations. Remove the mould from the loading apparatus. Determine the moisture content of around 20 to 50 g of soil from the top 3 cm layer.

Table 3.23: Mixes with corresponding soaked CBR values.

Mix Description	**CBR**
Untreated Mix (SA5)	18.4
Mix Treated with 2% Cement (SA5C2)	25.6
Mix Treated with 3% Cement (SA5C3)	30.5
Mix Treated with 4% Cement (SA5C4)	37.2
Mix Treated with 2% Cement +0.6kg/m^3 chemical (SA5C2CH3)	29.8
Mix Treated with 3% Cement +0.6kg/m^3 chemical (SA5C3CH3)	58.8

3.7 Microstructural Analysis

SEM analyses and X-ray Diffraction (XRD) of the treated and untreated specimens were carried out by a Zeiss Gemini-1 Sigma 500 Emission Scanning Electron Microscope, Rigaku XRD-D1, respectively, to understand the underlying mechanisms of the effects of Nano-Si.

a) SEM

SEM analysis is a powerful tool in which a concentrated electron beam is utilized to produce a high magnification images of the surface topography. One of the most effective methods for figuring out the microstructure of cementitious materials is FE- Scanning electron microscopy. To study the effect of addition nanoparticles and cement, emphasis on the shape and microstructure becomes incumbent.

To identify the components in SA samples with cement and chemicals, SEM with an EDS extension were employed. Broken Soil-Aggregate samples were taken from the cubes that were tested for compressive strength to study the micro structure of the samples and the changes that are occurring in the samples throughout the process on the addition of cement and chemical. Also, this test was performed to check the reduction in voids after addition of cement and chemical

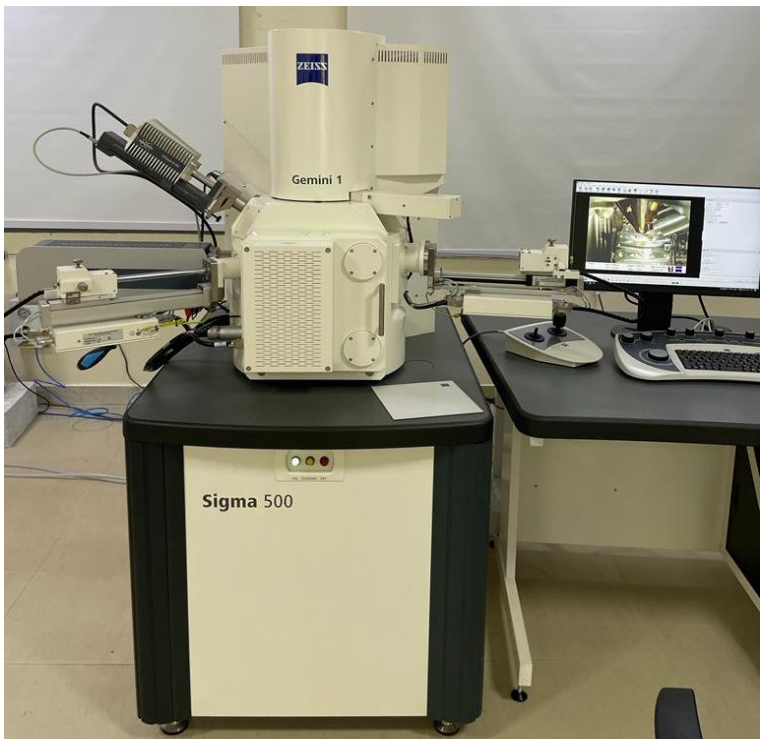

Figure 3.26: SEM equipment used in the study.

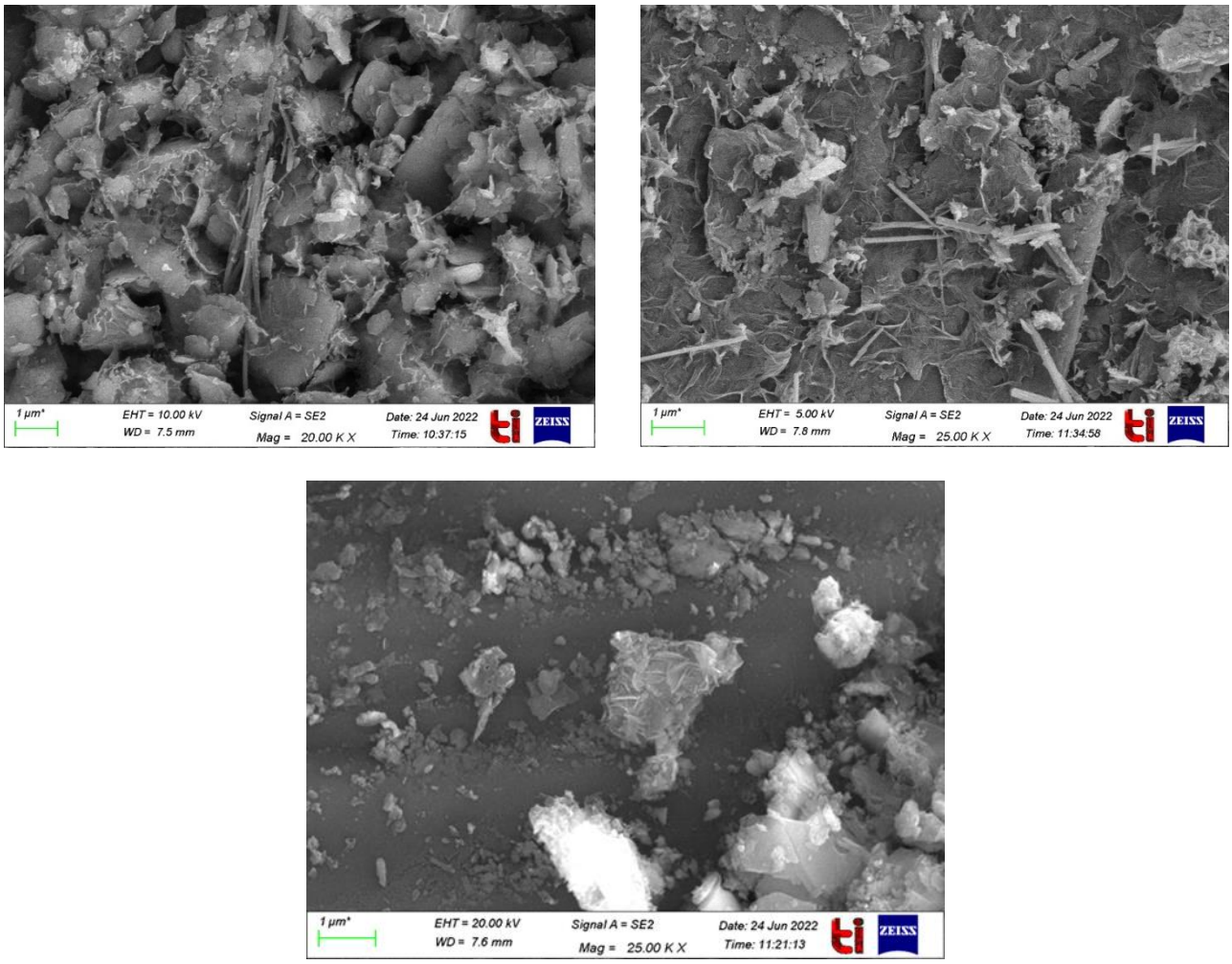

Figure 3.27: SEM images of (i) SA5C2CH3, (ii) SA5C3CH3, (iii) SA5C4CH3

The FE-SEM images clearly shows that with the increase in the percentage of cement the densification of the matrix increase, this is because with the addition of cement the porosity is reduced to a greater extend. The Mix with 4% of cement (SA5C4CH3) has a very dense composition because of the formation of compounds like SiO_2, $CaCO_3$ on the surface, which is reflected in the compressive strength of the sample.

b) Energy Dispersive X-Ray Spectroscopy (EDS)

Energy-dispersive X-ray spectroscopy (EDS, EDX, EDXS or XEDS), sometimes called energy dispersive X-ray analysis (EDXA or EDAX) or energy dispersive X-ray microanalysis (EDXMA), is an analytical technique used for the elemental analysis or chemical characterization of a sample.

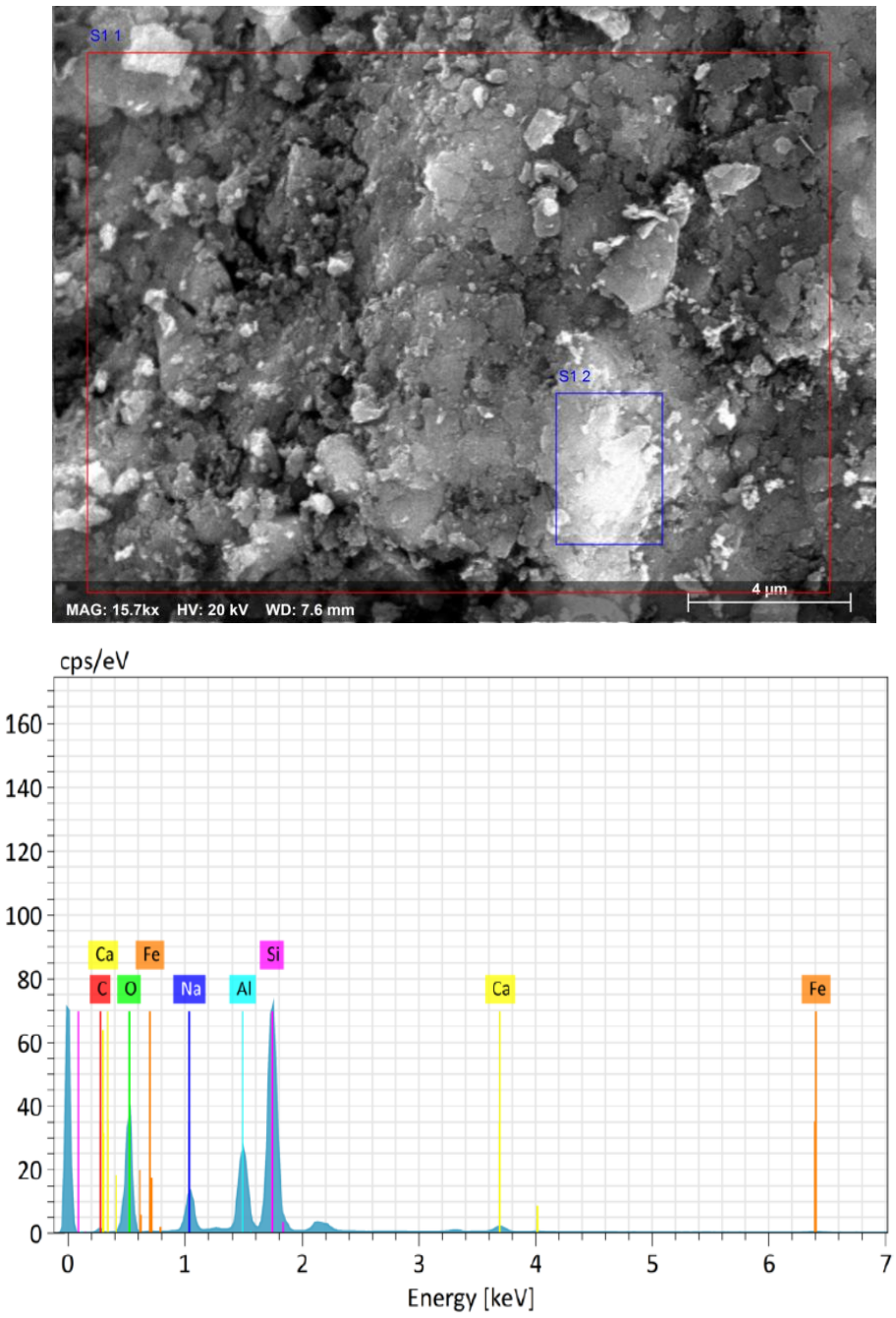

Figure 3.28: EDS analysis at position S1 2

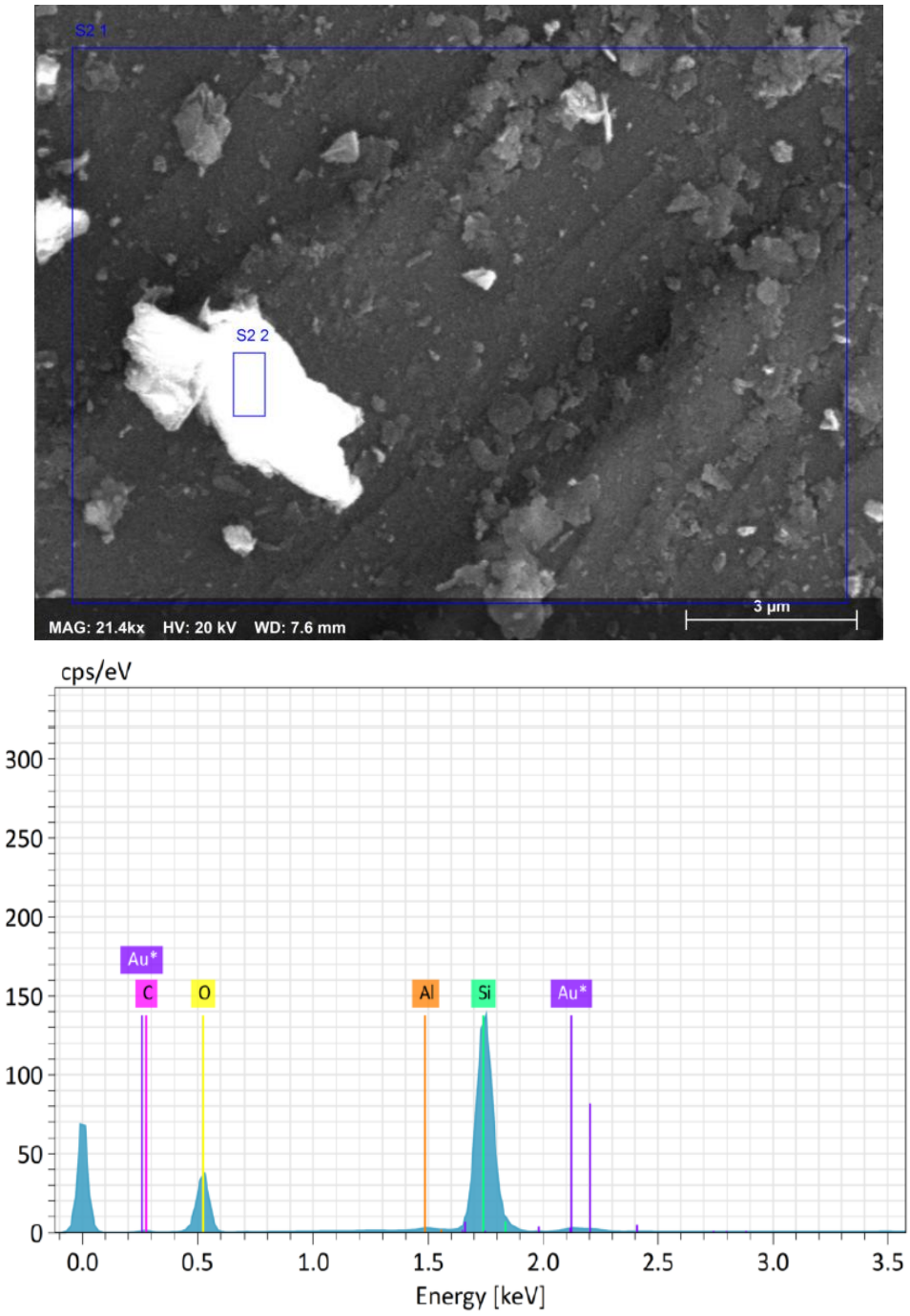

Figure 3.29: EDS analysis at position S2 2

The EDS analysis on white chunk clearly shows the formation of SiO_2 phase. The XRD analysis of the samples are manifested by the results of EDS.

c) X-Ray Diffraction (XRD)

An essential analytical tool for characterising soil aggregate samples is X-ray diffraction (XRD). Both qualitative and quantitative analysis are done using it. The fundamental idea behind how it operates is that when crystalline material diffracts X-rays, the result is an XRD pattern made up of peaks with different intensities at distinctive diffraction angles.

For micro structural analysis the soil-aggregate powdered sample after sieving was placed on acetone spatula and kept on the XRD machine. The speed of scanning was fixed at 2^0 per minute and 2θ ranged from $0\text{-}50^0$.

Figure 3.30: XRD Equipment

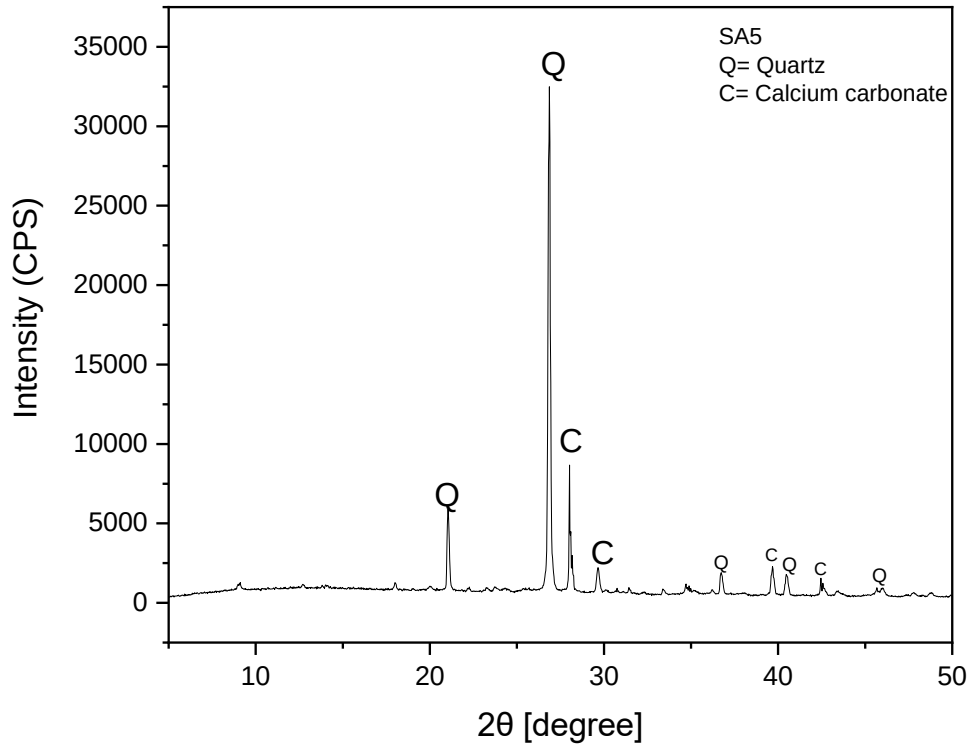

Figure 3.31: XRD analysis of SA5

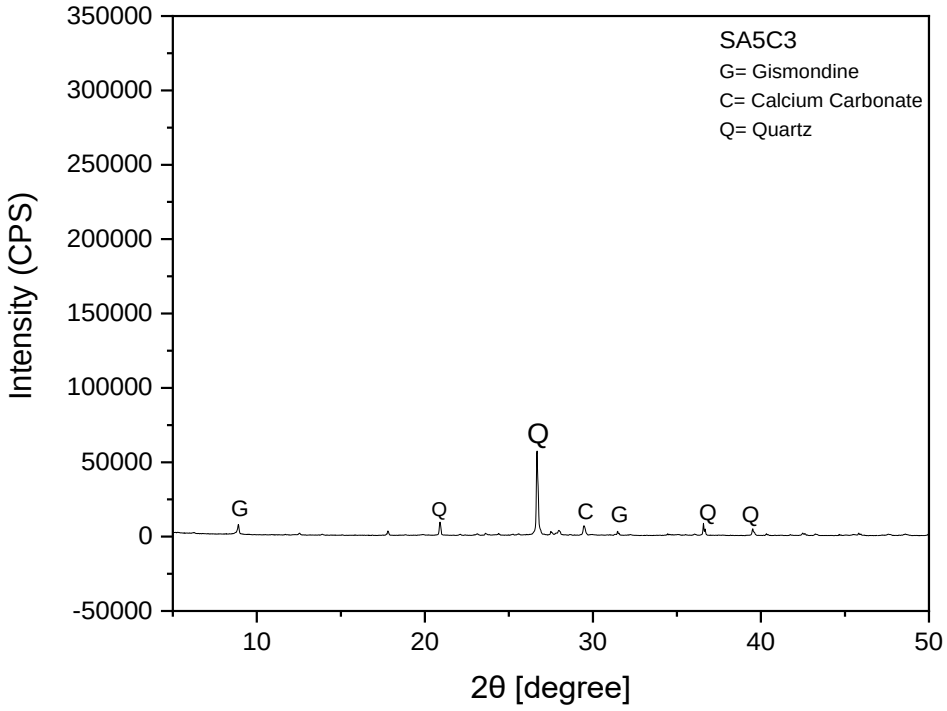

Figure 3.32: XRD analysis of SA5C3

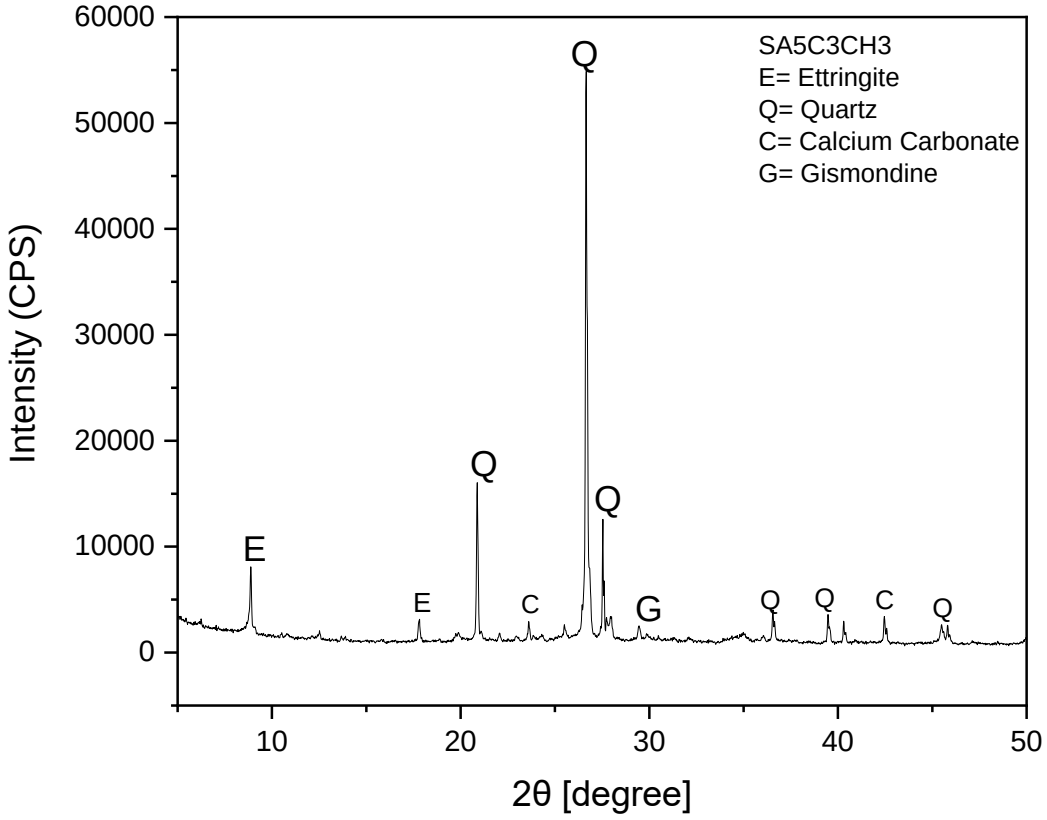

Figure 3.33: XRD analysis of SA5C3CH3

The XRD analysis of different samples SA5, SA5C3, SA5C3CH3 are shown in figure 3.30, figure 3.31, figure 3.32 respectively. All the samples exhibit $Si0_2$ as major phase along with $CaCO_3$. Apart from these crystalline phases $CaSiAl_2O_6.H_2O$ phase is also present in SA5C3 sample.

CHAPTER - 5

RESULTS AND DISCUSSIONS

5.1 General

This chapter deals with the investigation of the results from the different tests performed on different mixes for use as Cement Treated Sub-bases. Tests were performed for compressive strengths, compaction, California bearing ratio and the Deflectometric evaluation. The strength characteristics of CTSB consisting of aggregates of varying sizes, Fine aggregates (Soil), cement and chemical additives are reviewed in this chapter. The deflectometric investigations using light weight Deflectometer are also discussed.

5.2 Effect of different SA (Soil Aggregate) mixes on Compaction.

The optimal moisture content and maximum dry density of 7 mixtures (Soil + Aggregate) were investigated in this study. The graphs clearly show that as the percentage of aggregates increases the maximum dry density while the optimal moisture content decreases. The graphical illustration of the MDD and OMC for seven mixes are shown below,

Figure 4.8 depicts the fluctuations in optimal moisture content (OMC) and maximum drying density (MDD) of residual soil with various course aggregate percentages. As can be seen, the addition of aggregates increased the MDD while decreasing the soil's OMC.

.

Table 5.1: OMC and MDD of mixes with different Aggregates to Soil proportions

Mix No.	Mix type (Control Mix)	OPTIMUM MOISTURE CONTENT AND MAXIMUM DRY DENSITY	
		OMC	*MDD*
1	SA1-20% Soil 80% Aggregates	5.01	2.25
2	SA2-30% Soil 70% Aggregates	5.03	2.22
3	SA3-40% Soil 60% Aggregates	5.07	2.21
4	SA4-50% Soil 50% Aggregates	5.35	2.20
5	SA5-60% Soil 40% Aggregates	6.08	2.16
6	SA6-70% Soil 30% Aggregates	6.22	2.13
7	SA7-80% Soil 20% Aggregates	6.48	2.09

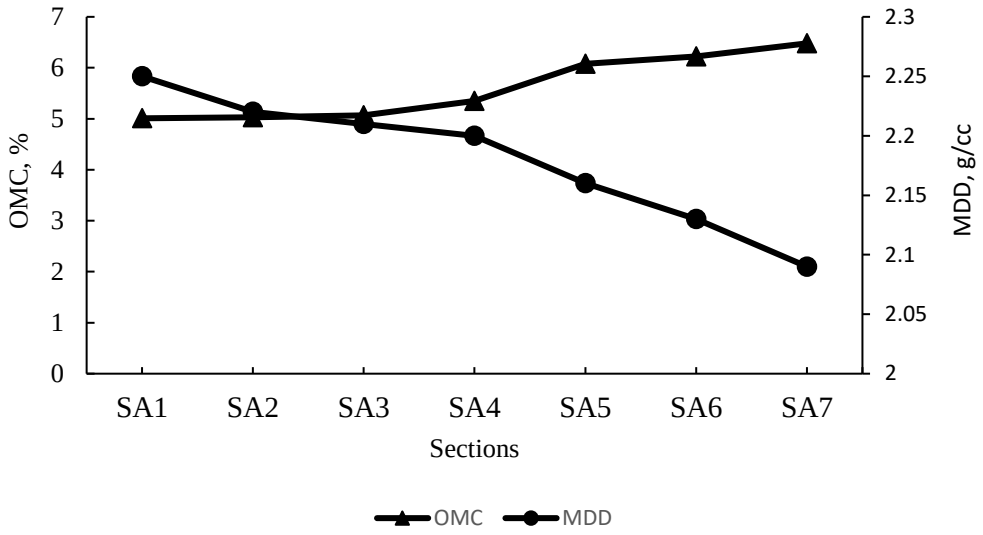

Figure 5.1 Variation of OMC/MDD for different mixes.

From the Modified proctor results, the MDD value decreased as the percentage of the aggregates is decreased and vice versa however the OMC value increased as the percentages of soil increased.

5.3 Effect of cement and chemical on Unconfined Compressive Strength.

The strength of the mixtures with varying proportions of soil and aggregates was tested using UCS on an ACTM (Automatic compression testing machine). The maximum unconfined compressive strength for SA5 (60 percent soil and 40 percent aggregates) was 1.7 MPa.

Figure 5.2 (i)ACTM machine (ii)UCS values for Mix 5 (SA5)

S.No.	Mix type (Control Mix)	Average Unconfined Compression Strength (MPa)

1	20% Soil 80% Aggregates (SA1)	0.6
2	30% Soil 70% Aggregates (SA2)	0.8
3	40% Soil 60% Aggregates (SA3)	0.86
4	50% Soil 50% Aggregates (SA4)	1.33
5	60% Soil 40% Aggregates (SA5)	1.76
6	70% Soil 30% Aggregates (SA6)	1.26
7	80% Soil 20% Aggregates (SA7)	1.03

Table 5.2: Average UCS of different Soil-Aggregate Mixes

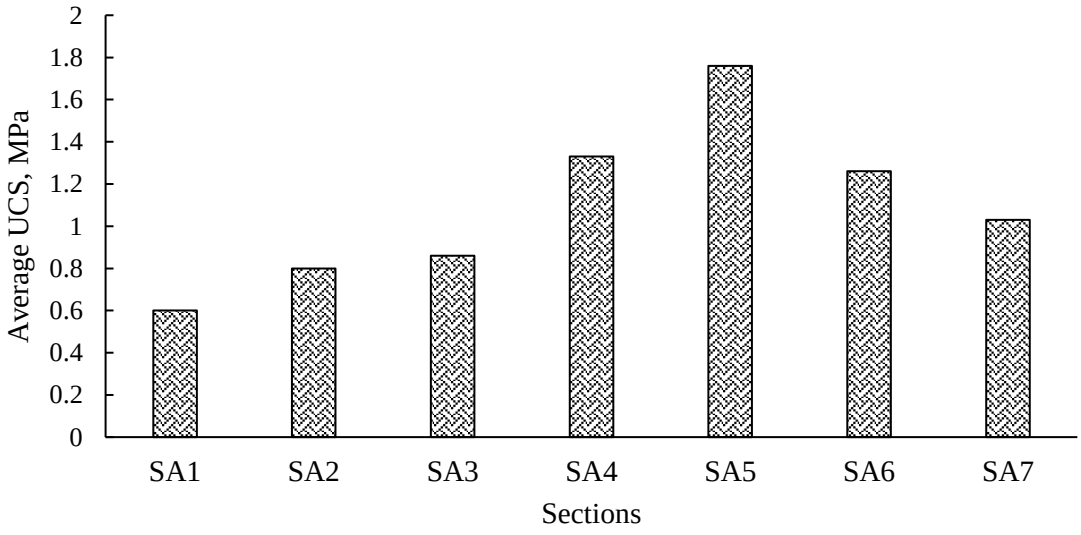

Figure 5.3: Average UCS values for different control samples

SA5 mix was chosen for further analysis (because of its high strength) and was subjected to several cement treatments (2%, 3%, and 4%). The average UCS values with increasing cement percentages are shown in the figure 5.4

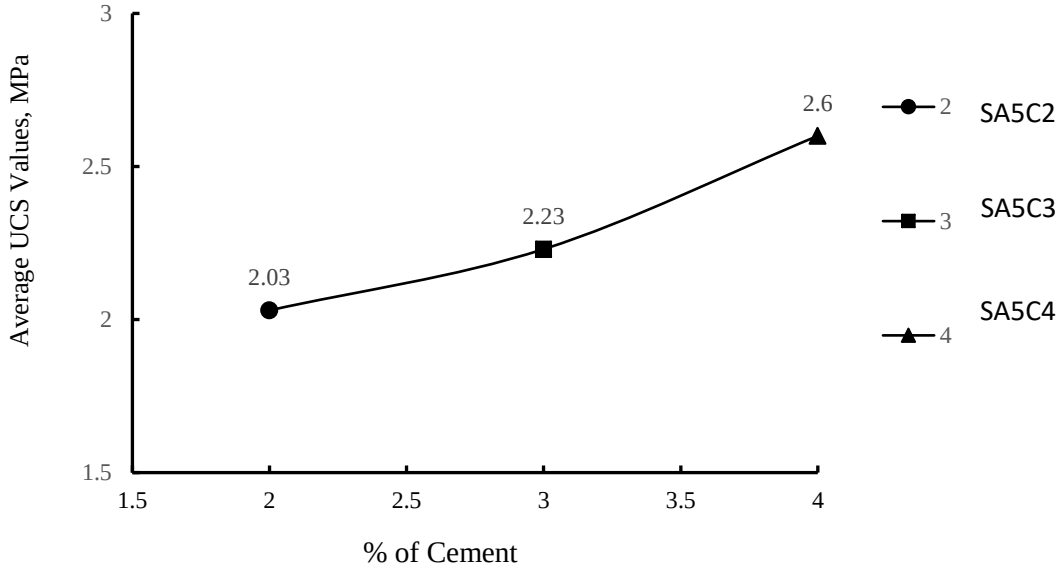

Figure 5.4: Average UCS values of the mix (SA5) treated with different proportions

The graph above clearly shows that when the cement percentage increases, the average UCS values increase, but because only 1.5-3 MPa strength is required for CTSB as per IRC 37-2018, there is no need to exceed the cement percentage beyond 4 percent as it will be uneconomical. The earlier studies have also shown that with increase in the cement proportions there is an increase in the efficacy (Singh *et al.*, 2020) Different proportions of cement were then treated with varying proportions of chemicals and tested for unconfined compressive strength, and is graphically shown in figure 5.5.

The variation of average UCS with addition of chemical is shown in the figure 5.5. the graph clearly depicts that as the percentage of the chemical increases the UCS increases till 0.6kg/m^3 of chemical dosage, after which the UCS value drops.

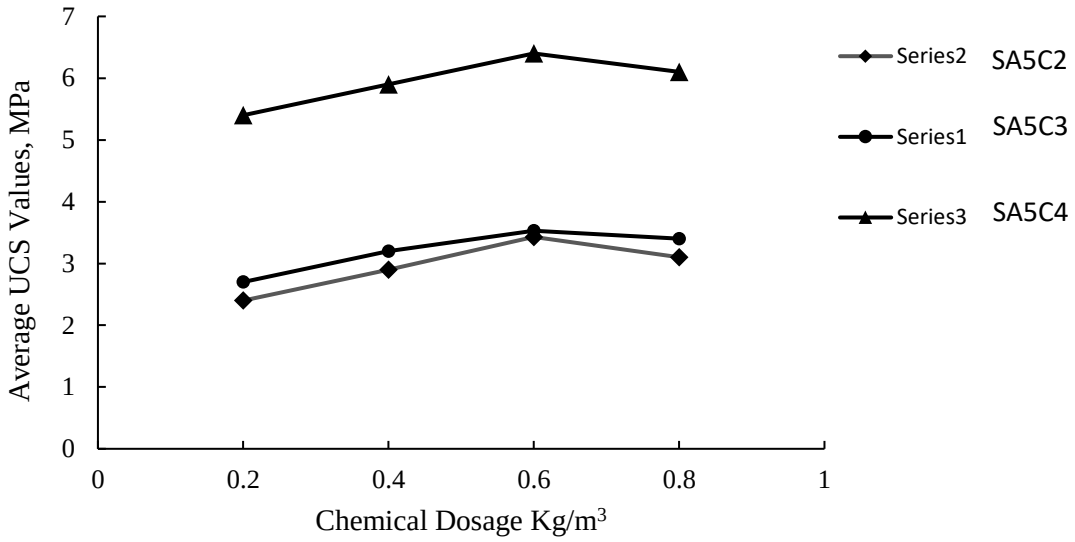

Figure 5.5: variation of UCS values with increase in the chemical and cement proportion.

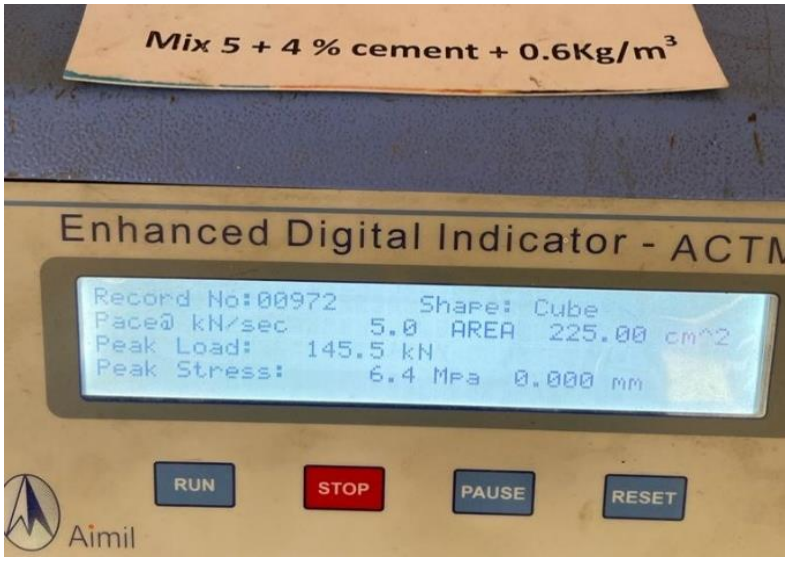

Figure 5.6: UCS values for (SAC4CH3)

The compressive strength increases as the proportion of chemical dosage increases until the dosage reaches 0.6kg/m3, after which it falls, as illustrated in the graph shown above. The compressive strength of 4 per cent cement with a chemical addition increased dramatically compared to other two mixes. The Increase in the compressive strength is because the addition of cement increases compressive strength, as evidenced by previous research (Okyay and Dias, 2010) (Chew, Kamruzzaman and Lee, 2004). The addition of more than 4% cement produce excessive hydration heat, which causes cracks resulting in the failure of the layer.

5.4 Effect of cement and chemical on California Bearing Ratio (CBR)

The California Bearing Ratio of untreated soil, cement treated, and treated with cement and chemical are depicted graphically in the figure 4.7. It's clear from the graph that with the increase in the percentage of cement the CBR value increases and continues to increase with the addition of chemical. The CBR value for the SA5 mix that just contained soil aggregate (60:40) was 18.4%, but with the addition of cement, the value increases to 37.2% for SA5C4. After treating the mixes with chemical the value of the CBR continued to increase and reached to a vale of 58.8% for SA5C3CH3. Comparing all these CBR values the addition of cement and chemical increased the CBR value by 219%.

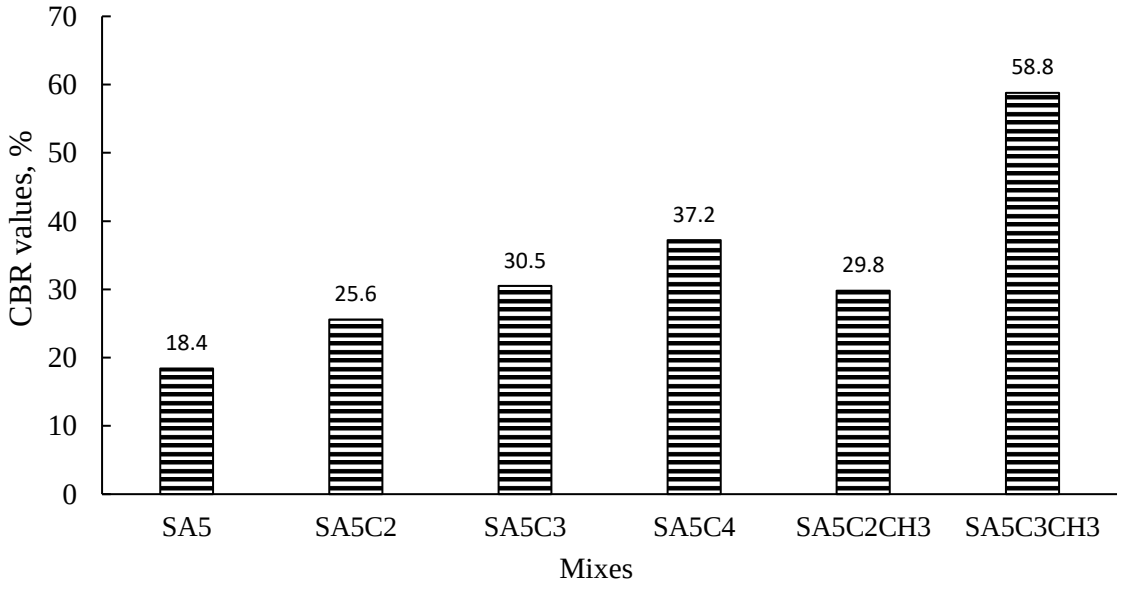

Figure 5.7: CBR values for different mixes.

5.5 Field Testing Results

5.5.1 Effect of cement and chemical on Field Unconfined Compressive Strength.

After laying different proportions of Control mix, cement treated and chemically treated sub-base layer 4on 60m long road, samples (150mm cubical moulds) were collected using both a heavy weight hammer and a DLC hammer for UCS testing. The samples were then tested using an automatic compression testing machine (ACTM) for 7-day UCS, the results of which are displayed in the figure 5.8.

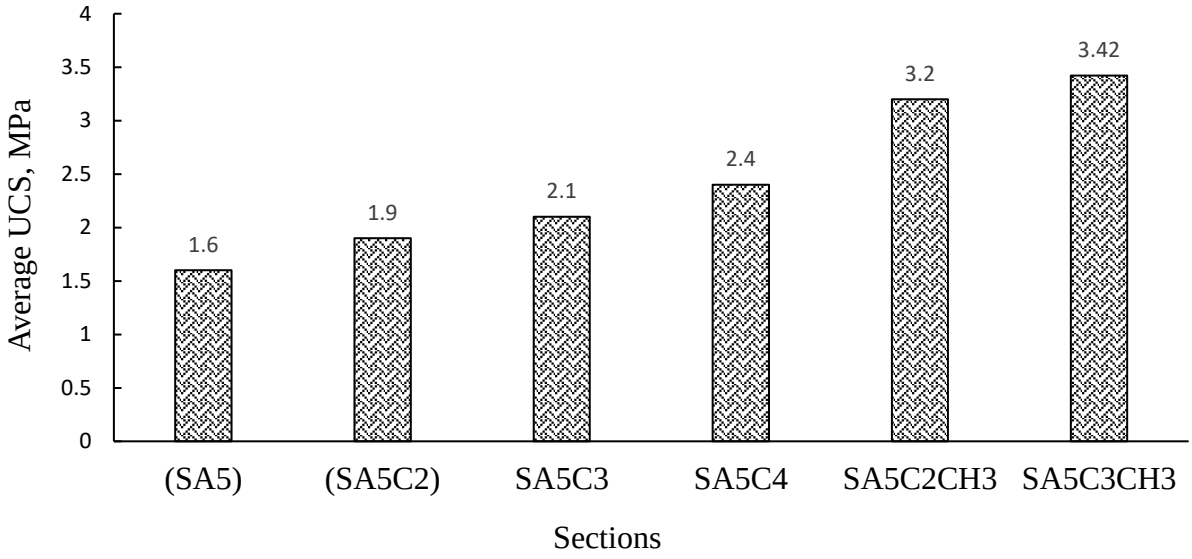

Figure 5.8: Field 7-day UCS values of different Mixes.

The unconfined compressive strength value increased and continued to improve with the addition of chemicals and cement, as shown by the 7-day UCS value, which is also noted in earlier literature when treating the mix with cement and chemical. The 7-day UCS value for the SA5 mix without chemical and cement was 1.6 MPa, and it continued to rise to 3.52 MPa for SA5C3CH3 as cement and chemical were added.

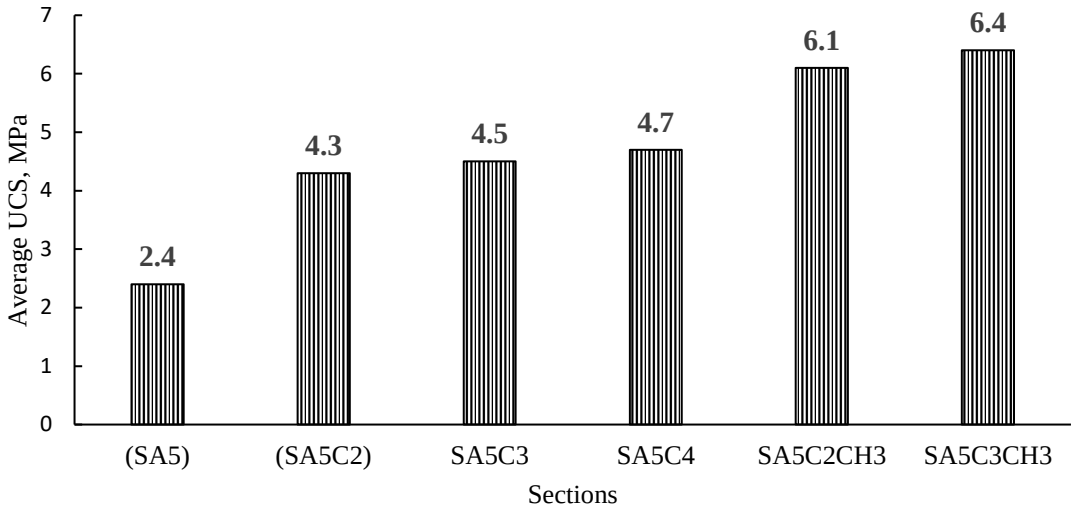

Figure 5.9: Field 28-day UCS values of different mixes

5.5.2. Effect of cement and chemical on Deflectometric Study:

LWD is a quick test method for the compaction quality of soils and unbound base courses in road construction. The soil dynamic LWD modulus, which is empirically associated to the degree of compaction of the soil, is measured by the light weight deflectometer. The modulus and the deflection values for different sections on the field is graphically shown in the figure 4.9 and 4.10 respectively.

The modulus and the deflection are inversely related with one another. The graph clearly depicts that with the increase in the additives the modulus value increases and the deflection values decreases. This is due to the fact that the voids in the untreated mix are filled by cement and the remaining voids are filled by the chemical making the mix dense and ultimately raising the modulus value, which is shown by the microstructural analysis and the X-ray diffraction of the samples.

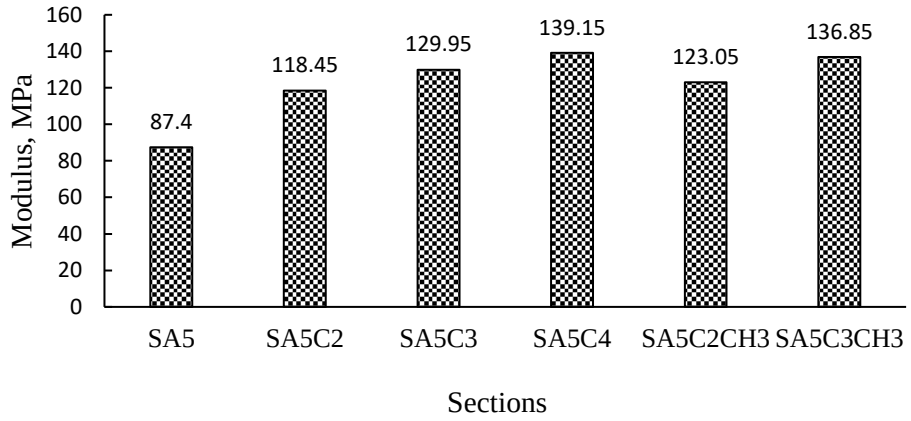

Figure 5.10: Modulus values of different sections on field at the time of laying

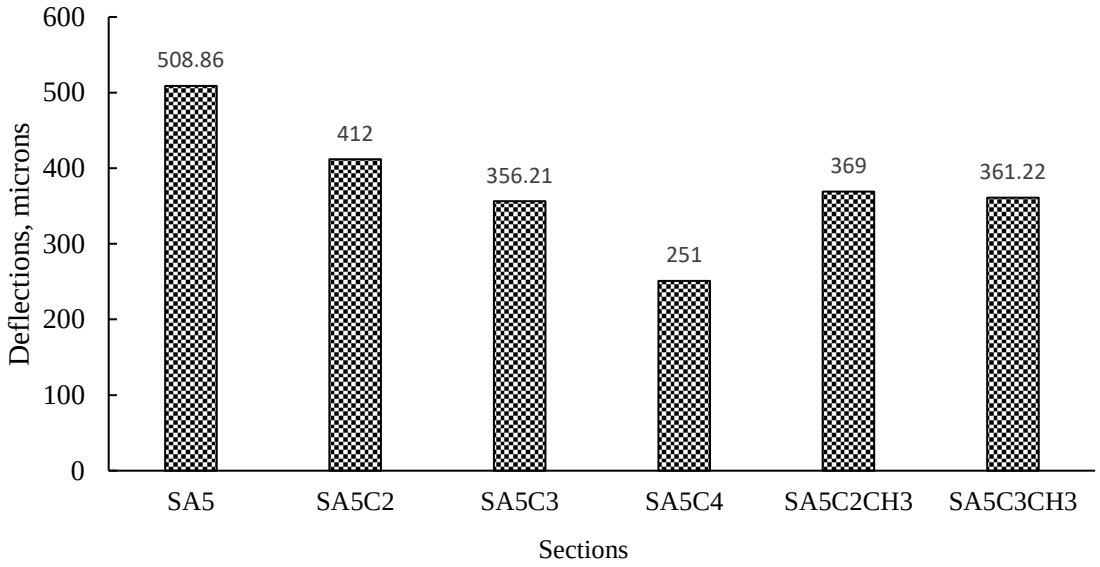

Figure 5.11: Deflection values of different field mixes at the time of laying

The deflection values of different sections are graphically shown in the figure 5.11. Although these values were measured shortly after laying in order to check the degree of compaction using deflection values, the largest deflection is for SA5, which has the least modulus, and the minimum deflection is for SA5C4 having highest modulus.

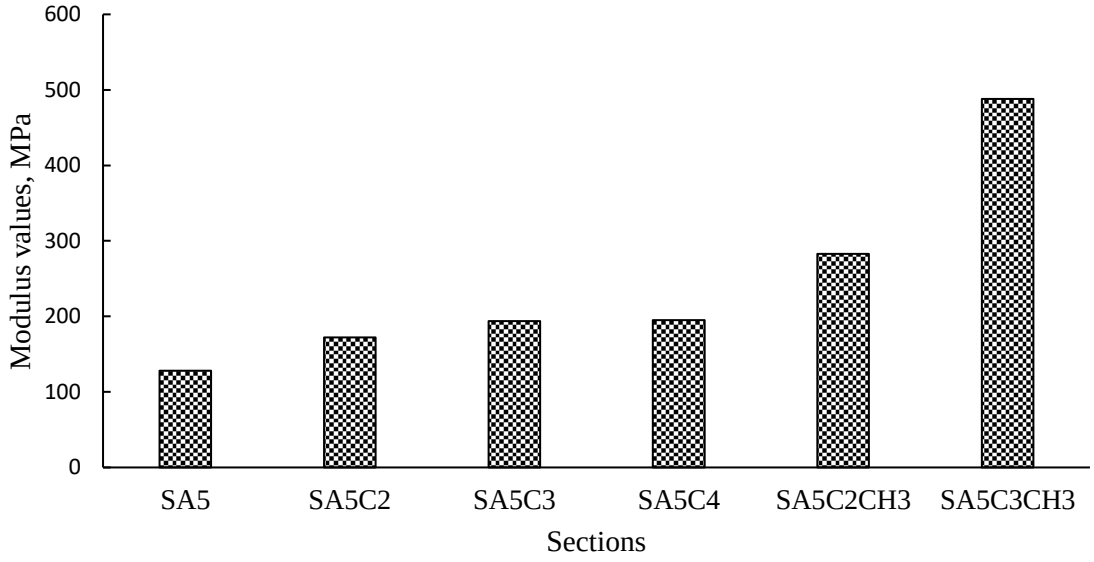

Figure 5.12: 28-day modulus values for different field mixes

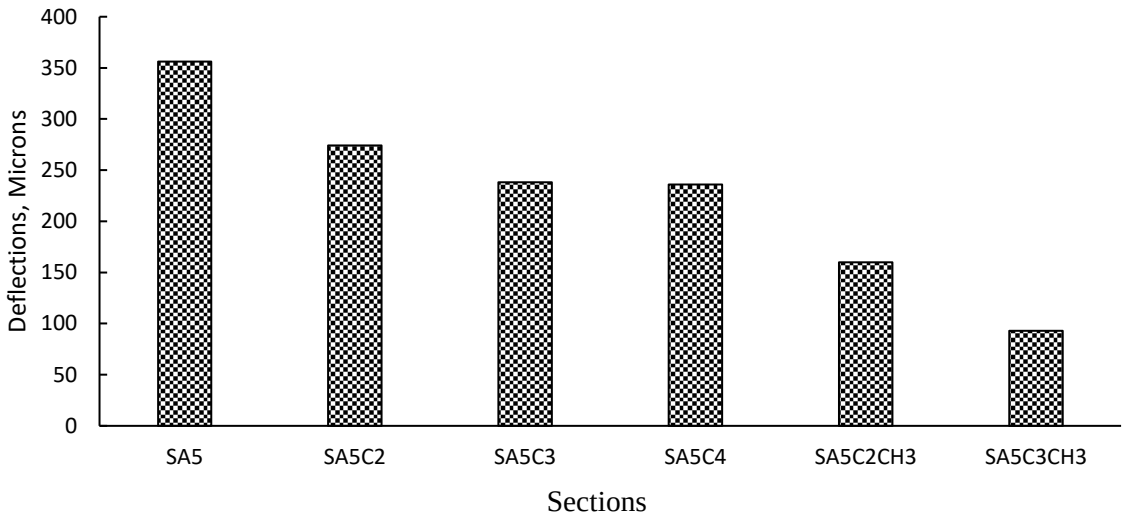

Figure 5.13: 28-day Deflection values of different field mixes

The LWD test was again performed after 28 days from laying of the layer to check the modulus and deflection values, the results of which are shown in the figure 5.12 and 5.13 respectively. The comparison of modulus/ deflection values at the time of laying and 28 days are shown in the figure 5.14, where the mix with least deflection and highest modulus is SA5C3CH3.

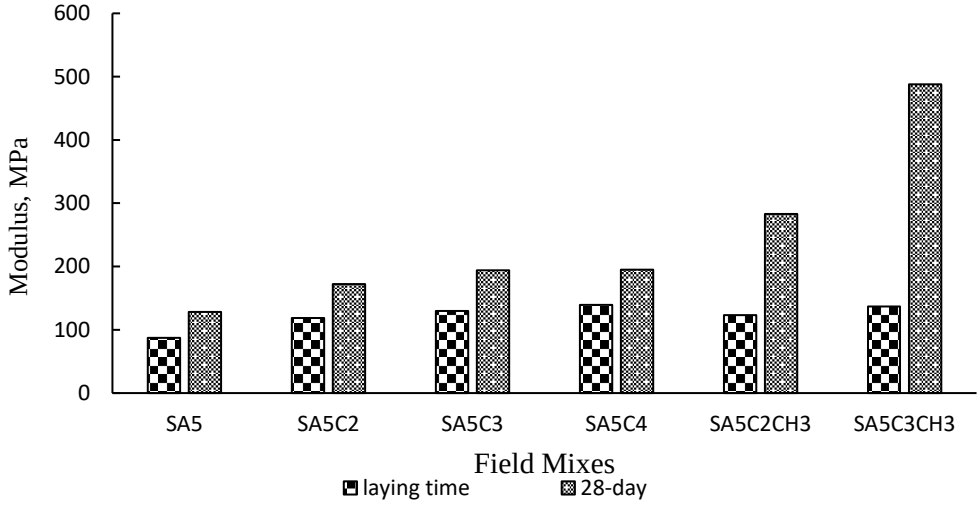

Figure 5.14: Modulus values at 28th-day and at the time of laying.

5.6 Micro Structural Analysis

The X ray diffraction pattern of SA5, SA5C3, SA5C3CH3 are shown in figure 5.15 . All the samples exhibit $Si0_2$ as major phase along with $CaCO_3$. Apart from these crystalline phases $CaSiAl_2O_6.H_2O$ phase is also present in SA5C3 sample. The addition of Nano-chemicals in SA5C3 sample, SiO_2, $CaCO_3$, $CaSiAl2O_6$. H_2O and $Ca_6Al_2(SO_4)_3OH_{12}.26\ H_2O$ are observed as shown in figure 3.32. the addition of nanoparticles further enhances the volume fraction of

Quartz (SiO_2) phase. Moreover, the nanoparticle of SiO_2 also increased the capacity of water absorption and formed the hydroxyl group.

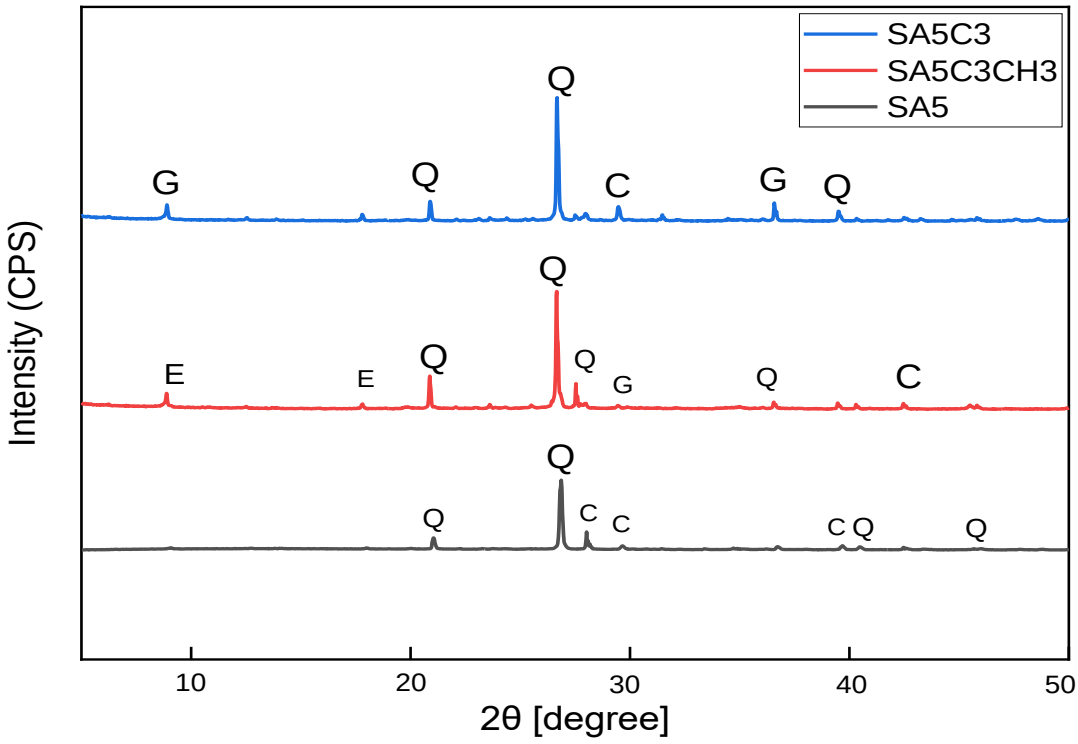

Figure 5.15: XRD Analysis of different samples.

Morphology of synthesized samples is observed using FE-SEM as shown in figures 5.16 (a,b,c) The FE-SEM images of SA5, SA5C3 and SA5C3CH3 are taken on the solid samples. The images of solid SA5 contains large particles of SiO_2 while small particles may correspond to $CaCO_3$. it can be observed from the FE-SEM images that the addition of cement reduces the samples' porosity and enhances the binding among the various constituents. The addition of Nano chemicals in SA5C3 sample some rod type of morphology is also observed. It could be related to $Ca_6Al_2(SO_4)_3\ OH_{12}.26\ H_2O$ crystalline phase.

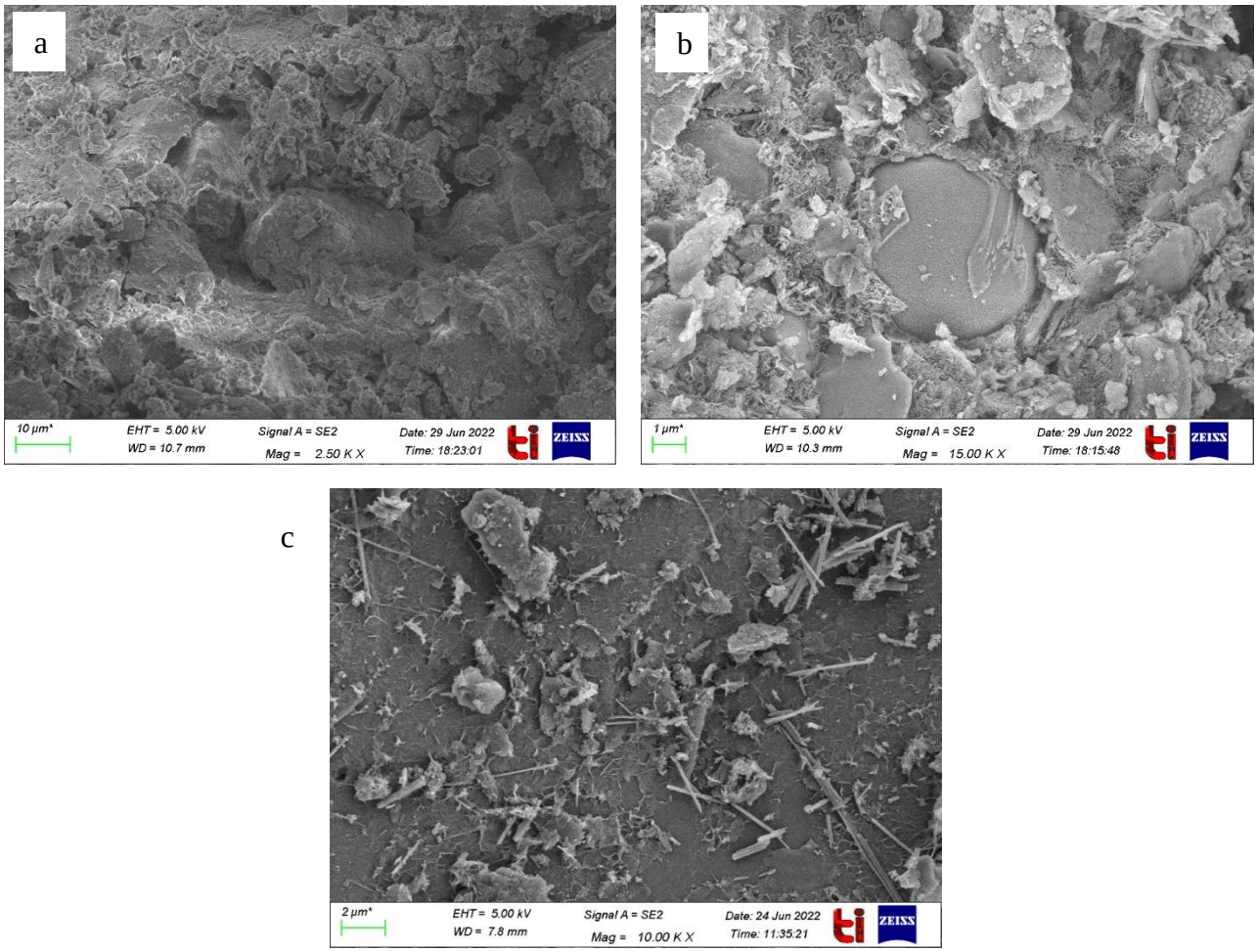

Figure 5.16: SEM Images of (a)SA5 (b)SA5C3 (c)SA5C3CH3

The addition of cement in SA5 increases the mechanical strength of the sample approximately 1.5 times because of the matrix's reduction in porosity, which is clear from the SEM images. Interestingly addition of nanoparticles in SA5C3 sample enhances the mechanical strength which is 3 times higher than SA5 sample because of the formation of ettringites which results in the densification of the matrix shown in figure 5.15(c). The addition of nanoparticles decreased the porosity of the mix, resulting in high strength.

CHAPTER 4
FIELD STUDY

4.1 Deflectometric Studies:

LWD, a dynamic stiffness device, has recently picked up steam as a portable and affordable tool for determining in-situ reactions such as deflections and surface modulus on thin bound and unbound layers(Guzzarlapudi, Adigopula and Kumar, 2016). The in-situ interactions were investigated using a popular method known as back-calculation to estimate layer moduli. These in-situ responses were also utilized to predict the residual life of the in-service pavement and define alternative maintenance techniques such as overlays. LWD devices can also be utilized as a quality control/quality assurance and structural evaluation tool by analysing in-situ compacted stiffness. However, in India, the use of LWD for structural evaluation is restricted to low-volume roads(Guzzarlapudi, Adigopula and Kumar, 2016) like PMGSY Roads.

4.2 Lightweight Deflectometer (LWD)

This method is in accordance with the ASTM E 2583-07. This is a type of plate-bearing test. The load is a force pulse generated by a falling weight (mass) that is transmitted via a plate sitting on the material to be evaluated by a buffer system. The test instrument can move about by hand or using a dolly. A Schematic layout of the Lightweight Deflectometer (LWD) is shown in the figure 4.1. The weight is lifted to the point where it will produce the desired force pulse when dropped. The weight is dropped, and the vertical movement or deflection of the surface is measured with appropriate equipment. At the same site, many tests at the same drop height (various heights are optional) can be performed.

The peak deflection caused by the force pulse is measured at each location in micrometres, millimetres, mils, or inches. The peak force transmitted by the falling weight is measured in kN or lbf, or as the mean stress (the force divided by the load plate area) in kN/m2(kPa) or psi, depending on the application.

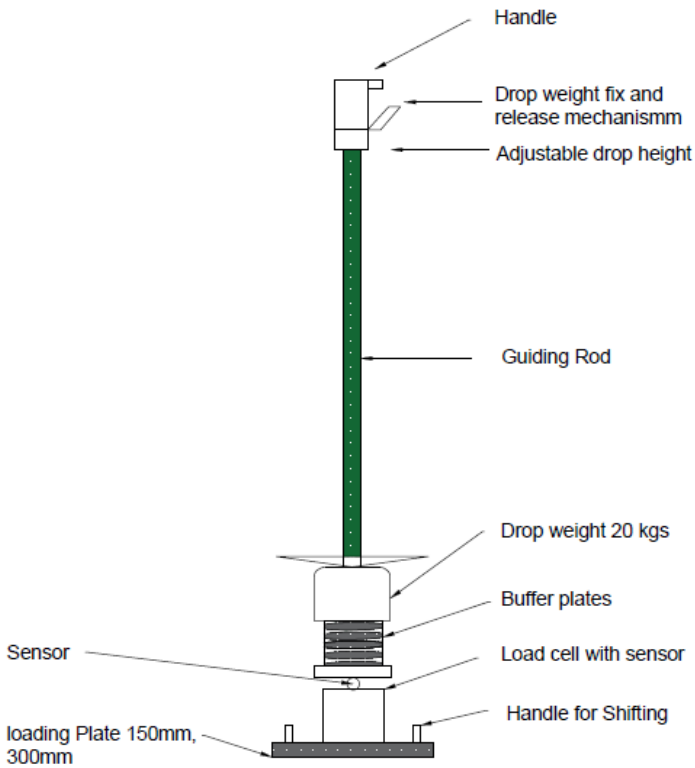

Figure 4.1: A Schematic layout of Lightweight Deflectometer (LWD)

4.2.1 Significance:

The determination of surface deflections as a result of the application of an impulse load is covered by this test method. The resulting deflections are measured at the centre of the applied load, as well as at different distances away from the load. Deflections can be utilized to assess in-situ material characteristics of the pavement layers or can be directly linked to pavement performance. The LWD can be used to ensure Quality control and quality assurance of compacted layers, structural evaluation of load carrying capacity, and thickness requirements for highway and airfield pavements are all examples of data applications.

4.2.2 Procedure:

Place the instrument above the test point you want to check. The test surface must be as clean and smooth as possible. It is recommended that a thin coating of fine sand be spread over the test point on gravel surfaces. This aids in the uniform contact of the load plate with the surface. To improve load distribution, an appropriate rubber cushion can be employed. Make that the loading plate and sensors are resting on a firm and stable test surface. Raise the falling weight to the appropriate height and let it fall freely.

Figure 4.2: LWD Apparatus

Note the peak surface deflections and peak load that result. Compare the outcomes of at least two falling weight sequences. Note the variability in the report if the difference is larger than 63 percent for any sensor. Additional testing at the same or different stress levels may be performed.

4.3 Field Test:

The field work was performed so as to compare lab data to that of field. IRC recommends that the lab values should be 1.5 times more than that of the field values. The LWD test was performed on the field to check the in-situ compaction to ensure proper compaction at the time of laying and to take the samples for unconfined compressive strength values to check weather the UCS values are in the limits as per the IRC codal provisions.

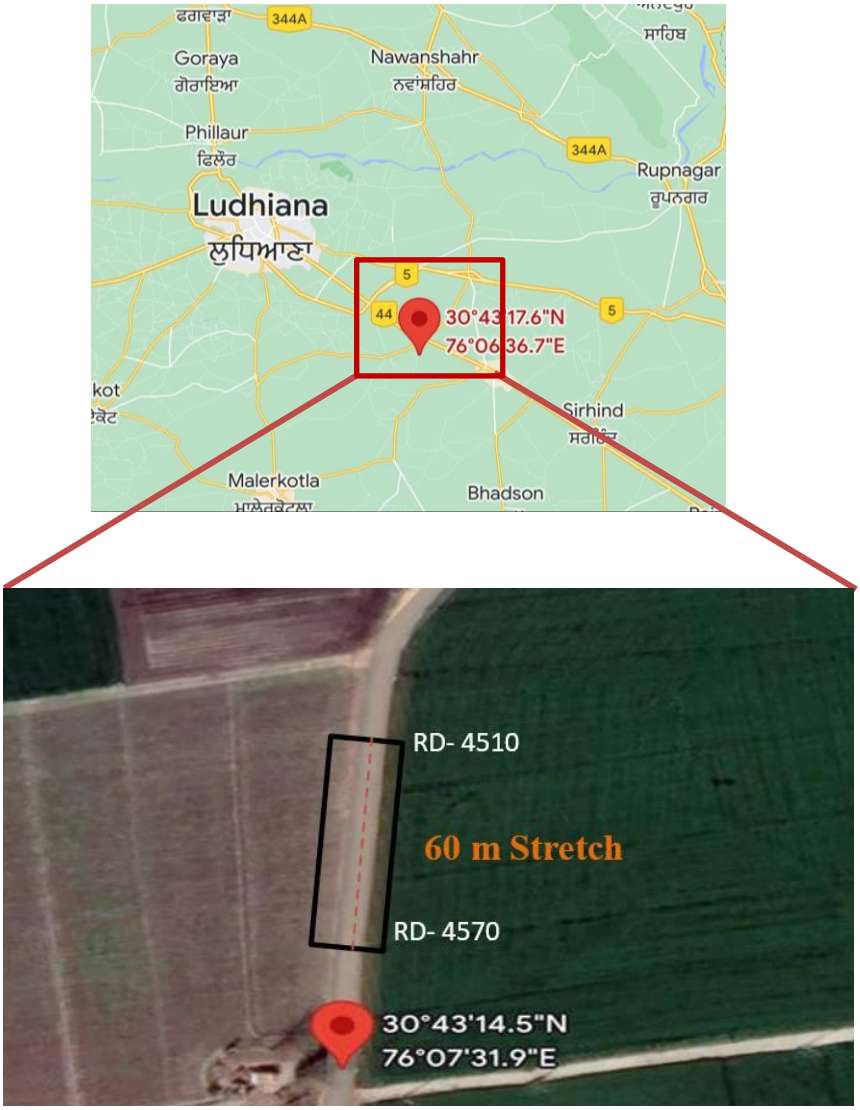

Figure 4.3: Site location (Bija)

The test was performed on field located in Bija, a district in Punjab. The figure above shows the location of PMGSY site with an intermediate lane width of 5.5m. A total of 60 meters of road were set up and separated into different portions. The road was separated lengthwise into two sections so that the mix is laid on one side while leaving the other accessible to traffic. The cement content and optimal water content were determined, and then the cement was spread in different portions as per the calculations, followed by the ideal water content. A rotavator (machine used for blending) was used to mix the soil, aggregate, cement, and water.

Figure 4.4: Marked area for spreading of cement.

To avoid damaging the rotavator's blades and perhaps delaying construction, aggregates larger than 40 mm should be eliminated from the soil-aggregate mixture. To ensure a consistent distribution of cement, mark the length and width for spreading the cement bags. Spread cement manually or mechanically as per the specification.

Figure 4.5: Spreading of Cement on different sections

Figure 4.6 : A Rotavator: Blending of cement, soil and aggregates.

The moisture content of the field was measured with a moisture meter and found to be 2.8 percent. The amount of water to be added was calculated accordingly for each mix. Seven mixtures were set out on the field, with one portion serving as a control, three sections containing cement, and the final three sections containing cement and chemical.

Figure 4.7: Moisture Meter for field moisture content.

After the field moisture was checked, the chemical was poured inside tanker as shown in the figure 4.8. Calculate the water of compaction (OMC - NMC + 2%) and then add water to the water tanker.

Figure 4.8: Mixing Chemical (Terracil and Zycobond)

Figure 4.9: Spreading Chemical (Terracil and Zycobond) on Sections.

After a tanker of 4500 liters was used to disperse water and chemical (in some areas), 4-5 rounds of rotavator were ensured so that the water, mixture, and chemical in some places were properly mixed. After proper mixing, a sample was taken from each portion for UCS testing, and the moulds were filled using both a heavyweight and a DLC hammer.

Figure 4.10: Collection of samples for UCS from field using (i) Heavy Hammer (ii) DLC Hammer

The road was ready for compaction after mixing. Three-wheel/drum static road roller was employed for compaction of sub-base. To ensure correct compaction at each spot, a lightweight deflectometer was utilized to check the in-situ compaction of soil. After the compaction was completed, the sections were then marked for the LWD test. 4 points were chosen from each section, and LWD tests were performed on them.

Figure 4.11: Compaction using 3 drum roller

Figure 4.12: Samples for 7-day UCS testing

Table 4.1: Different mixes with corresponding 7-day UCS value.

Section No.	Mix details	Mix Nomenclature	Average 7-day UCS values (MPa)
1	Soil aggregate Control Mix	SA5	1.6
2	Mix +2% cement	SA5C2	1.9
3	Mix +3% cement	SA5C3	2.1
4	Mix +4% cement	SA5C4	2.4
5	Mix +2% cement +0.6 kg/m^3	SA5C2CH3	3.2
6	Mix +3% cement +0.6 Kg/m^3	SA5C3CH3	3.42

Table 4.1 and 4.2 shows field 7-day and 28-day unconfined compressive strength of different mixes respectively. As it is clear from the table the UCS value increases as the percentage of the cement increases and continues to increase as the chemical is added. Moreover, the addition of chemicals water proofs the surface besides increasing its strength, making it behave like a water-repellent layer as can be seen in figure 4.2.

Figure 4.13: Waterproofing effect on compacted chemically treated sub-base

Table 4.2: Different mixes with corresponding 28-day UCS value.

Section No.	Mix details	Mix No.	Average 28-day UCS values (MPa)
1	Soil aggregate Control Mix	(SA5)	2.4
2	Mix +2% cement	(SA5C2)	4.3
3	Mix +3% cement	SA5C3	4.5
4	Mix +4% cement	SA5C4	4.7
5	Mix +2% cement +0.6 Kg/m^3	SA5C2CH1	6.1
6	Mix +3% cement +0.6 Kg/m^3	SA5C3CH2	6.4

4.4 Field Deflectometer testing

LWD test was performed on different points on 6 sections both after laying and after 28 days to compare the modulus and deflection values. At the time of laying the LWD was performed to check the degree of compaction using deflection values. The ratio of the in-situ density to the highest laboratory dry density is used to define the degree of compaction. By using empirical connections between the LWD modulus and degree of compaction, it can be indirectly determined from the LWD. Utilizing LWD is one of the most used correlations for assessing the level of compaction. The road plan and different points for LWD testing is shown in figure 4.13.

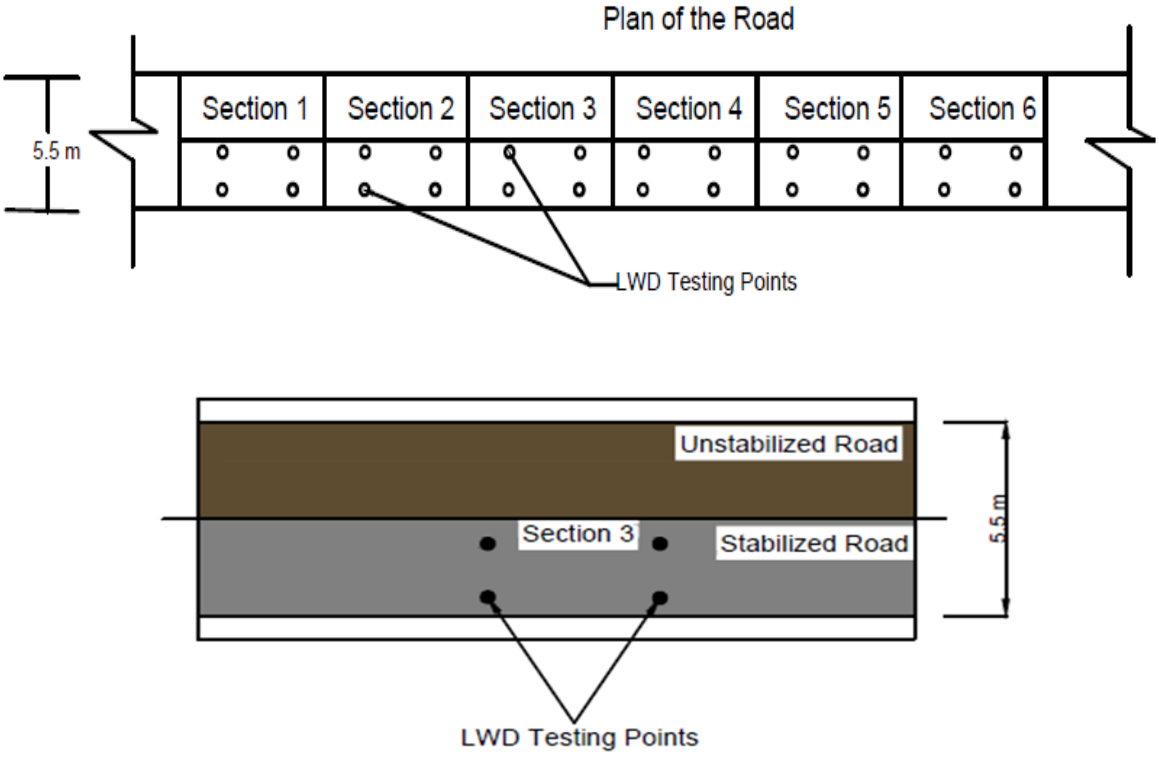

Figure 4.14 Plan of the Road and points for LWD testing

Figure 4.15: Marking of points for LWD test.

A total of 4 points were taken on each section, and one point involved six drops of Base-weight (20kgs). Out of the six drops first three are considered as the seating loads, and the final drop is used for the evaluation. Table 4.3 shows the average value of different parameters used in LWD testing. This data was taken just after laying on the sub-base layer to check the modulus and deflection values of the layer.

Table 4.3: Average (Deflection, Modulus, Stress and Load) data for different sections.

Section No.	**Description**	**Radius**	**Average Load**	**Average Stress**	**Distance (G1)**	**Average Deflection(D1)**	**Average E-Mod (MPa)**
1	SA5	150	12.02	169.96	0	508.86	87.4
2	SA5C2	150	11.48	162.56	0	412	118.45
3	SA5C3	150	12.01	162.93	0	356.21	129.95
4	SA5C4	150	12.15	172.04	0	251	139.15
5	SA5C2CH3	150	11.52	162.95	0	369	123.05
6	SA5C3CH3	150	11.31	159.8	0	361.22	136.85

Table 4.4: Average (Deflection, Modulus, Stress and Load) data for different sections after 28 days.

Section Description	**Radius**	**Average Load**	**Average Stress**	**Distance (G1)**	**Average Deflection(D1)**	**Average E-Mod (MPa)**
SA5	150	12.02	169.96	0	356	128
SA5C2	150	11.48	162.56	0	274	172
SA5C3	150	12.01	162.93	0	238	194
SA5C4	150	12.15	172.04	0	236	195
SA5C2CH1	150	11.9	172.6	0	160	283
SA5C3CH2	150	11.31	172.7	0	93	488

The LWD test was again performed after 28 days from laying of the layer to check the modulus and deflection values, the results of which are shown in the table 4.4. The higher strength of SA5C3CH3 is confirmed by XRD and SEM analysis.

CHAPTER 6

ANALYSIS AND DESIGN OF PAVEMENT SECTION

6.1 General

The pavement structure is a linear elastic multi-layered system, and when the wheel loads are applied on the top surface of the pavement structure, it can produce two types of strains:

1. Tensile strain E_t at the bottom of the bituminous layer.
2. Vertical strain, E_v on the top of the subgrade layer.

These two pavement design factors limit the bituminous layer from cracking and rutting. When the critical horizontal tensile strain (E_t) value exceeds the allowable strain value, cracking occurs on the top surface of the bituminous layer, and the pavement distresses due to fatigue; when the vertical compressive strain (E_v) value exceeds the allowable strain value, permanent deformation (rutting) occurs on the surface of the pavement structure due to subgrade overloading, and the pavement may distress due to rutting. Figure 5.1 depicts a three-layered pavement system and its critical section.

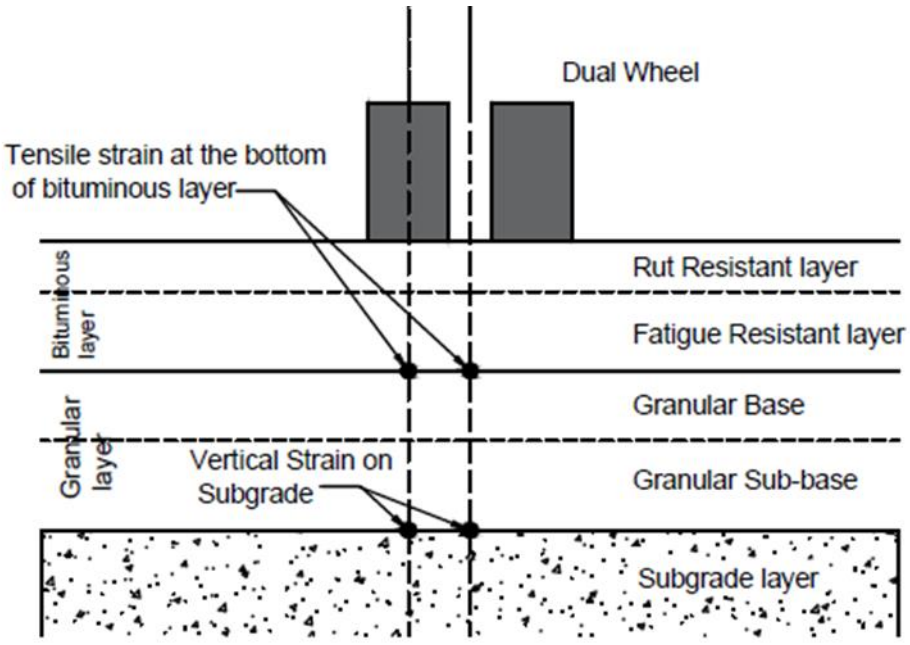

Figure 6.1: A pavement section with bituminous layer(s), granular base and GSB showing the locations of critical strains

6.2 Steps Involved in the Design of Pavements

a) Selected a trial composition

A robust subgrade, a well-drained sub-base strong enough to bear construction traffic loads, and a resistant layer to resist cracking, rutting, and moisture should help the designer in selecting the pavement composition in a high-performing pavement.

b) Selecting layer thickness

The designer's experience should be used to choose the trial thicknesses of the various layers that make up the pavement, while keeping in mind the minimum thicknesses indicated in these Guidelines and other relevant Specifications based on functional and constructability concerns.

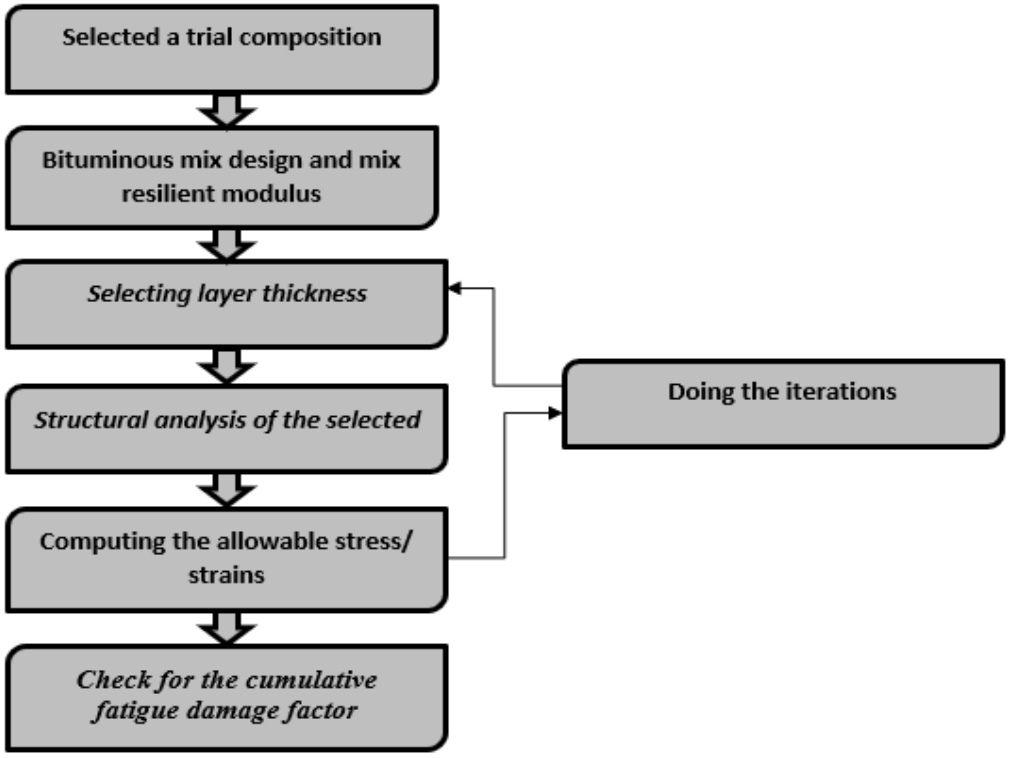

Figure 6.2:Flow chart for design of pavement.

c) Structural analysis of the selected pavement structure

The pavement structure is analyzed using IIT Pave software. Various inputs include layer thicknesses, poisons ratio, resilient modulus of different layers, standard axle load of 80 kN distributed over four wheels (20 kN on each wheel), and tyre pressure of 0.56 MPa, are required. The axle load under consideration and contact pressure of 0.80 MPa will be considered for fatigue damage analysis of cement-treated bases.

d) Computing the allowable stress/ strains

To establish the allowable strains in the bituminous layer and subgrade for the selected design traffic, utilize the fatigue and rutting performance (limited strain) models provided in IRC 37-2018(Koti Marg & Puram, n.d.). The pavement design period in terms of cumulative standard axles, and the resilient modulus value of the bottom layers are used as inputs to the models.

e) Doing the iterations

Changing the layer thickness may be necessary for a few iterations until the strains computed by IIT paving are less than the permissible strains derived from performance models.

f) Check for the cumulative fatigue damage factor

The cumulative fatigue damage analysis is required when using a cementitious base (CTB) in the pavement to ensure that the cumulative damage caused by the expected axle load spectrum does not exceed unity.

6.3 Pavement analysis and Results for conventional pavement (IRC-37, 2018)

Elastic modulus of Subgrade = 63 MPa

GSB and WMM combined modulus = $0.2*(400)^{0.45}*63 = 186.76$ MPa

Modulus of bituminous layer = 3 000 MPa

Subgrade rutting

$N_R = 4.1656 \times 10^{-08} [1/\varepsilon_v]^{4.5337}$

For 5 msa traffic (low Volume Roads)

$5*10^6 = 4.1656 \times 10^{-08} [1/\varepsilon_v]^{4.5337}$

E_v = 784.3 microns

Fatigue cracking

$N_f = 1.6064*C*10^{-04} [1/\varepsilon t]^{3.89}*[1/M_{Rm}]^{0.854}$

$5*10^6 = 1.6064*2.556*10^{-04} [1/\varepsilon_t]^{3.89} * [1/3000]^{0.854}$

E_t = 465 microns

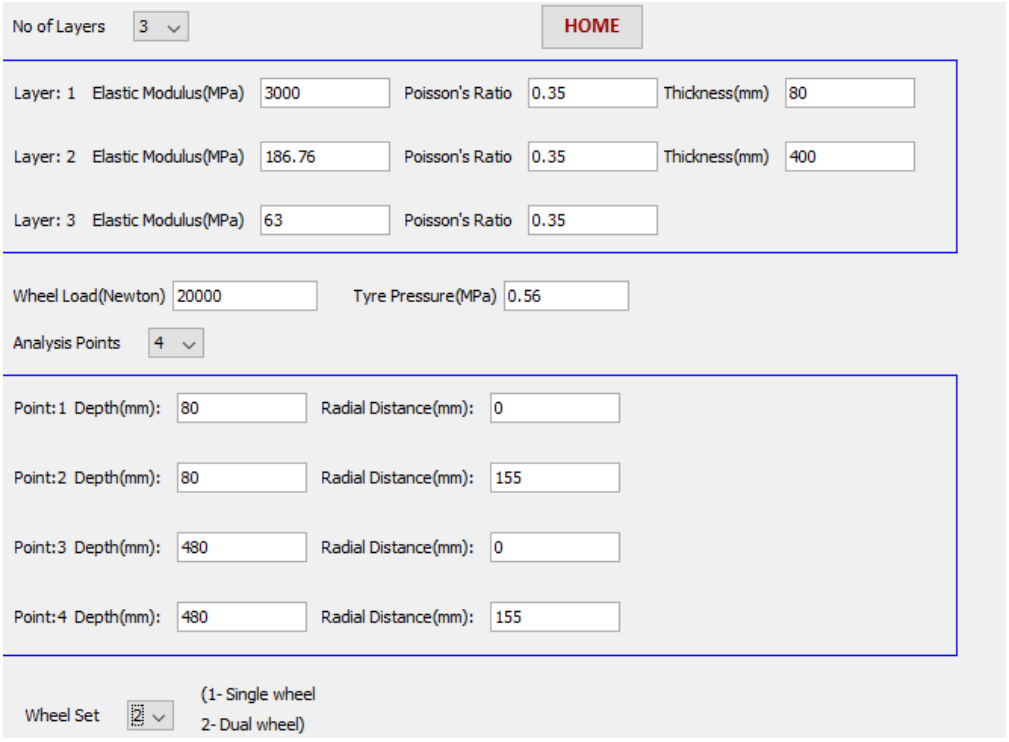

Figure 6.3: IIT Pave Input Screen for conventional section

Table 6.1: Allowable Stress and Actual Strain for 5 MSA with Granular Sub-Base

Distress Type	**Allowable stress**	**Actual Strains**
Subgrade Rutting	784.3 microns	548 microns
Fatigue Cracking	465 microns	318.6 microns

```
No. of layers                3
E values (MPa)          3000.00  186.76   63.00
Mu values                  0.350.350.35
thicknesses (mm)           80.00  400.00
single wheel load (N) 20000.00
tyre pressure (MPa)        0.56
Dual  Wheel
  Z         R       SigmaZ       SigmaT      SigmaR      TaoRZ       DispZ       epZ         epT         epR
 80.00     0.00-0.2104E+00 0.1233E+01 0.1003E+01-0.1935E-01 0.5783E+00-0.3310E-03 0.3186E-03 0.2150E-03
 80.00L    0.00-0.2104E+00-0.2945E-01-0.4379E-01-0.1935E-01 0.5783E+00-0.9891E-03 0.3186E-03 0.2150E-03
 80.00   155.00-0.1529E+00 0.8353E+00 0.7320E-02-0.9119E-01 0.5844E+00-0.1493E-03 0.2954E-03-0.7718E-04
 80.00L 155.00-0.1529E+00-0.2518E-01-0.7673E-01-0.9119E-01 0.5844E+00-0.6275E-03 0.2954E-03-0.7718E-04
480.00     0.00-0.3026E-01 0.4098E-01 0.3366E-01-0.5546E-02 0.3837E+00-0.3019E-03 0.2131E-03 0.1602E-03
480.00L    0.00-0.3018E-01 0.3064E-02 0.5833E-03-0.5546E-02 0.3838E+00-0.4993E-03 0.2131E-03 0.1599E-03
480.00   155.00-0.3288E-01 0.4451E-01 0.3895E-01-0.8259E-02 0.3976E+00-0.3325E-03 0.2270E-03 0.1868E-03
480.00L 155.00-0.3289E-01 0.3281E-02 0.1408E-02-0.8244E-02 0.3976E+00-0.5480E-03 0.2269E-03 0.1868E-03
```

Figure 6.4: Strain Values from IIT Pave

Pavement analysis and Results for pavement with chemical stabilized Sub-Base (Section-6)

Elastic modulus of Subgrade = 63 MPa

Modulus of chemical stabilized Sub-Base = 488 MPa

Modulus of WMM = 350 MPa

Modulus of bituminous layer =3 000 MPa

Subgrade rutting

$N_R = 1.4100 \times 10^{-08} [1/\varepsilon_v]^{4.5337}$

For 5 msa traffic

$5*10^6 = 4.1656 \times 10^{-08} [1/\varepsilon_v]^{4.5337}$

E_v = 784.3 microns

Fatigue cracking

$N_f = 1.6064*C*10^{-04} [1/\varepsilon t]^{3.89}*[1/M_{Rm}]^{0.854}$

$5*10^6 = 1.6064*2.556*10^{-04} [1/\varepsilon_t]^{3.89} * [1/3000]^{0.854}$

E_t = 465 microns

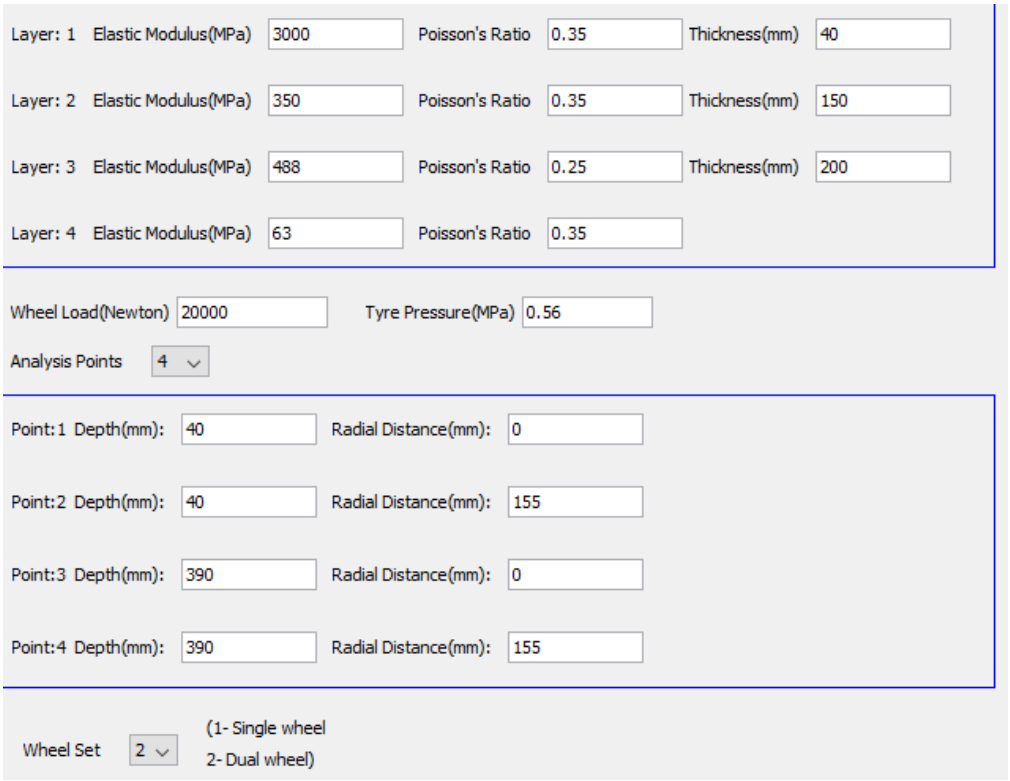

Figure 6.5: IIT Pave Input Screen for SA5C3CH3

Table 6.2: Allowable Stress and Actual Strain for 5 MSA with chemically stabilized Sub-Base (Section-6)

Distress Type	Allowable stress	Actual Strains
Subgrade Rutting	784.3 microns	566 microns
Fatigue Cracking	465 microns	192.1 microns

```
No. of layers                4
E values (MPa)         3000.00  350.00  488.00   63.00
Mu values                0.350.350.250.35
thicknesses (mm)         40.00  150.00  200.00
single wheel load (N) 20000.00
tyre pressure (MPa)       0.56
Dual  Wheel
  Z        R      SigmaZ      SigmaT     SigmaR     TaoRZ      DispZ      epZ        epT        epR
 40.00    0.00-0.4630E+00 0.6097E+00 0.5585E+00-0.1334E-01 0.5438E+00-0.2906E-03 0.1921E-03 0.1691E-03
 40.00L   0.00-0.4630E+00-0.1491E+00-0.1550E+00-0.1334E-01 0.5438E+00-0.1019E-02 0.1921E-03 0.1691E-03
 40.00  155.00-0.1313E+00-0.1434E-02-0.9428E+00-0.1368E+00 0.4943E+00 0.6638E-04 0.1248E-03-0.2988E-03
 40.00L 155.00-0.1313E+00-0.6264E-01-0.1725E+00-0.1368E+00 0.4943E+00-0.1402E-03 0.1248E-03-0.2988E-03
390.00    0.00-0.3228E-01 0.1241E+00 0.9669E-01-0.5691E-02 0.3938E+00-0.1792E-03 0.2213E-03 0.1511E-03
390.00L   0.00-0.3228E-01 0.2294E-02-0.9688E-03-0.5690E-02 0.3938E+00-0.5198E-03 0.2212E-03 0.1512E-03
390.00  155.00-0.3496E-01 0.1347E+00 0.1083E+00-0.1056E-01 0.4084E+00-0.1961E-03 0.2384E-03 0.1708E-03
390.00L 155.00-0.3495E-01 0.2588E-02-0.5685E-03-0.1056E-01 0.4084E+00-0.5660E-03 0.2384E-03 0.1708E-03
```

Figure 6.6 : Actual Strain Values from IIT Pave for SA5C3CH3

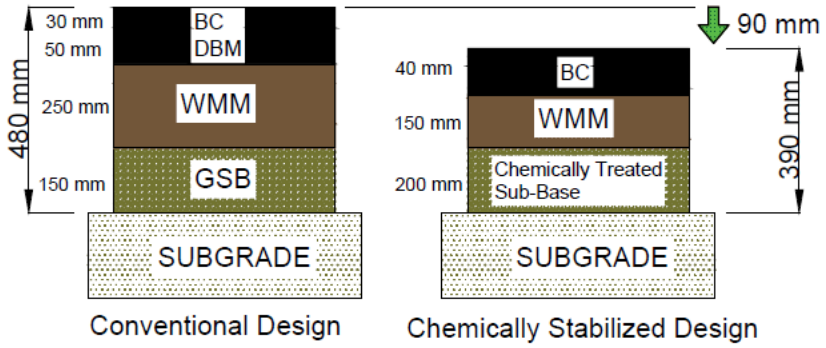

Figure 6.7: Thickness comparison of Conventional design and Chemically treated design.

The difference in thickness in the conventional design and the chemically treated design is shown in the figure 5.3. IRC 37 doesn't recommend DBM layer for traffic volume less than 10 MSA

Table 6.3: Allowable Stresses and Actual Strains for different sections.

Section Description	E-Mod (MPa)	Allowable subgrade rutting stress	Allowable fatigue cracking stress	Actual subgrade rutting stress	Actual fatigue cracking stress
Conventional section	186.76	784.3 microns	465 microns	548 microns	318.6 microns
SA5	128			612.3 microns	207 microns
SA5 C2	172			611.6 microns	204.4 microns
SA5C3	194			611.1 microns	203.7 microns
SA5C4	195			610.5 microns	203.6 microns
SA5C2CH3	283			608.1 microns	199.9 microns
SA5C3CH3	488			566 microns	192.1 microns

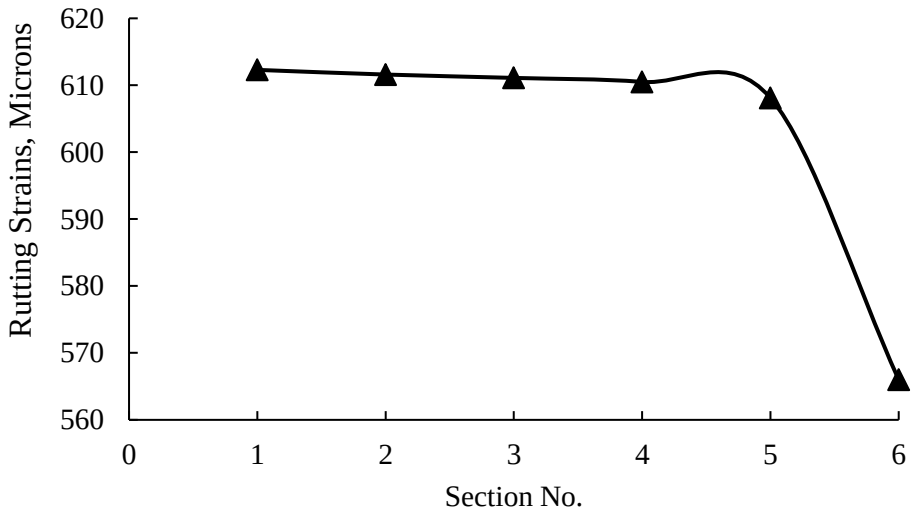

Figure 6.8 : Variation of Strain values (Rutting) for different sections

The allowable and actual strain values from IIT pave is listed in table 5.3. The table depicts that with the increase in the modulus values the strain value decreases for both bottom bituminous layer and top of subgrade

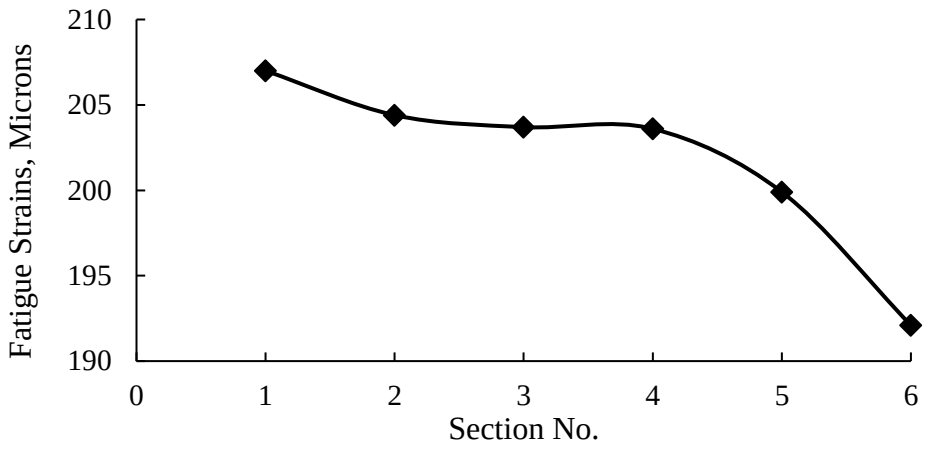

Figure 6.9 : Variation of Strain values (Rutting) for different sections

The strain values (both rutting and fatigue) are reduced as the modulus values are increased. The strain values are reduced because when the layer's modulus increases, the surface becomes stiffer, transferring less stress to the bottom layers. The figure shows a graphical representation of various strains (Rutting and Fatigue) on different sections.

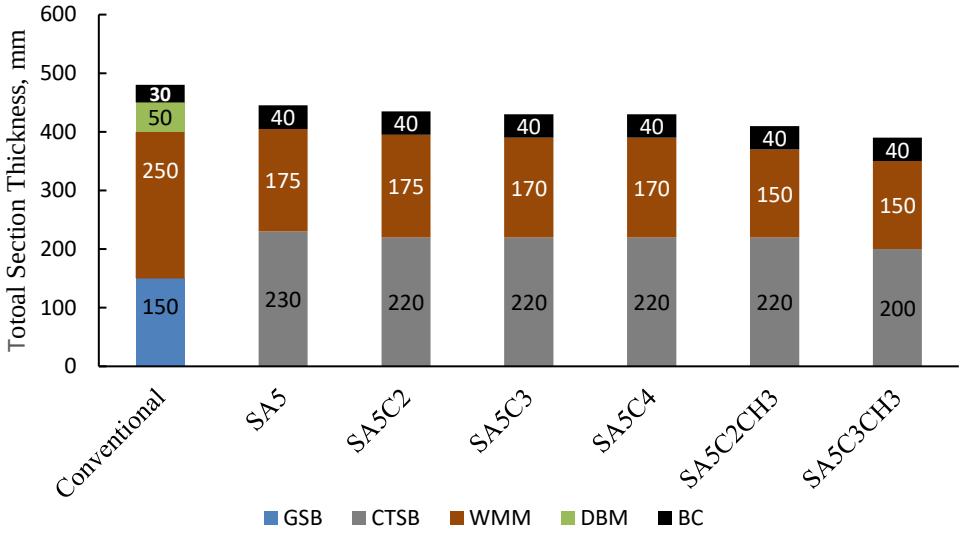

Figure 6.10 : Sections with corresponding design thicknesses

The figure graphically depicts the layer thickness of various portions. When comparing the conventional section to the optimum Section (SA5C3CH2), the thickness is lowered to 90 mm, and the DBM layer is removed (as per IRC-37, 2018), resulting in significant cost savings for low-traffic roads.

6.4 Cost Analysis

Because of the massive investment in transportation sector, cost analysis becomes one of the crucial factors in the transportation industry. In India, where there is very high growth in this sector, certain modifications in different aspects are made to make it as economical as possible. Inputs used to estimate the cost of a roadway construction project with any section are the road's length, the road's width, the layer's thickness, and the cost of 1cumec of material. The table 6.4 shows the cost analysis of a conventional low volume road (5 MSA traffic)

Bituminous concrete Layer

Length of road: 1000m

Width of road: 7m

Thickness of asphalt layer :0.03m

Therefore, volume of asphalt:

V= 1000*7.0*0.03 =210m^3

Cost of Bituminous concrete Layer = 12,138 /m^3

Total Cost of BC layer = 210*12,138= Rs 25,48,980/=

DBM Layer

Length of DBM bed = 1000m

Breadth of DBM bed = 7m 45

Thickness of DBM layer =0.05m

Volume of DBM layer = L*B*H

1000*7*0.05= 350 m^3

Cost of DBM layer = 11,013 /m^3

Total cost of DBM layer= 11013 * 350 = Rs 38,54,550/=

WMM Layer

Length of WMM bed = 1000m

Breadth of WMM bed = 7m

Thickness of WMM layer =0.25m

Volume of WMM layer = L*B*H

1000*7*0.25=1750m3

Rate of WMM = 2803.65 /m^3

Total cost of WMM = 1750*2803.65 = Rs, 49,06,387/=

GSB Layer:

Length of GSB bed = 1000m

Breadth of GSB bed = 7m

Thickness of GSB layer =0.15m

Volume of GSB layer = L*B*H

1000*7*0.2=1050 m^3

Cost of GSB = 2658.10 /m^3

Total cost of GSB layer= 1050* 2658.10 = 27,91,005/=

Table 6.4: Quantity and cost per Km for Low volume Road (Conventional Section).

Case I – Conventional pavement section							
Layers	**Thickness (mm)**	**Width (m)**	**Length (m)**	**Quantity (m^3)**	**Cost Incurred (INR)**	**Amount (Lacs)**	**Total Amount (lacs)**
BC	30	7	1000	210	12,138	25.48	140.99
DBM	50			350	11,013	38.54	
WMM	250			1750	2803.65	49.06	
GSB	150			1050	2658.10	27.91	

Table 6.5: Quantity and cost per Km for Low volume Road (Chemically stabilized section).

Case II – Optimal pavement section (6)							
Layers	**Thickness (mm)**	**Width (m)**	**Length (m)**	**Quantity (m^3)**	**Cost Incurred (INR)**	**Amount (Lacs)**	**Total Amount (lacs)**
BC	40	7	1000	280	12,138	33.98	105.9
WMM	150			1050	2803.65	29.43	
Chemically treated Sub-base	200			1400	3020.25	42.28	

When comparing the conventional section with the ideal/optimal section for roads with design traffic of 5 msa (low volume roads), the cost and thickness are reduced by 33.4 % and 23%, respectively. The graphical comparison of different layers in conventional and chemically stabilized section is shown in the figure below

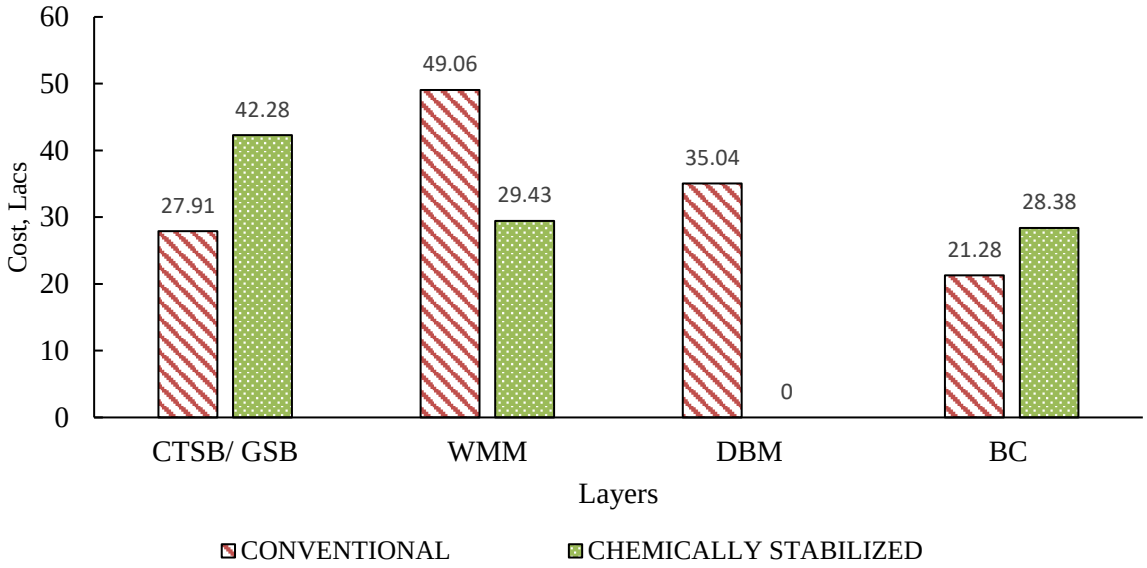

Figure 6.11: Comparison of cost for conventional and Chemically stabilized section.

The graph shown above depicts a Comparison between the conventional design and the most optimal design section (SA5C3CH3). It is evident that using the traditional design is quite expensive and that using chemically stabilized sub-bases can lower the cost by roughly 33.4%.

CHAPTER 7
CONCLUSION

In this study, the mix design and analysis of flexible pavement for low-volume roads produce noteworthy findings about the thickness of various layers and the overall thickness of the pavement section, respectively. This study's significant findings can be summarised as follows:

1. The 7-Day UCS values increased as the percentages of the cement and chemical is increased. The optimum percentage value of cement and chemical are 3% and 0.6kg/m^3 respectively. The 7 days UCS strength of chemically based cement treated mix was approximately 103.4% more than the control mix.
2. A similar trend is observed in 28-days UCS strength. The 28-days UCS strength of chemically based cement treated mix was approximately 80% more than the control mix.
3. With the addition of cement and chemical, the CBR value increased from 18.4% for SA5 (60%soil and 40% aggregates) mix to 58.8% for SA5C3CH3 (60%soil and 40% aggregates+ 3% cement + 0.6kg/m^3 chemical). The increase in the percentage of CBR value is 219%.
4. The most ideal chemically based cement treated section has a thickness of 390mm for a traffic count of 5 msa compared to 480mm for the conventional section. There has been a 23% reduction in thickness.
5. The chemically based cement treated section was 33.4% cheaper than the conventional pavement section for low volume roads.
6. The Deflectometric studies show an increase in the modulus as the chemical and cement dosage increases. The SA5C4 mix has the highest modulus at the time of laying because of the high cement percentage. After 28 days, SA5C3CH3 mix has the highest modulus and the least amount of deflection.
7. The microstructural analysis shows that the addition of nanoparticles in SA5C3 (60%soil and 40% aggregates+ 3% cement) sample enhances the mechanical strength which is 3 times higher than SA5 sample because of the formation of rod like structures (ettringites) which results in the densification of the matrix.

The recommended course aggregate to fine aggregate (Locally available soil) ratio should be 40:30 with 3% of cement and 0.6kg/m^3 chemical (Terracil and Zycobond) for low volume

traffic roads (< 5msa traffic volume). To ensure adequate mixing of aggregates and soil, a rotavator should be allowed to pass several times and chemicals should be mixed under competent supervision.

A thorough Deflectometric study should be carried out using Falling weight deflectometer on the existing chemically based cement treated sub-base road so that the same technology can be implemented on the national highways.

REFERENCES

1. Al-Rawas, A. A., Hago, A. W., & Al-Sarmi, H. (2005). Effect of lime, cement and Sarooj (artificial pozzolan) on the swelling potential of an expansive soil from Oman. Building and Environment, 40(5), 681–687.
2. Ateş, A. (2016). Mechanical properties of sandy soils reinforced with cement and randomly distributed glass fibers (GRC). Composites Part B: Engineering, 96, 295–304.
3. Baghini, M. S., Ismail, A., & Karim, M. R. bin. (2015). Evaluation of cement-treated mixtures with slow setting bitumen emulsion as base course material for road pavements. Construction and Building Materials, 94, 323–336.
4. Brooks, R. M. (2009). Soil stabilization with fly ash and rice husk ash. International Journal of Research and Reviews in Applied Sciences, 1(3), 209–217.
5. Buazar, F. (2019). Impact of biocompatible nanosilica on green stabilization of subgrade soil. Scientific Reports, 9(1), 1–9.
6. Catton, M. D. (1941). Research on the physical relations of soil and soil-cement mixtures. Highway Research Board Proceedings, 20.
7. Chew, S. H., Kamruzzaman, A. H. M., & Lee, F. H. (2004). Physicochemical and engineering behavior of cement treated clays. Journal of Geotechnical and Geoenvironmental Engineering, 130(7), 696–706.
8. Consoli, N. C., Rosa, D. A., Cruz, R. C., & Dalla Rosa, A. (2011). Water content, porosity and cement content as parameters controlling strength of artificially cemented silty soil. Engineering Geology, 122(3–4), 328–333.
9. Farzadnia, N., Ali, A. A. A., & Demirboga, R. (2013a). Characterization of high strength mortars with nano alumina at elevated temperatures. Cement and Concrete Research, 54, 43–54.
10. Farzadnia, N., Ali, A. A. A., & Demirboga, R. (2013b). Characterization of high strength mortars with nano alumina at elevated temperatures. Cement and Concrete Research, 54, 43–54.
11. Gayathri, M. S., & Pal, S. K. (2021). Comparison of Compaction Characteristics of Non-conventional Conventional Stabilizers. Proceedings of the Indian Geotechnical Conference 2019, 727–737.

12. Givi, A. N., Rashid, S. A., Aziz, F. N. A., & Salleh, M. A. M. (2010). Experimental investigation of the size effects of SiO2 nano-particles on the mechanical properties of binary blended concrete. Composites Part B: Engineering, 41(8), 673–677.
13. Guefrech, A., Mounanga, P., & Khelidj, A. (2011). Experimental study of the effect of addition of nano-silica on the behaviour of cement mortars Mounir. Procedia Engineering, 10, 900–905.
14. Guzzarlapudi, S. D., Adigopula, V. K., & Kumar, R. (2016a). Comparative studies of lightweight deflectometer and Benkelman beam deflectometer in low volume roads. Journal of Traffic and Transportation Engineering (English Edition), 3(5), 438–447.
15. Guzzarlapudi, S. D., Adigopula, V. K., & Kumar, R. (2016b). Comparative studies of lightweight deflectometer and Benkelman beam deflectometer in low volume roads. Journal of Traffic and Transportation Engineering (English Edition), 3(5), 438–447.
16. Guzzarlapudi, S. D., Adigopula, V. K., & Kumar, R. (2016c). Comparative studies of lightweight deflectometer and Benkelman beam deflectometer in low volume roads. Journal of Traffic and Transportation Engineering (English Edition), 3(5), 438–447.
17. Kawashima, S., Hou, P., Corr, D. J., & Shah, S. P. (2013). Modification of cement-based materials with nanoparticles. Cement and Concrete Composites, 36, 8–15.
18. Kumar, H., Raju, P. G., & Verma, A. K. (2020). Black Cotton Soil in Highway Construction. Helix-The Scientific Explorer| Peer Reviewed Bimonthly International Journal, 10(01), 144–148.
19. Madurwar, K. v, Dahale, P. P., & Burile, A. N. (2013). Comparative study of black cotton soil stabilization with RBI Grade 81 and sodium silicate. International Journal of Innovative Research in Science, Engineering and Technology, 2(2), 493–499.
20. Montepara, A., Tebaldi, G., Marradi, A., & Betti, G. (2012). Effect on pavement performance of a subbase layer composed by natural aggregate and RAP. Procedia-Social and Behavioral Sciences, 53, 980–989.
21. Nima, F., Ali, A. A. A., & Demirboga, R. (2012). Development of nanotechnology in high performance concrete. Advanced Materials Research, 364, 115–118.
22. Okyay, U. S., & Dias, D. (2010). Use of lime and cement treated soils as pile supported load transfer platform. Engineering Geology, 114(1–2), 34–44.
23. Padmavathi, V., Nirmala Peter, E. C., Rao, P. N., & Padmavathi, M. (2018). Stabilization of soil using terrasil, zycobond and cement as admixtures. International Congress and Exhibition" Sustainable Civil Infrastructures: Innovative Infrastructure Geotechnology", 163–170.

24. Pagar, S., D, A., Rahul, R., Sangale, Y., & Patil, Y. (2018, May). Cement Treated Sub-Base for Bituminous Pavement.
25. Patel, N. A., Mishra, C. B., Dave, S. K., & Parmar, D. K. (2015). Investigating the Modifications in Properties of Clayey Soil Utilizing ppc for Variable Dynamic Compaction. International Journal of Research in Engineering and Technology.
26. Patel, N. A., Mishra, C. B., & Pancholi, V. v. (2015a). Scientifically surveying the usage of Terrasil chemical for soil stabilization. Int. J. Res. Advent Technol, 3(6), 77–84.
27. Patel, N. A., Mishra, C. B., & Pancholi, V. v. (2015b). Scientifically surveying the usage of Terrasil chemical for soil stabilization. Int. J. Res. Advent Technol, 3(6), 77–84.
28. Patel, N. A., Mishra, C. B., Parmar, D. K., & Gautam, S. B. (2015). Subgrade soil stabilization using chemical additives. International Research Journal of Engineering and Technology (IRJET), 2(4), 1089–1095.
29. Patil, B. M., & Patil, K. A. (2013). Effect of pond ash and RBI Grade 81 on properties of subgrade soil and base course of flexible pavement. International Journal of Civil and Environmental Engineering, 7(12), 966–971.
30. Prabakar, J., Dendorkar, N., & Morchhale, R. K. (2004). Influence of fly ash on strength behavior of typical soils. Construction and Building Materials, 18(4), 263–267.
31. Prasad, A., & Reddy, C. N. V. S. (2011). The Potential of Cement Stabilized Gravelly Soils as Construction Material. Proc. of Indian Geotechnical Conference-2011, Kochi, India, 493–496.
32. Raghwa, A., & Sonthwal, E. V. K. (2021). REVIEW OF IMPROVING PROPERTIES OF SOIL USING FLY-ASH AND TERRA-ZYME.
33. Rathod, R. G. (2017). Efficient way to improve subgrade property of pavement by chemical stabilization. Int. J. Eng. Res. Appl, 7(1), 83–86.
34. Samal, K. P. (n.d.). Performance of Low Cost Materials for Stabilization of Black Cotton Soil: A Review.
35. Shirahatti, P. N., Kallimani, P. M., & Rajashekhar, M. S. (2016). Application of geo-textile and terrasil chemical to reduce permeability of soil. International Journal for Scientific Research & Development (IJSRD), 4(06).
36. Shooshpasha, I., & Shirvani, R. A. (2015). Effect of cement stabilization on geotechnical properties of sandy soils. Geomech Eng, 8(1), 17–31.

37. Singh, G., Jain, S., Tiwari, D., Dave, S. M., & Singh, A. (2020a). Assessment of modulus using falling weight deflectometer and cores for stabilized layer. Materials Today: Proceedings, 32, 698–705.
38. Singh, G., Jain, S., Tiwari, D., Dave, S. M., & Singh, A. (2020b). Assessment of modulus using falling weight deflectometer and cores for stabilized layer. Materials Today: Proceedings, 32, 698–705.
39. Singh, G., & Yadav, R. K. (2018). Effect of RBI grade 81 on index properties and compaction characteristics of fine grained soil.
40. Stefanidou, M., & Papayianni, I. (2012). Influence of nano-SiO2 on the Portland cement pastes. Composites Part B: Engineering, 43(6), 2706–2710.
41. Zabielska-Adamska, K. (2008). Laboratory compaction of fly ash and fly ash with cement additions. Journal of Hazardous Materials, 151(2–3), 481–489.
42. Zahoor, S., & Jassal, K. (2020). Sub-Grade Stabilization using Nano Particles.

ANNEXURE – O1

For 5 msa traffic the strain values are calculated using equations from IRC 37-2018

For 5 msa traffic (low Volume Roads)

$5*10^6 = 4.1656 \times 10^{-08} [1/\varepsilon_v]^{4.5337}$

E_v = 784.3 microns

Fatigue cracking

$N_f = 1.6064*C*10^{-04} [1/\varepsilon t]^{3.89}*[1/M_{Rm}]^{0.854}$

$5*10^6 = 1.6064*2.556*10^{-04} [1/\varepsilon_t]^{3.89} * [1/3000]^{0.854}$

E_t = 465 microns

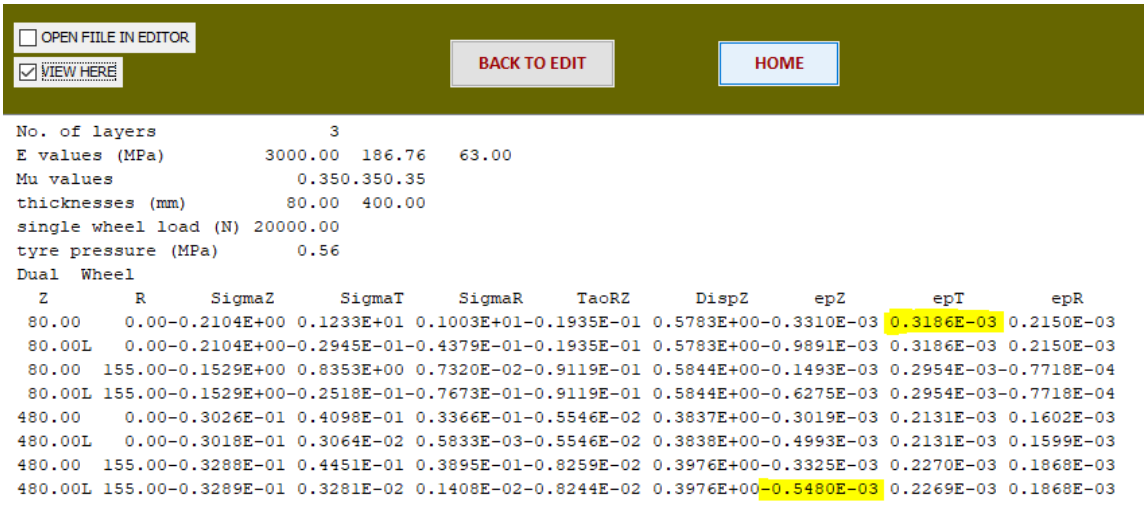


```
No. of layers                3
E values (MPa)          3000.00  186.76   63.00
Mu values                  0.350.350.35
thicknesses (mm)           80.00  400.00
single wheel load (N) 20000.00
tyre pressure (MPa)        0.56
Dual  Wheel
  Z         R       SigmaZ       SigmaT      SigmaR      TaoRZ       DispZ       epZ         epT         epR
 80.00     0.00-0.2104E+00 0.1233E+01 0.1003E+01-0.1935E-01 0.5783E+00-0.3310E-03 0.3186E-03 0.2150E-03
 80.00L    0.00-0.2104E+00-0.2945E-01-0.4379E-01-0.1935E-01 0.5783E+00-0.9891E-03 0.3186E-03 0.2150E-03
 80.00   155.00-0.1529E+00 0.8353E+00 0.7320E-02-0.9119E-01 0.5844E+00-0.1493E-03 0.2954E-03-0.7718E-04
 80.00L 155.00-0.1529E+00-0.2518E-01-0.7673E-01-0.9119E-01 0.5844E+00-0.6275E-03 0.2954E-03-0.7718E-04
480.00     0.00-0.3026E-01 0.4098E-01 0.3366E-01-0.5546E-02 0.3837E+00-0.3019E-03 0.2131E-03 0.1602E-03
480.00L    0.00-0.3018E-01 0.3064E-02 0.5833E-03-0.5546E-02 0.3838E+00-0.4993E-03 0.2131E-03 0.1599E-03
480.00   155.00-0.3288E-01 0.4451E-01 0.3895E-01-0.8259E-02 0.3976E+00-0.3325E-03 0.2270E-03 0.1868E-03
480.00L 155.00-0.3289E-01 0.3281E-02 0.1408E-02-0.8244E-02 0.3976E+00-0.5480E-03 0.2269E-03 0.1868E-03
```

Figure 1:Actual strain values for conventional section.

The figure is taken from IIT pave where the vertical compressive strain at the top of subgrade is given by ep_z and the horizontal tensile strains at the bottom of the bottom bituminous layer is shown by ep_t.

```
No. of layers                4
E values (MPa)          3000.00  350.00  128.00   63.00
Mu values                  0.350.350.250.35
thicknesses (mm)           40.00  175.00  230.00
single wheel load (N) 20000.00
tyre pressure (MPa)        0.56
Dual  Wheel
  Z         R       SigmaZ       SigmaT      SigmaR      TaoRZ       DispZ       epZ         epT         epR
 40.00     0.00-0.4529E+00 0.6782E+00 0.6164E+00-0.2197E-01 0.6486E+00-0.3020E-03 0.2070E-03 0.1792E-03
 40.00L    0.00-0.4529E+00-0.1363E+00-0.1435E+00-0.2197E-01 0.6486E+00-0.1014E-02 0.2070E-03 0.1792E-03
 40.00   155.00-0.1242E+00 0.6802E-01-0.8887E+00-0.1722E+00 0.6097E+00 0.5435E-04 0.1408E-03-0.2897E-03
 40.00L 155.00-0.1242E+00-0.5113E-01-0.1627E+00-0.1722E+00 0.6097E+00-0.1409E-03 0.1408E-03-0.2897E-03
445.00     0.00-0.3355E-01 0.2806E-01 0.2120E-01-0.6297E-02 0.4075E+00-0.3583E-03 0.2434E-03 0.1763E-03
445.00L    0.00-0.3356E-01 0.3824E-02 0.6938E-03-0.6299E-02 0.4075E+00-0.5579E-03 0.2433E-03 0.1762E-03
445.00   155.00-0.3653E-01 0.3046E-01 0.2470E-01-0.1024E-01 0.4229E+00-0.3931E-03 0.2610E-03 0.2048E-03
445.00L 155.00-0.3654E-01 0.4218E-02 0.1599E-02-0.1023E-01 0.4229E+00-0.6123E-03 0.2610E-03 0.2049E-03
```

Figure 2: Actual values for SA5

The strains values on the top of subgrade (ep_z) and on the bottom of the bottom bituminous layers (ep_t) are 566 microns and 192.1 microns respectively which are less than the allowable values, hence the design is safe.

OPEN FILE IN EDITOR

VIEW HERE

BACK TO EDIT

HOME

```
No. of layers                4
E values (MPa)          3000.00  350.00  172.00   63.00
Mu values                 0.350.350.250.35
thicknesses (mm)          40.00  175.00  220.00
single wheel load (N) 20000.00
tyre pressure (MPa)        0.56
Dual  Wheel
  Z         R       SigmaZ       SigmaT      SigmaR      TaoRZ       DispZ       epZ         epT         epR
 40.00     0.00-0.4552E+00 0.6659E+00 0.6060E+00-0.1936E-01 0.6171E+00-0.3001E-03 0.2044E-03 0.1774E-03
 40.00L    0.00-0.4552E+00-0.1388E+00-0.1458E+00-0.1936E-01 0.6171E+00-0.1016E-02 0.2044E-03 0.1774E-03
 40.00   155.00-0.1261E+00 0.5533E-01-0.8986E+00-0.1638E+00 0.5752E+00 0.5636E-04 0.1380E-03-0.2913E-03
 40.00L 155.00-0.1261E+00-0.5350E-01-0.1648E+00-0.1638E+00 0.5752E+00-0.1419E-03 0.1380E-03-0.2913E-03
435.00     0.00-0.3342E-01 0.4196E-01 0.3237E-01-0.6330E-02 0.4037E+00-0.3023E-03 0.2455E-03 0.1758E-03
435.00L    0.00-0.3343E-01 0.4044E-02 0.7963E-03-0.6333E-02 0.4037E+00-0.5575E-03 0.2455E-03 0.1759E-03
435.00   155.00-0.3645E-01 0.4565E-01 0.3730E-01-0.1054E-01 0.4190E+00-0.3325E-03 0.2641E-03 0.2035E-03
435.00L 155.00-0.3641E-01 0.4452E-02 0.1596E-02-0.1060E-01 0.4191E+00-0.6116E-03 0.2641E-03 0.2029E-03
```

Figure 3: Actual strain values of (SA5C2)

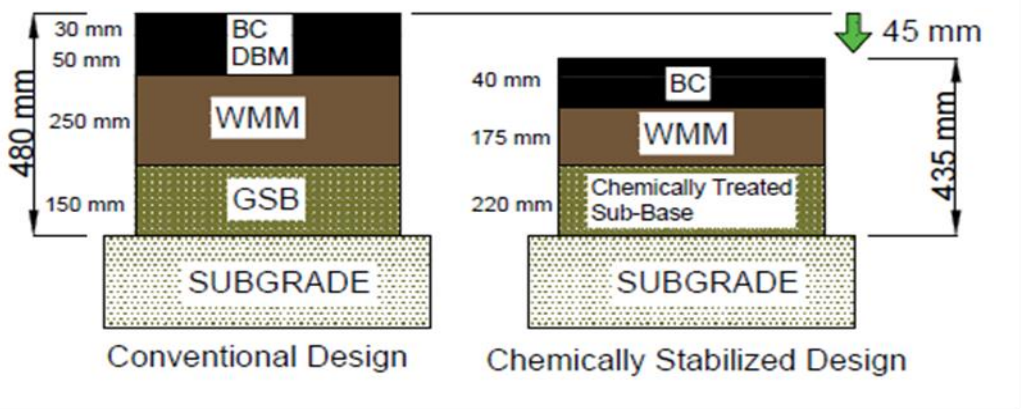

Figure 4: Comparison of conventional section with SA5C2

OPEN FILE IN EDITOR

VIEW HERE

BACK TO EDIT

HOME

```
No. of layers                4
E values (MPa)          3000.00  350.00  194.00   63.00
Mu values                 0.350.350.250.35
thicknesses (mm)          40.00  170.00  220.00
single wheel load (N) 20000.00
tyre pressure (MPa)        0.56
Dual  Wheel
  Z        R      SigmaZ      SigmaT      SigmaR      TaoRZ       DispZ       epZ         epT         epR
 40.00     0.00-0.4557E+00 0.6626E+00 0.6032E+00-0.1851E-01 0.6078E+00-0.2996E-03 0.2037E-03 0.1769E-03
 40.00L    0.00-0.4558E+00-0.1395E+00-0.1464E+00-0.1851E-01 0.6078E+00-0.1016E-02 0.2037E-03 0.1769E-03
 40.00  155.00-0.1266E+00 0.5189E-01-0.9015E+00-0.1613E+00 0.5650E+00 0.5691E-04 0.1372E-03-0.2918E-03
 40.00L 155.00-0.1266E+00-0.5418E-01-0.1654E+00-0.1613E+00 0.5650E+00-0.1422E-03 0.1372E-03-0.2918E-03
430.00     0.00-0.3348E-01 0.4874E-01 0.3779E-01-0.6339E-02 0.4032E+00-0.2841E-03 0.2457E-03 0.1751E-03
430.00L    0.00-0.3348E-01 0.4012E-02 0.7203E-03-0.6339E-02 0.4032E+00-0.5577E-03 0.2457E-03 0.1751E-03
430.00  155.00-0.3643E-01 0.5300E-01 0.4322E-01-0.1073E-01 0.4185E+00-0.3118E-03 0.2645E-03 0.2014E-03
430.00L 155.00-0.3642E-01 0.4435E-02 0.1490E-02-0.1073E-01 0.4185E+00-0.6111E-03 0.2645E-03 0.2014E-03
```

Figure 5: Actual strain values for section (SA5C3)

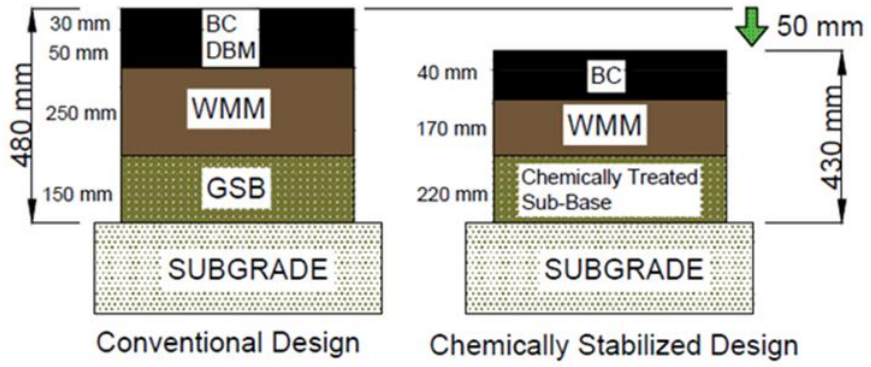

Figure 6: Comparison of conventional section with SA5C3

```
No. of layers                4
E values (MPa)          3000.00  350.00  195.00   63.00
Mu values                 0.350.350.250.35
thicknesses (mm)          40.00  170.00  220.00
single wheel load (N) 20000.00
tyre pressure (MPa)        0.56
Dual  Wheel
  Z        R      SigmaZ      SigmaT      SigmaR      TaoRZ       DispZ       epZ         epT         epR
 40.00     0.00-0.4558E+00 0.6623E+00 0.6029E+00-0.1846E-01 0.6073E+00-0.2995E-03 0.2036E-03 0.1769E-03
 40.00L    0.00-0.4558E+00-0.1395E+00-0.1465E+00-0.1846E-01 0.6073E+00-0.1016E-02 0.2036E-03 0.1769E-03
 40.00  155.00-0.1267E+00 0.5164E-01-0.9017E+00-0.1611E+00 0.5644E+00 0.5695E-04 0.1372E-03-0.2918E-03
 40.00L 155.00-0.1267E+00-0.5422E-01-0.1654E+00-0.1611E+00 0.5644E+00-0.1422E-03 0.1372E-03-0.2918E-03
430.00     0.00-0.3344E-01 0.4900E-01 0.3799E-01-0.6333E-02 0.4030E+00-0.2830E-03 0.2455E-03 0.1749E-03
430.00L    0.00-0.3345E-01 0.4007E-02 0.7184E-03-0.6333E-02 0.4030E+00-0.5572E-03 0.2455E-03 0.1750E-03
430.00  155.00-0.3643E-01 0.5329E-01 0.4348E-01-0.1071E-01 0.4182E+00-0.3109E-03 0.2642E-03 0.2014E-03
430.00L 155.00-0.3639E-01 0.4429E-02 0.1485E-02-0.1072E-01 0.4183E+00-0.6105E-03 0.2642E-03 0.2011E-03
```

Figure 7: Actual strain values of (SA5C4)

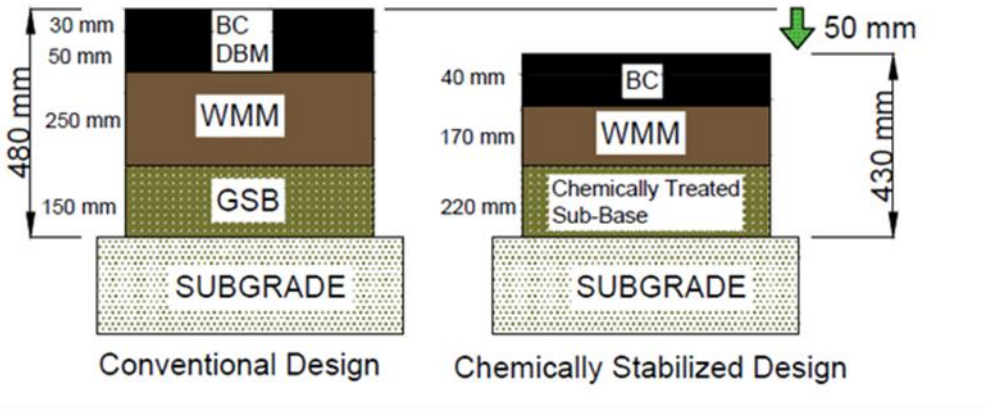

Figure 8: Comparison of conventional section with SA5C4

```
No. of layers                4
E values (MPa)         3000.00  350.00  283.00   63.00
Mu values                0.350.350.250.35
thicknesses (mm)         40.00  150.00  220.00
single wheel load (N) 20000.00
tyre pressure (MPa)       0.56
Dual  Wheel
  Z        R      SigmaZ      SigmaT      SigmaR      TaoRZ       DispZ       epZ         epT         epR
 40.00     0.00-0.4581E+00 0.6455E+00 0.5886E+00-0.1621E-01 0.5818E+00-0.2967E-03 0.1999E-03 0.1743E-03
 40.00L    0.00-0.4581E+00-0.1426E+00-0.1492E+00-0.1621E-01 0.5818E+00-0.1017E-02 0.1999E-03 0.1743E-03
 40.00   155.00-0.1285E+00 0.3419E-01-0.9159E+00-0.1525E+00 0.5362E+00 0.6002E-04 0.1332E-03-0.2943E-03
 40.00L  155.00-0.1285E+00-0.5714E-01-0.1680E+00-0.1525E+00 0.5362E+00-0.1421E-03 0.1332E-03-0.2943E-03
410.00     0.00-0.3368E-01 0.7504E-01 0.5856E-01-0.6289E-02 0.4028E+00-0.2370E-03 0.2432E-03 0.1704E-03
410.00L    0.00-0.3368E-01 0.3605E-02 0.2099E-03-0.6289E-02 0.4028E+00-0.5558E-03 0.2432E-03 0.1704E-03
410.00  155.00-0.3658E-01 0.8176E-01 0.6622E-01-0.1111E-01 0.4182E+00-0.2600E-03 0.2627E-03 0.1941E-03
410.00L 155.00-0.3661E-01 0.4031E-02 0.8328E-03-0.1112E-01 0.4182E+00-0.6081E-03 0.2627E-03 0.1942E-03
```

Figure 9: Actual strain values of (SA5C2CH3)

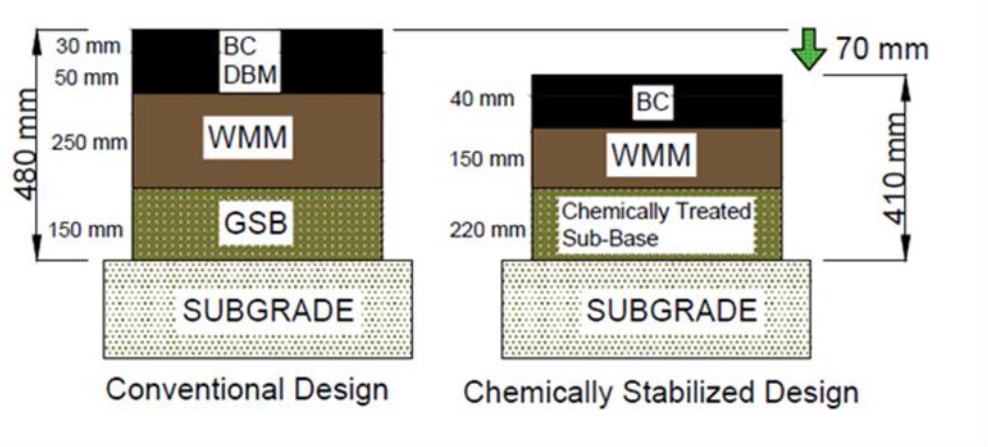

Figure 10: Comparison of conventional section with SA5C2CH3

```
No. of layers                4
E values (MPa)          3000.00  350.00  488.00   63.00
Mu values                  0.350.350.250.35
thicknesses (mm)          40.00  150.00  200.00
single wheel load (N) 20000.00
tyre pressure (MPa)        0.56
Dual  Wheel
  Z         R       SigmaZ       SigmaT      SigmaR      TaoRZ       DispZ       epZ         epT         epR
 40.00     0.00-0.4630E+00 0.6097E+00 0.5585E+00-0.1334E-01 0.5438E+00-0.2906E-03 0.1921E-03 0.1691E-03
 40.00L    0.00-0.4630E+00-0.1491E+00-0.1550E+00-0.1334E-01 0.5438E+00-0.1019E-02 0.1921E-03 0.1691E-03
 40.00   155.00-0.1313E+00-0.1434E-02-0.9428E+00-0.1368E+00 0.4943E+00 0.6638E-04 0.1248E-03-0.2988E-03
 40.00L 155.00-0.1313E+00-0.6264E-01-0.1725E+00-0.1368E+00 0.4943E+00-0.1402E-03 0.1248E-03-0.2988E-03
390.00     0.00-0.3228E-01 0.1241E+00 0.9669E-01-0.5691E-02 0.3938E+00-0.1792E-03 0.2213E-03 0.1511E-03
390.00L    0.00-0.3228E-01 0.2294E-02-0.9688E-03-0.5690E-02 0.3938E+00-0.5198E-03 0.2212E-03 0.1512E-03
390.00   155.00-0.3496E-01 0.1347E+00 0.1083E+00-0.1056E-01 0.4084E+00-0.1961E-03 0.2384E-03 0.1708E-03
390.00L 155.00-0.3495E-01 0.2588E-02-0.5685E-03-0.1056E-01 0.4084E+00-0.5660E-03 0.2384E-03 0.1708E-03
```

Figure 11: Actual strain values of (SA5C3CH3)

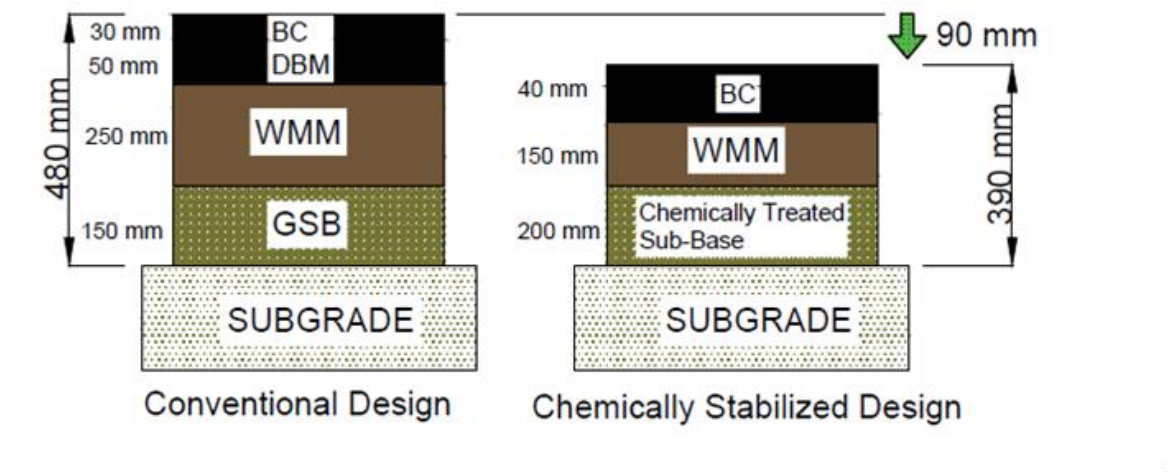

Figure 12: Comparison of conventional section with SA5C3CH3

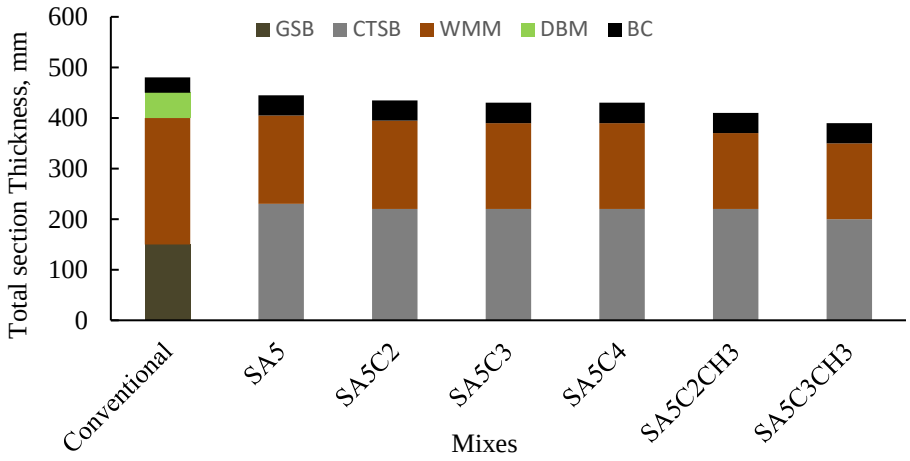

Figure 13: Thickness comparison of different sections

Curiginal

Document Information

Analyzed document	Thesis combined.pdf (D141784664)
Submitted	2022-07-06 12:17:00
Submitted by	Dr. Har Singh
Submitter email	harsingh@thapar.edu
Similarity	5%
Analysis address	harsingh.thapar@analysis.urkund.com

Sources included in the report

SA **Chaudhary Devi Lal University, Sirsa / Final File.doc** 2
Document Final File.doc (D135724029)
Submitted by: saranalok@gmail.com
Receiver: saranalok.cdlu@analysis.urkund.com

SA **Rajiv Gandhi Proudyogiki Vishwavidyalaya / thesis...vijay.docx** 2
Document thesis...vijay.docx (D139916867)
Submitted by: ashokgagorni@gmail.com
Receiver: ashokgagorni.rgpv@analysis.urkund.com

SA **Thapar Institute Of Engineering And Technology / Thesis work (2).docx** 1
Document Thesis work (2).docx (D75674249)
Submitted by: manpreetsingh2@thapar.edu
Receiver: manpreetsingh2.thapar@analysis.urkund.com

SA **Jagan Nath University / Thesis Happy Sharma 03.07.2019 Mtech- Transportation.pdf** 2
Document Thesis Happy Sharma 03.07.2019 Mtech- Transportation.pdf (D54336995)
Submitted by: vivek.sharma@jagannathuniversity.org
Receiver: vivek.sharma.akshay@analysis.urkund.com

W URL: https://www.ijream.org/papers/ICRTET0171.pdf 4
Fetched: 2022-04-03 12:07:48

SA **Savutribai Phule Pune University / Project Report on A Study of Cement Treated Base and Sub base in Flexible Pavement. Amar Gavane SVCP.docx** 1
Document Project Report on A Study of Cement Treated Base and Sub base in Flexible Pavement. Amar Gavane SVCP.docx (D55043841)
Submitted by: plag.sinhgad@sinhgad.edu
Receiver: plag.sinhgad.unipune@analysis.urkund.com

SA **AISECT UNIVERSITY(Rabindranath Tagore University) / sanjay sir civil.docx** 1
Document sanjay sir civil.docx (D51450047)
Submitted by: researchcellau@gmail.com
Receiver: researchcellau.rtu@analysis.urkund.com

SA **RIMT University / 19-M-CE-1191 Sanna Manzoor.docx** 2
Document 19-M-CE-1191 Sanna Manzoor.docx (D119698848)
Submitted by: sandeep.singla@rimt.ac.in
Receiver: sandeep.singla.rimt@analysis.urkund.com